

University of Alberta

Understanding AI-PAM Assisted Oil Sands Tailings Treatment

by

Lina Guo

A thesis submitted to the Faculty of Graduate Studies and Research
in partial fulfillment of the requirements for the degree of

Master of Science

in

Chemical Engineering

Chemical and Material Engineering

©Lina Guo

Fall 2012

Edmonton, Alberta

Permission is hereby granted to the University of Alberta Library to reproduce single copies of this thesis and to lend or sell such copies for private, scholarly or scientific research purposes only. Where the thesis is converted to, or otherwise made available in digital form, the University of Alberta will advise potential users of the thesis of these terms

The author reserves all other publication and other rights in association with the copyright in the thesis, and except as herein before provided, neither the thesis nor any substantial portion thereof may be printed or otherwise reproduced in any material form whatsoever without the author's prior written permission.

Acknowledgment

I would love to convey my sincere gratitude to Drs. Zhenghe Xu and Jacob Masliyah for their intelligent guidance and generous support throughout this project. I have been educated not only academic knowledge but also the proper attitude for questions, challenges and criticisms.

Special appreciation to Dr. Yadi Maham for his valuable advices during the final stage of thesis writing. I am also thankful for the great help of Dr. Xianhua Feng in polymer synthesis and his contribution to the progress of this work. I would like to thank Dr. Lana Alagha for the helpful discussions.

I acknowledge Mr. Jim Skwarok and Ms. Shaiou-Yin Wu for their patience with sharing their experience of laboratory work. I would also like to thank Ms Lisa Carreiro and Ms. Leanne Swekla for being accommodating.

The financial support from the Natural Sciences and Engineering Research Council of Canada through the NSERC Industrial Research Chair in Oil Sands Engineering is gratefully appreciated. My sincere thanks also go to Champion Technologies for their inspiration during my internship.

It is my honor to work in the oil sands engineering research group. Thank all the administrative and academic staff at the Chemical and Materials Engineering Department for being responsive.

At last, my deepest gratitude goes to my family and friends. I am forever grateful to my family for their love, support and understanding. My endless thanks always go to all my friends for their companionship and encouragement.

Abstract

Built on the established success of Al-PAM, an in-house synthesized, organic-inorganic hybrid polymer, for flocculation and filtration of fresh oil sands extraction tailings, this research is to understand working mechanism of Al-PAM, focusing on the effect of Al-PAM properties (molecular weight and aluminum content), tailings characteristics (fines content and bitumen content) and temperature on flocculation and filtration of oil sands laboratory extraction tailings. Based on fundamental knowledge established through this study, an appealing solution to fresh oil sands tailings treatment by filtering the sediment of flocculated fresh oil sands extraction tailings was proposed and tested.

Al-PAM of higher molecular weight or/and high Al content was identified to be more effective in flocculating fines in oil sands tailings and hence filtration. Removal of bitumen from laboratory extraction tailings did not improve flocculation and filtration of oil sands tailings by Al-PAM. Effective flocculation of ultra-fines particles in fresh tailings was determined to be a critical contributor to outstanding performance of Al-PAM in flocculation and filtration of oil sands laboratory extraction tailings. It was also found that temperature (22 and 45 °C) had little effect on settling and filtration of laboratory oil sands extraction tailings. Filtration of sediments after flocculation of laboratory oil sands extraction tailings was found about 3 times more efficient than filtration of the entire flocculated tailings suspensions.

Table of Contents

Chapter 1 Introduction.....	1
1.1 Oil sands.....	1
1.2 Oil sands extraction processes.....	2
1.2.1 Clark Hot Water Extraction (CHWE).....	2
1.2.2 SAGD and other extraction processes.....	5
1.3 Oil sands tailings.....	5
1.3.1 Challenges of tailings treatment and management.....	7
1.3.2 Current technologies for oil sands tailings treatment.....	9
1.4 Previous work prior to this study.....	16
1.5 Objectives of this work.....	18
1.6 Organization of thesis.....	19
Chapter 2 Literature Review.....	26
2.1 Basics of particle aggregation.....	26
2.1.1 Electrical double layer.....	26
2.1.2 DLVO theory.....	27
2.1.3 Coagulation and flocculation.....	28
2.2 Properties of polymer flocculants.....	31
2.2.1 Charge of polymers.....	32
2.2.2 Structure of polymers.....	33
2.3 Flocculation application in oil sands tailings treatment.....	35
2.3.1 Combination of flocculation and filtration in oil sands tailings treatment.....	36
Chapter 3 Materials and Experiments.....	42
3.1 Materials.....	42
3.1.1 Polymers.....	42

3.1.2 Al-PAM preparation and measurement.....	45
3.1.3 Model fine tailings.....	53
3.1.4 Laboratory extraction tailings.....	54
3.2 Procedures for settling and filtration experiment.....	56
3.2.1 Isokinetic sampling.....	56
3.2.2 Settling tests.....	58
3.2.3 Filtration tests.....	60
Chapter 4 Settling and Filtration.....	64
4.1 Settling.....	64
4.1.1 Settling curve and ISR.....	65
4.1.2 Discussion.....	67
4.2 Filtration.....	72
4.2.1 Specific resistance of filtration.....	73
4.2.2 Filtration curves and data processing.....	76
Chapter 5 Effect of Polymer Properties on Oil Sands Tailings Treatment.....	85
5.1 Effect of molecular weight.....	85
5.1.1 Settling behavior.....	85
5.1.2 Filtration performance.....	90
5.1.3 Summary.....	98
5.2 Effect of aluminum content	99
5.2.1 Settling behavior.....	100
5.2.2 Filtration performance.....	104
5.2.3 Summary.....	107
Chapter 6 Effect of Tailings Characteristics.....	110
6.1 Effect of bitumen content.....	110
6.1.1 Laboratory extraction tailings.....	110

6.2 Effect of fines in supernatant.	118
6.2.1 Test procedure.....	118
6.2.2 Supernatant-refilling experiment of model fines tailings.....	120
6.2.3 Supernatant-refilling experiment of laboratory extraction tailings.....	121
6.2.4 Discussion.....	122

Chapter 7 A Proposal of AI-PAM Assisted Filtration for Oil Sands

Tailings Treatment.....127

7.1 Settling behaviour at different temperatures.....	127
7.1.1 Settling tests.....	128
7.1.2 Discussion.....	130
7.2 Filtration performance at different temperatures.....	133
7.2.1 Model fines tailings.....	134
7.2.2 Laboratory extraction tailings.....	136
7.2.3 Discussion	138
7.3 Comparison of direct filtration of whole tailings to filtration of sediments.....	139
7.3.1 Procedure for Sediment filtration experiment	139
7.3.2 Model fines tailings.....	140
7.3.3 Laboratory extraction tailings.....	140
7.3.4 Summary.....	143
7.4 A design of dewatering system.....	143

Chapter 8 Conclusions and Future Work.....149

8.1 Conclusions.....	149
8.2 Recommendation for future work.....	149

Appendices.....151

Appendix A - Further investigation of Al-PAM structure.....	151
Appendix A-I Settling behaviour.....	151
Appendix A-II Filtration performance.....	155
Appendix B - Effect of bitumen content on settling and filtration of diluted mature fine tailings.....	167

List of Tables

Table 3-1 Physical properties of polymer flocculants used in this study.....	43
Table 3-2 Relationship between pH and aluminum ion species.....	46
Table 3-3 Colloid characteristics of Al-PAMs freshly prepared and after one night storage.....	48
Table 3-4 Aluminum content of Al-PAMs.....	52
Table 3-5 Ion concentration of Aurora process water (mg/L).....	54
Table 3-6 Composition of laboratory extraction tailings (wt%).....	55
Table 3-7 Experimental conditions of laboratory extraction tests (pH=8.4)	56
Table 4-1 List of linear fit of $t/V-V$ and SRF for laboratory extraction tailings: 11 wt% solids with 25 wt% fines at pH=8.4.....	80
Table 5-1 Effect of molecular weight on SFR of flocculated model fine tailings.....	93
Table 5-2 Effect of molecular weight on SRF of flocculated laboratory extraction tailings.....	97
Table 5-3 Physical properties of AIPAM6R and AIPAM6H.....	100
Table 5-4 Effect of Al content on SRF of flocculated model fine tailings.....	105
Table 5-5 Effect of Al content on SRF of flocculated laboratory extraction tailings.....	106

Table 6-1 Composition of laboratory extraction tailings prepared from SYN ore (wt%).....	112
Table 6-2 SRFs of flocculated laboratory extraction tailings by Al-PAMs at selected dosage.....	116
Table 6-3 Composition of laboratory extraction tailings prepared from POSYN ore (wt%).....	117
Table 6-4 SRFs of the supernatant filtration tests.....	125
Table 7-1 SRFs of flocculated model fine tailings by Al-PAM at different temperatures.....	136
Table 7-2 SRFs and filtration rates of flocculated laboratory extraction tailings by Al-PAM at different temperatures.....	138
Table 7-3 SRFs of flocculated whole tailings and sediments.....	142
Table A-1 SRFs of flocculated tailings by Al-PAM and mixture of (PAM+Colloid)at selected dosages.....	157
Table A-2 Characteristics of polymers.....	158
Table A-3 Sediment volume of flocculated laboratory extraction tailings by different polymers at different dosages.....	160

List of Figures

Figure 1.1 Schematic flowchart of bitumen production.....	2
Figure 1.2 Schematic representation of a typical CHWE bitumen extraction process.....	4
Figure 1.3 Schematic representation of conventional oil sands extraction and tailings management system.....	6
Figure 1.4 Schematics of the CT process.....	11
Figure 1.5 Schematics of TT or paste technology process.....	12
Figure 2.1 Distribution of ions in Stern-model of electrical double layer system.....	27
Figure 2.2 General illustration of interaction energy profile of particle surface in electrolyte solution (DLVO).....	28
Figure 2.3 Schematic aggregates by (a) coagulation; and (b) flocculation.....	30
Figure 2.4 Schematic flocculation mechanisms of particles: (a) bridging; (b) charge neutralization	31
Figure 2.5 Image of PAM, a linear polymer with long chain.....	33
Figure 2.6 Examples of branched polymers: (a) branched polymer with arms of the composition similar to backbones or graft polymer with compositions of branches being different from backbones;	

(b) star polymer; (c) comb polymer; and (d) dendritic polymer..	34
Figure 3.1 Set-up for colloid preparation.....	46
Figure 3.2 Schematics of Al-PAM synthesis.....	49
Figure 3.3 Schematics of Al-PAM structure.....	50
Figure 3.4 Setup for synthesis of Al-PAM (a) before put on protection from exposure to light; (b) with protection from exposure to light; and (c) schematics of Al-PAM synthesis setup.....	51
Figure 3.5 (a) Particle size distribution of kaolinite in model fine tailings; and (b) photograph of model fine tailings in the process of settling.....	53
Figure 3.6 (a) Impeller fit for a 20-L pail; and(b) mechanical stirrer suitable for a 20-L pail.....	57
Figure 3.7 (a) Masterflex® heavy duty pump; (b) disposable plastic pipette of 23 mL in volume.....	58
Figure 3.8 (a) Home-made baffle and customized impeller for 250-mL beakers; and (b) mechanical stirrer used for mixing tailings in 250-mL beakers.....	58
Figure 3.9 Setup for settling experiment.....	59
Figure 3.10 Setup for the filtration experiment.....	60
Figure 4.1 Schematics of a typical settling curve.....	65
Figure 4.2 Settling curve of flocculated laboratory extraction tailings by	

2 ppm MF1011.....	66
Figure 4.3 Initial settling rates of flocculated laboratory extraction tailings by MF1011 and Al-PAMs at different dosages.....	67
Figure 4.4 Schematic representation of the bridging model under (a) a correct mixing; and (b) an excessive mixing.....	69
Figure 4.5 Theoretical results of a filtration experiment.....	74
Figure 4.6 A general flow for filtration data processing and corresponding plotting.....	77
Figure 4.7 Original filtration curve plotted according to released filtrate against filtration time.....	78
Figure 4.8 Derived filtration curve plotted as percent water left in the slurry against filtration time.....	78
Figure 4.9 Derived filtration curve plotted as moisture content in filter cake against filtration time.....	79
Figure 4.10 Derived filtration curve plotted as t/V against filtrate volume.....	79
Figure 5.1 (a) Initial settling rate of 5 wt% kaolinite suspensions as a function of Al-PAM dosage; and (b) settling of flocculated model fine tailings with 10 ppm AlPAM8R (Al-PAM dosage ppm is expressed in terms of tailings slurry).....	86
Figure 5.2 Supernatant turbidities of model fine tailings with 5 wt% kaolinite	

at different dosages of Al-PAMs.....	87
Figure 5.3 Initial settling rates of flocculated laboratory extraction tailings by MF1011 and Al-PAMs (pH=8.4).....	88
Figure 5.4 Supernatant turbidities of laboratory extraction tailings (11 wt% solids with 26 wt% fines) at different dosages of MF1011 and Al-PAMs (pH=8.4).....	89
Figure 5.5 Filtration of flocculated model fine tailings by (a) MF1011; (b) AIPAM4R; (c) AIPAM6R; and (d) AIPAM8R (pH=8.4, flocculant dosage is shown in reference to mass of tailings).....	91
Figure 5.6 SRFs of flocculated model fine tailings with 5 wt% kaolinite by MF1011.....	92
Figure 5.7 Filtration of flocculated laboratory extraction tailings by (a) MF1011; (b) AIPAM4R; (c) AIPAM6R; and (d) AIPAM8R.....	95
Figure 5.8 Effect of molecular weight on (a) filtration performance; (b) filtration rate; and (c) final filter cake moisture of tailings SYN704HB at optimum dosage of each polymer.....	96
Figure 5.9 Comparison of SRF at selected dosages of different polymers.....	97
Figure 5.10 Initial settling rates of flocculated model fine tailings with 5 wt% kaolinite by Al-PAM with different Al content at room temperature 22°C, pH=8.4.....	101

Figure 5.11 Initial settling rates of flocculated laboratory extraction tailings (11 wt% solids with 26 wt% fines) by Al-PAM with different Al content at room temperature 22°C, pH=8.4.....	102
Figure 5.12 (a) supernatant turbidities of flocculated laboratory extraction tailings; and (b) zeta potential of particles in supernatant of flocculated laboratory extraction tailings by Al-PAMs with different Al content.....	103
Figure 5.13 Filtration of flocculated model fine tailings by (a) AIPAM6R with lower Al content; and (b) AIPAM6H with higher Al content.....	104
Figure 5.14 Filtration of flocculated laboratory extraction tailings by (a) AIPAM6R with lower Al content; and (b) AIPAM6H with higher Al content.	106
Figure 6.1 Initial settling rates of flocculated laboratory extraction tailings by (a) AIPAM4R; (b) AIPAM6R; (c) AIPAM8R; and (d) MF1011.....	111
Figure 6.2 Supernatant turbidities of flocculated laboratory extraction tailings by (a) AIPAM4R; (b) AIPAM6R; (c) AIPAM8R; and (d) MF1011.....	113
Figure 6.3 Filtration of flocculated laboratory extraction tailings at selected dosages of different polymers.....	115

Figure 6.4 Effect of bitumen content on (a) initial settling rate; and (b) moisture content in filter cake of flocculated laboratory extraction tailings (prepared from POSYN ore) by AIPAM8R at selected dosages.....	117
Figure 6.5 Schematics of supernatant-refilling filtration experiment.....	119
Figure 6.6 Filtration to supernatant of flocculated model fine tailings by MF1011 and Al-PAM as (a) percent of water left in tailings; and (b) moisture content of filter cake as a function of filtration time.....	120
Figure 6.7 (a) filtration to supernatant of flocculated laboratory extraction tailings by Al-PAM and MF1011; (b) photograph of cross section of filter cake from flocculated tailings with refilled supernatant with MF1011; and (c) photograph of cross section of filter cake from flocculated tailings with refilled supernatant with Al-PAM.....	121
Figure 6.8 A schematic diagram of different filter cake structures.....	123
Figure 6.9 Linear fit of $t/V - V$ for (a) model fine tailings; and (b) laboratory extraction tailings (pH=8.4).....	124
Figure 7.1 Schematics of set-up for settling at 45°C.....	128
Figure 7.2 Settling behaviour of the flocculated model fine tailings by AIPAM8R at (a) 22 °C (R.T.); and (b) 45°C (H.T.).....	129

Figure 7.3 Settling behaviour of the flocculated laboratory extraction tailings by AIPAM8R at (a) 22 °C (R.T.); and (b) 45°C (H.T.)..	129
Figure 7.4 Schematics of conformation at different temperatures.....	132
Figure 7.5 Schematics of set-up for filtration at 45°C.....	134
Figure 7.6 Comparison of filtration performance of the flocculated model fine tailings by AIPAM8R at 22 °C (R.T.) to 45 °C (H.T.) as (a) percent of water left in tailings; and (b) moisture content of filter cake as a function of filtration time.	135
Figure 7.7 Comparison of filtration performance of the flocculated laboratory extraction tailings by AIPAM8R at 22 °C (R.T.) to 45 °C (H.T.) as (a) percent of water left in tailings; and (b) moisture content of filter cake as a function of filtration time.	137
Figure 7.8 Effect of temperature on SRF of flocculated laboratory extraction tailings by Al-PAM.....	137
Figure 7.9 Filtration to the sediments of flocculated model fine tailings by MF1011 and Al-PAM.....	140
Figure 7.10 Filtration to the sediments of flocculated laboratory extraction tailings by MF1011 and Al-PAM.....	141
Figure 7.11 Images of flocs in sediment of flocculated laboratory extraction tailings by Al-PAM and MF1011.....	143
Figure 7.12 Concept of a novel two-step filtration process for treating large	

volume of oil sands extraction tailings: filtration of sediments	
after flocculation and thickening.....	144
Figure 7.13 Procedure of concept tests.....	145
Figure 7.14 Comparison of filtration of whole tailings to sediments	
flocculated by (a) MF1011; and (b) Al-PAM.....	146
Figure A-1 Settling behaviour of model fine tailings with AIPAM8R,	
(PAM + Colloid) mixture, PAM, respectively before	
shaking.....	152
Figure A-2 Settling behaviour of model fine tailings with AIPAM8R,	
(PAM + Colloid) mixture, PAM, respectively after	
shaking.....	153
Figure A-3 (a) Settling behaviour of laboratory extraction tailings with	
AIPAM8R, (PAM + Colloid) mixture, PAM, respectively, before	
shaking; and (b) photograph of flocs for flocculated tailings by	
Al-PAM.....	154
Figure A-4 (a) Settling behaviour of laboratory extraction tailings with	
AIPAM8R, (PAM + Colloid) mixture, PAM, respectively, after	
shaking; (b) photograph of released flocs of flocculated tailings	
by (PAM + Colloid) mixture after shaking.....	155
Figure A-5 Filtration performances of flocculated (a) model fine tailings;	
and (b) laboratory extraction tailings by Al-PAM or mixture of	

(PAM+Colloid).....	156
Figure A-6 Comparisons of initial settling rate of flocculated (a) model fine tailings; and (b) laboratory exaction tailings with PAM, MF1011 and Al-PAM.	159
Figure A-7 Solids content in sediment of flocculated laboratory extraction tailings with polymers addition at different dosages.....	161
Figure A-8 Schematics of why sediment of MF1011 is more compact than Al-PAM.....	162
Figure A-9 TGA curves of H-1(Al-PAM), PAM, and Al(OH) ₃ /PAM blend.....	164
Figure A-10 (a)&(b) Adhesion force of a single PAM chain to clay; (c)&(d) Adhesion force of Al-PAM to clay.....	165
Figure A-11 Schematics of flocs by (a) single chain polymer; and (b) star-like polymer with the similar chain length.....	166
Figure B-1 Comparisons of (a) settling; (b) water left percent in the total water of tailings; and (c) moisture content in the filter cake of the diluted MFT with different bitumen content at selected dosages of each polymer.....	168

Chapter 1 Introduction

1.1 Oil sands

The largest deposit of oil sands was discovered in the Athabasca region of northern Alberta, Canada. Athabasca oil sands (Cretaceous McMurray Formation) are a mixture of bitumen, minerals and water in varying proportions. It contains on average 12% bitumen, 84-85% mineral solids and 3-6% water by weight [1]. Minerals are predominately sands quartz, silts and clays. The main clay components are 40-70% kaolinite, 30-45% illite and up to 10% mixed layer illite/smectite, which is believed to be largely responsible for the processing and compaction problems in oil sands extraction and fines tailings disposal [2].

It was estimated that approximately 300 billion barrels of bitumen would be recoverable from the Alberta oil sands. Bitumen is heavy petroleum which has a very high viscosity at ambient temperature. Like conventional crude oil, bitumen can be refined to various fuels after upgrading. Therefore, oil sands are an important energy source not only for Canada but also for the world. Figure 1.1 shows the general process of bitumen production for surface mining.

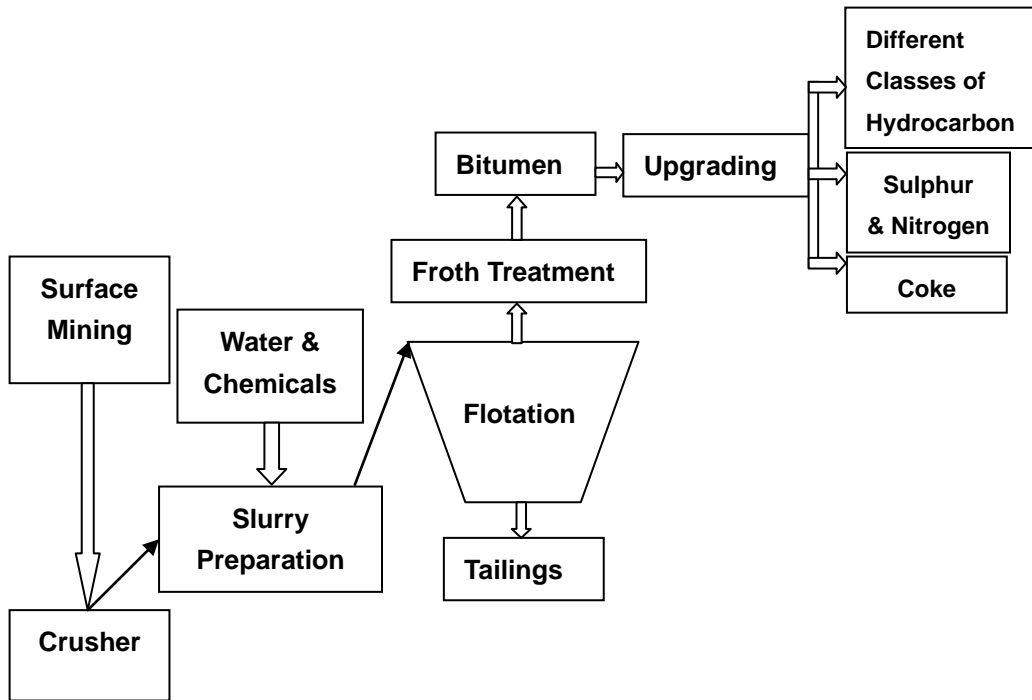


Figure 1.1 Schematic flowchart of bitumen production [3].

1.2 Oil sands extraction processes

1.2.1 Clark Hot Water Extraction (CHWE)

Historically, the potential of oil sands as an energy source has not been fully realized until 1920s. A scientist, Dr. Karl Clark, working at Alberta Research Council, Edmonton, Canada, developed a method for extracting bitumen from oil sands using hot water. The extraction process was named after him as Clark Hot Water Extraction (CHWE) process. The basic concept of CHWE is mixing hot water to open-pit mined oil sands, and

floating bitumen to the top of the mixture [3]. Now, an improved process of the CHWE [4] is used in the surface mining operations by bitumen producers.

Figure 1.2 is a schematic representation of the CHWE bitumen extraction process from mining to upgrading. In this process, oil sands after being mined and crushed, are delivered through hydrotransport pipeline while being mixed with hot water, steam, caustic and a small amount of air [5, 6]. Heat reduces the viscosity of bitumen and mechanical shear helps to separate bitumen from sands [3]. The mixture slurry with liberated and aerated bitumen is then pumped to a gravity separation vessel. The bitumen aggregates float up to the top of vessels as froth due to their lower density than the density of mixture slurry. Meanwhile the heavier solids settle to the bottom, forming tailings [3]. The middlings with unrecovered bitumen are sent to the flotation cells or hydrocyclones for further bitumen recovering [3]. Chemicals, such as naphtha or paraffinic diluents, are used to reduce the viscosity of bitumen in the froth treatment. The density difference between water and oil facilitates removal of water and solids [3]. The naphtha-based froth treatment uses centrifuge and/or inclined plate settler [1]. After removing solvents from the diluted bitumen in a diluent recovery unit, the bitumen product is upgraded to produce synthetic crude

oil [1]. In the end, the tailings waste goes to the tailings ponds or thickeners for water-waste management.

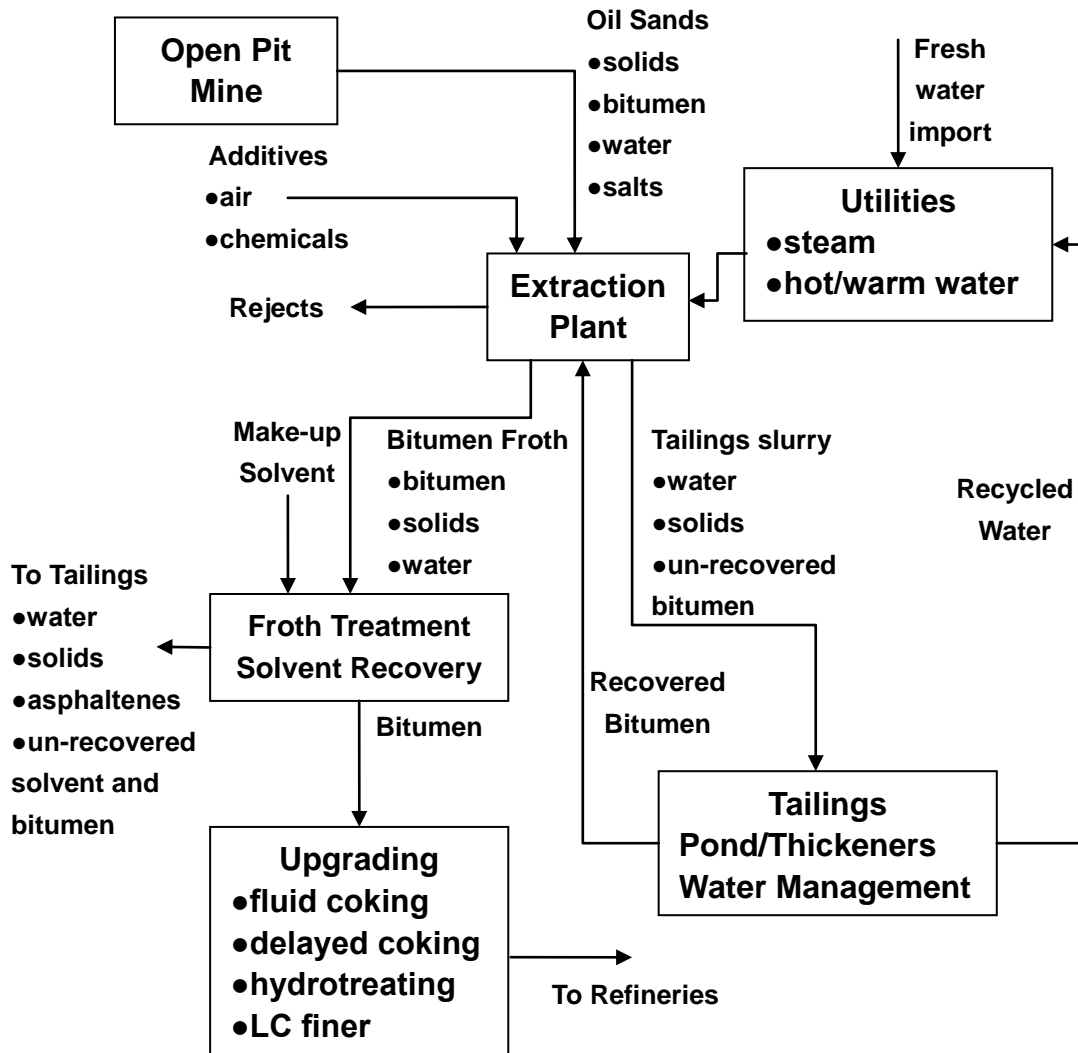


Figure 1.2 Schematic representation of a typical CHWE bitumen extraction process [7].

1.2.2 SAGD and other extraction processes

SAGD-Steam Assisted Gravity Drainage is another main industrial process for bitumen production. It is most commonly used in in-situ operation [8]. In the late 1970s, Roger Butler and his colleagues at Imperial Oil developed SADG, which has made it feasible to recover bitumen for about 85% of the oil sands resource located underground in deep formation [3]. Cyclic Steam Stimulation (CSS), Vapour Extraction Process (VAPEX), Toe to Heel Air Injection (THAI) and Supercritical Fluid Extraction (SFE) are also experimental extraction methods for in-situ oil sands extraction [9, 10].

1.3 Oil sands tailings

The oil sands tailings generated from oil sands extraction process are a complex mixture of water, sands, and silt clays. Tailings slurry has approximately 45-55 wt% solids which contains about 82 wt% sands and 18 wt% fines (diameter < 44 μm) [11], unrecovered hydrocarbons and dissolved chemicals [12].

A conventional oil sands extraction and tailings management system is shown in Figure 1.3.

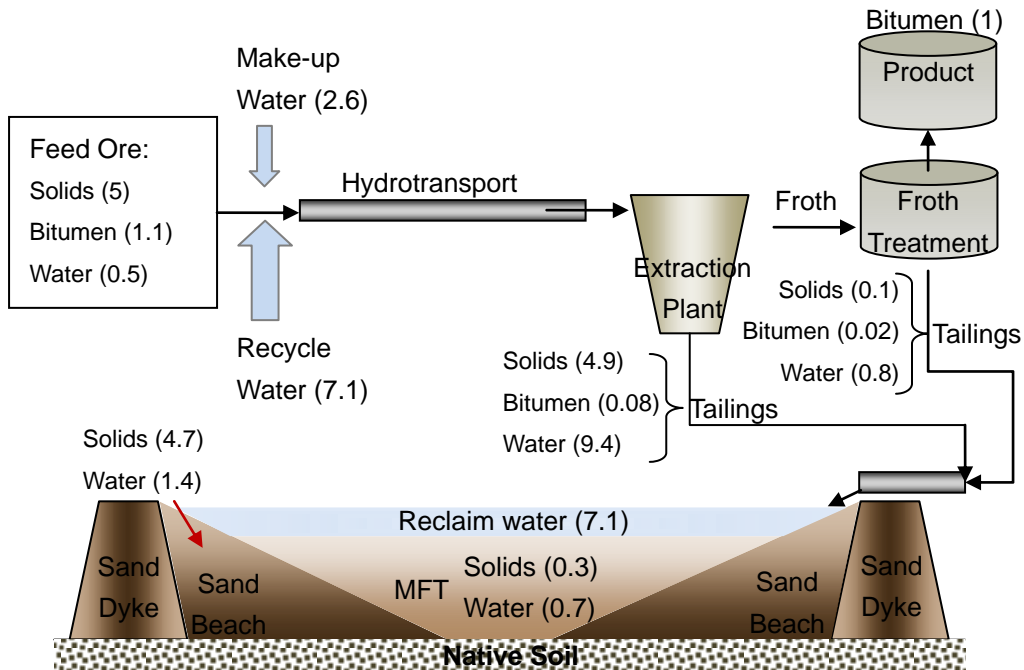


Figure 1.3 Schematic representation of conventional oil sands extraction and tailings management system [13, 14].

Here, the numbers in Figure 1.3 represent mass of each component. For example, in the feed ore, the mass of solids is 5, bitumen is 1.1 and water is 0.5. Therefore, for the whole system, according to mass balance:

$$\text{Input} = \text{“Feed Ore”} + \text{“Water”} = 5 + 1.1 + 0.5 + 2.6 + 7.1 = 16.3;$$

$$\text{Output} = \text{“Bitumen”} + \text{“Tailings”} = 1 + (4.9 + 0.08 + 9.4) + (0.1 + 0.02 + 0.8) = 16.3$$

Traditionally, the tailings stream is pumped into large tailings ponds. The coarse solids settle out quickly and form sand dykes and sand beaches.

After settling for a few days, only a small fraction of smaller solid particles (smaller than 44 μm) remain in the upper part of the tailings pond. The water in this part is pumped back to the extraction plant. Below this depth of the tailings pond, fines form suspension which is very stable. After 2–3 years, the solids concentration of the suspension reaches 30-35% by weight and the suspension is usually referred to as mature fine tailings (MFT). Due to the high content of fines, dehydration of the MFT is extremely slow and it would take several centuries for the MFT to consolidate completely [5, 15].

1.3.1 Challenges of tailings treatment and management

Tailings treatment becomes increasingly important. With the increase of bitumen production, more tailings streams are produced which enlarges tailings ponds. The tailings ponds not only hold a large amount of water which can otherwise be recycled for plant use in the extraction process, but also pose threats to the environment because the water in tailings ponds is slightly alkaline and contains many types of toxic chemicals. It is responsibility of oil sands researchers to provide solutions to the tailings problems.

It is well known that fine solids in tailings ponds are present in a suspension state. Natural settling of such fines takes years to come to its final density which is still less than 40% solids. With higher production of bitumen extracted from oil sands, more tailings are generated and sent to tailings ponds. If tailings cannot be quickly treated, tailings ponds will grow and occupy a larger area of land. For example, in 2009, tailings ponds covered 130 square kilometers of area, which is as large as the City of Vancouver [16]. Apparently, reclamation of tailings ponds is urgent. More importantly, quick treatment of tailings will provide more recycled water for bitumen extraction operations. It has been found that to produce one cubic meter of synthetic crude oil (i.e., upgraded bitumen) in a mining operation requires about 2 - 4.5 m³ of fresh water [17]. The currently licensed volume of water diverted from Athabasca River by the oil sands mining operations is more than twice as that of municipal needs of Calgary [17]. The Energy Resources Conservation Board (ERCB) of Alberta calls for operators to reduce tailings by capturing or extracting the fine particles from the process water and then storing the captured dry solids in disposal areas. The details of ERCB suggestions as outlined in its Directive 074, 2009 are as follows:

1. Capture a minimum portion of fine particles (below 44 microns) from the

tailings. The capture rate (defined as a percentage of total fine particles in the mined oil sands) increases over three milestone years: 20% by June 30, 2010; 30% by June 30, 2012; and 50% by June 30, 2013.

2. Create dedicated disposal areas to store the captured fines particles.
3. Ensure the disposal areas meet the ERCB's minimum standards for "trafficability". To meet the ERCB requirements, the captured tailings have to be solid enough to allow a bulldozer, but not necessarily a wheeled vehicle, to travel over it [16].
4. Prepare annual plans and reports on tailings.

1.3.2 Current technologies for oil sands tailings treatment

The main objective of treating the oil sands tailings is to remove water so that a trafficable load-bearing surface can be produced to realize the subsequent reclamation within a practical time-frame, and the consequential deposit is no longer mobile and thus it will no longer have a need of dam-like containment [14]. The technologies could have been divided into five groups, which are physical/mechanical processes (e.g. CT and TT), natural processes, chemical/biological amendments, mixtures/co-disposal and permanent storage [14]. Here, CT and TT as physical/mechanical processes are given a little bit more introduction.

1.3.2.1 Composite/consolidated tailings (CT) technology

Oil sands tailings treatment has been studied since the beginning of commercial oil sands operations. The researchers used divalent cations or organic flocculants to aggregate clays in the tailings [18, 19]. A composite or consolidated tailings (CT) technology has been developed and successfully used for MFT reclamation [20]. The CT process is shown schematically in Figure 1.4. In this process, MFT with 30 wt% solids from tailings pond is mixed with coarse sands of fresh tailings concentrated via hydrocyclones to 70 wt% solids. After mixing, gypsum is introduced into the mixture. The water released from the CT process can be used for the bitumen extraction process. The CT deposit after one year of consolidation contains about 80 wt% solids. It is a geotechnically stable material and can be reclaimed as a solid landscape [21].

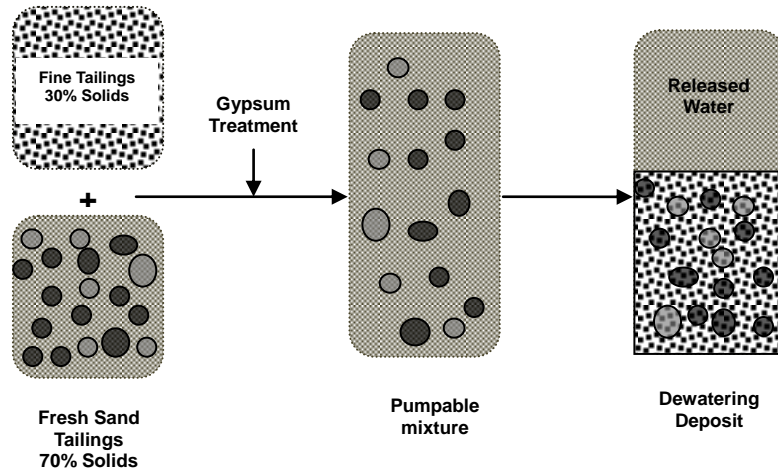


Figure 1.4 Schematics of the CT process [21].

Although CT technology accelerates water release from the tailings and reclamation of tailings ponds, it also creates some issues. For example, increased calcium ions content as a result of gypsum use, adversely affects bitumen extraction of certain types of ores [22, 23], and will raise a challenge of scaling in pipes, valves and other processing equipment. In addition, high concentrations of salts in the runoff water released from CT process also influence the quality of reclamation [19]. Therefore, the recycle water from CT process needs to be treated to be free of mineral solids before sending back to bitumen extraction operation.

1.3.2.2 Thickened tailings (TT) or paste technology

As stated above, the CT process is able to reduce the volume of MFT already existing in the tailings ponds. However, it would be better to treat the fresh tailings as early as possible rather than waiting for several years for the MFT to form. In this manner, the containment of fluid fine tailings in an external tailings disposal area during operations could be reduced or eliminated.

A technology named thickened tailings (TT) or paste technology was adopted for treating fine tailings from oil sands.

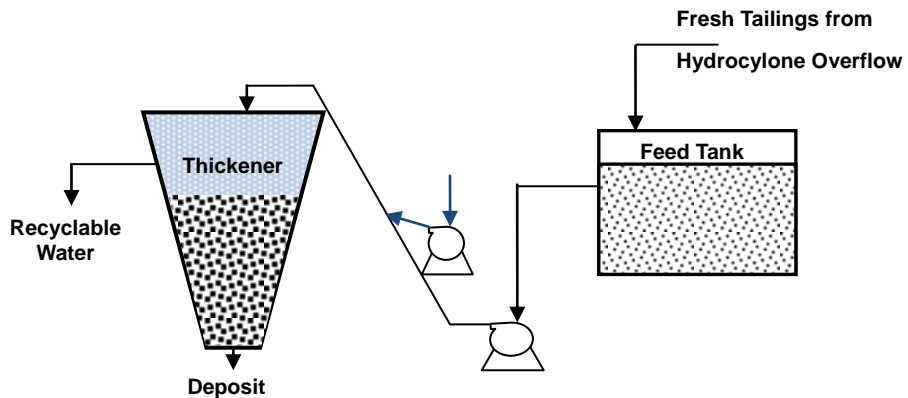


Figure 1.5 Schematics of TT or paste technology process.

In this process (see Figure 1.5), fresh fluid fine tailings (from hydrocyclone overflow of the whole tailings feed) are sent to a thickener together with added synthetic organic flocculants. The warm overflow water from the

thickener is recycled to the extraction process and the underflow (flocculated fines) from the thickener is pumped to the tailings ponds. When the thickened tailings are of high solids content, say, 50-60 wt%, the TT deposits can be reclaimed as dry land in a relatively short time [24, 25]. Otherwise, when the TT solids content is about 30 wt%, it needs to be further treated. The flocculation of fluid fine tailings is dependent on the properties of tailings and flocculants, such as the mineralogy, particle size of solids, pH, and water chemistry of slurry, feed dilution, hydrodynamic conditions, molecular weight and charge density of polymer flocculants.

The TT technology provides a possible solution to reduce tailings storage, which is a serious tailings problem existing in the present and future oil sands processing plants [26]. For example, by using thickeners, oil sands processing companies diminished containment requirement for tailings by producing higher density sludge of thickener underflow stream. Moreover, more energy savings were achieved by recycling more warm water from thickener overflow [2]. Compared to gypsum, polymer flocculants have fewer side effects on the quality of released water. However, the ability of dewatering and stability of the deposits obtained from the polymer application still need to be improved.

1.3.2.3 Other technologies for tailings treatment

The sediment produced by either CT or TT technology remains fluid and its containment in a deposit site. Further consolidation of the sediment and release of water to produce self-supportive dry tailings is required. As a result, more consolidation technologies have been developed for treating oil sands tailings. These technologies include natural drying, freeze thaw, centrifugation, and filtration.

Natural atmospheric drying has been practiced since ancient times. For drying fluid fine tailings or MFT using solar energy, the effective evaporation period is from April to November. The formation of surface crusts limits the evaporation [27]. Freeze-thaw is another natural process of drying but without need for externally provided energy, as long as the ground freezes during the winter. During the thaw of the frozen deposit, water is released from the reticulate ice formed during freezing while clay pads settle, developing a thaw strain and leading to a significant reduction in the deposit volume and hence release of water [28, 29]. Both methods are attractive as they utilize natural solar energy; however, they both require large area to allow for thin layers of MFT to dewater. For natural drying, it is important to note that water in the MFT cannot be recovered

because they are released into atmosphere directly during the evaporative process. Taking into account the temperature and daylight time difference for seasonal change, a combination of natural drying and freeze-thaw approach is usually used. The centrifuge works in accordance with the sedimentation principle, where the centrifugal acceleration causes more dense solids to separate. Industrial centrifuges can be classified as screen centrifuges which allow the liquid to pass through a screen, and decanter centrifuges in which there is no physical separation between the solid and liquid phases, rather than an accelerated settling due to centrifugal acceleration [30]. Thickener-centrifuge technology could be commercialized but its high capital and operation cost for operation and maintenance of oil sands fine tailings management is challenging.

An alternative to centrifugation for producing dry and stackable oil sands tailings is by filtration. In filtration, liquid in a suspension is forced to flow through interstitial voids of formed filter cake by pressure difference, vacuum, centrifugal force or a combination of them. During batch filtration, the filtrate volume flow rate depends on the driving force (e.g. pressure drop) across and resistance of the cake and filter medium.

1.4 Previous work prior to this study

Suitable flocculants for the alkaline oil sands tailings needs to be carefully chosen as the polymeric flocculants. There has been a need of robust polymer flocculants for effective oil sands tailings treatment with no harm to the bitumen recovery process.

There are some factors desirable for an effective polymer flocculant as outlined below:

1. Trivalent ions can compress electrical double layer most effectively [31];
2. A polymer flocculant with arms is able to “grab” more particles by flocculating small size particles due to an open structure [32, 33]; and
3. Inorganic–organic hybrid polymers with star-like structure are more shear resistant [34].

A novel inorganic-organic hybrid polymer, Al-PAM has all the advantages. Al-PAM has been found to be an effective polymer aid to settling and filtration of oil sands tailings. Details of Al-PAM structure and properties are discussed in chapter 3 and appendices.

Recently, Wang et al. [35] carried out a systematic study of flocculation and

filtration using tailings generated from laboratory hydrotransport extraction system (LHES). A commercial polymer Magnafloc1011 (Percol727) of high molecular weight (17.5 million Da) and an in-house synthesized, an inorganic-organic hybrid polymer, aluminum polyacrylamide (Al-PAM) of relatively low molecular weight (1 million Da). It was found that both polymers had outstanding ability to improve tailings settling performance. With the addition of Magnafloc1011 at its optimal dosage of 30 g/t solids, tailings settling was improved significantly, and reached consolidation stage within 30 seconds. For Al-PAM, a higher dosage of 50 g/t solids was needed to achieve a similar initial solids settling rate. The sediments formed by Magnafloc1011 were more compact than Al-PAM after 10 minutes of settling and consolidation, whereas the supernatant of the tailings treated by Al-PAM was much clearer than that by Magnafloc1011, both at their optimal dosages. The filtration tests of fresh oil sands extraction tailings with and without flocculant addition were conducted with a filter press at 15 kPa pressure, using filter paper of 2–5 μm pore sizes. The results showed remarkable filtration performance achieved by adding Al-PAM as a filtration aid. Not only the filtration rate was increased dramatically, but also more importantly, the moisture of the filter cake derived from flocculated tailings was less than 10 wt%. In contrast, the filtration performance of the fine tailings was not improved with the

application of optimal dosage of Magnafloc1011, and became even worse than filtration of fresh tailings without flocculant addition (blank) even though the flocculation was effective [35].

1.5 Objectives of this work

It has been found that Al-PAM is more effective than Magnafloc1011 in flocculation and filtration of fresh oil sands tailings. The objectives of this work are to further understand the mechanism of Al-PAM in flocculation and filtration of oil sands tailings, and consequently to research on developing an efficient way of recycling water from tailings waste produced from CHWE oil sands extraction. This project was carried out as follows:

1. A series of Al-PAMs with different molecular weight and aluminum content are synthesized and characterized.
2. Al-PAMs and Magnafloc1011 were used in flocculation and filtration of model fine tailings and laboratory extraction tailings. The residual bitumen content in the tailings feed was monitored and the final moisture content in the filter cake was measured. The performance of Al-PAM and Magnafloc1011 was correlated with their properties (molecular weight and aluminum content) and tailings properties (bitumen content and fines content).

3. Propose Al-PAM Assisted Filtration for oil sands tailings treatment.

Al-PAM and Magnafloc1011 were used in flocculation and filtration of model fine tailings and laboratory extraction tailings at a higher temperature (45°C) compared to room temperature (22°C). Filtration of sediments and filtration of whole tailings were compared as well.

1.6 Organization of thesis

The body of this thesis consists of 9 chapters. Chapter 1 provides basic background information of oil sands, bitumen extraction process and oil sands tailings issues. Chapter 2 presents an overview of the fundamentals of coagulation, flocculation and filtration including their mechanisms and application to oil sands treatment, and other literature reviews relevant to the present work. Chapter 3 describes the materials and experiments for synthesis of Al-PAMs, settling and filtration tests. Chapter 4 provides detail information on settling and filtration including data processing. Chapter 5 presents effects of polymer properties (Al-PAM molecular weight and aluminum content or charge density) on oil sands tailings treatment based on settling and filtration tests. Chapter 6 presents the effect of oil sands tailings characteristics (bitumen content and fines content) on tailings settling and filtration. Chapter 7 introduces the effect of temperature on

AI-PAM performance of tailings settling and filtration, and accordingly proposes an AI-PAM assisted flocculation-filtration dewatering method. Last chapter, chapter 8, is conclusions and future work of this study. Appendices present further investigation on structure of AI-PAM.

References

1. Masliyah, J. H., *Fundamentals of oil sands extraction*. in Course Pack. 2008: University of Alberta.
2. Chalaturnyk, R. J.; Scott, J. D.; Ozum, B., *Management of oil sands tailings*. Petroleum Science and Technology, 2002. **20**(9-10): p. 1025-1046.
3. Masliyah, J. H.; Gray, M. R., *Extracting and upgrading of oilsands bitumen*. in *Course Pack*. 2007: University of Alberta.
4. Clark, K. A.; Pasternack, D. S., *Hot water separation of bitumen from Alberta bituminous sand*. Industrial and Engineering Chemistry, 1932. **24**: p. 1410-1416.
5. FTFC (Fine Tailings Fundamentals Consortium), *Advances in oil sands tailings research*. 1995, Alberta Department of Energy. Oil Sands and Research Division.
6. Masliyah, J. H.; Zhou, Z. J.; Xu, Z. H.; Czarnecki, J.; Hamza, H.,

- Understanding water-based bitumen extraction from Athabasca oil sands*. Canadian Journal of Chemical Engineering, 2004. **82**(4): p. 628-654.
7. Masliyah, J. H.; Czarnecki, J.; Xu, Z. H., *Handbook on theory and practice of bitumen recovery from Athabasca oil sands*. Vol. Volume I: Theoretical Basis. 2011: Kingsley Knowledge Publishing.
 8. Alberta, G.O., *Fact sheet: Alberta's oil sands-the resource*. August 2010.
 9. Butler, R. M.; Mokrys, I. J., *Closed-loop extraction method for the recovery of heavy oils and bitumen underlain by aquifers: the vapex*. Journal of Canadian Petroleum Technology, 1998. **37**(4): p. 41-50.
 10. Xia, T. X.; Greaves, M.; Turta, A. T.; Ayasse, C., *THAI - A 'short-distance displacement' in situ combustion process for the recovery upgrading of heavy oil*. Chemical Engineering Research & Design, 2003. **81**(A3): p. 295-304.
 11. Beier, N.; Alostaz, M.; Segó, D., *Natural dewatering strategies for oil sands fine tailings*, in Tailings and Mine Waste 09 Conference. 2009: University of Alberta.
 12. *ERCB backgrounder on draft directive: Tailings performance criteria and requirements for oil sands mining schemes*. 2007.
 13. Beier, N.; Segó, D., *The oil sands tailings research facility*.

Geotechnical News, June, 2008.

14. *Oil sands tailings technology review*. 2010, OSRIN, BGC Engineering Inc.
15. Mazurek, K. A.; Chalaturnyk, R. J.; Rajaratnam, N.; Scott, J. D., *Transport of fine sand from a wellbore*. Journal of Canadian Petroleum Technology, 2002. **41**(4): p. 53-61.
16. Li, H. H., Long, J.; Xu, Z. H.; Masliyah, J. H., *Novel polymer aids for low-grade oil sand ore processing*. Canadian Journal of Chemical Engineering, 2008. **86**(2): p. 168-176.
17. Griffiths, M.; Taylor, A.; Woynillowicz, D., *Troubled waters, troubling trends, in technology and policy options to reduce water use in oil and oil sands development in Alberta*, R. Holmes, Editor. 2006, The Pembina Institute: Drayton Valley. p. 171.
18. Baillie, R. A.; Fear, J. V. D., *Method of reducing sludge accumulation from a tar sands hot water process*. 1975, Great Canadian Oil Sands Limited: Canada.
19. MacKinnon, M. D.; Matthews, J. G.; Shaw, W. H.; Cuddy, R. G., *Water quality issues associated with composite tailings (CT) technology for managing oil sands tailings*. International Journal of Mining, Reclamation and Environment, 2001. **15**(4): p. 235-256.
20. Matthews, J. G.; Shaw, W. H.; MacKinnon, M. D.; Cuddy, R. G.,

Development of composite tailings technology at Syncrude.

International Journal of Mining, Reclamation and Environment, 2002.

16(1): p. 24-39.

21. Mikula, R. J.; Munoz, V. A.; Kasperski, K.L.; Omotoso, O.E., *Commercial implementation of a dry landscape oil sands tailings reclamation option: consolidated tailings.* Natural Resources Canada, 1998.
22. Kasongo, T.; Zhou, Z.; Xu, Z. H.; Masliyah, J. H., *Effect of clays and calcium ions on bitumen extraction from Athabasca oil sands using flotation.* Canadian Journal of Chemical Engineering, 2000. **78**(4): p. 674-681.
23. Wallace, D.; Tipman, R.; Komishke, B.; Wallwork, V.; Perkins, E., *Fines/water interactions and consequences of the presence of degraded illite on oil sands extractability.* Canadian Journal of Chemical Engineering, 2004. **82**(4): p. 667-677.
24. Cymerman, G.; Kwong, T.; Lord, E.; Hamza, H.; Xu, Y., *Thickening and disposal of fine tails from oil sand processing.* in Polymers in Mineral Processing, Proceeding of the UBC-McGill Bi-Annual International Symposium on Fundamentals of 19 Mineral Processing 3rd. 1999. Quebec City.
25. Bushway, M. H.; Boardman, G. D.; McTernan, W. F., *Treatment of tar*

- sand process waters by means of two-stage, polymer-aided, air flotation*, in *Proceedings of the Industrial Waste Conference*. 1985.
26. Xu, Y.; Hamza, H.; Matthews, J., *Enlargement of fine particles in the oil sands industry - flocculation and thickening*. Particle Size Enlargement in Mineral Processing. in *Proceedings of the UBC-McGill Biennial International Symposium on Fundamentals of Mineral Processing*, 5th. 2004. Hamilton, ON, Canada.
27. Wells, R. R.; Langendoen, E.J.; Simon, A., *Modeling pre- and post-dam removal sediment dynamics: the Kalamazoo river, Michigan*. *Journal of the American Water Resources Association*, 2007. **43**(3): p. 773-785.
28. Dawson, R.; Segó, D.; Pollock, G., *Freeze-thaw dewatering of oil sands fine tails*. *Canadian Geotechnical Journal*, 1999. **36**(4): p. 587-598.
29. Hamza, A. A.; Taha, A. Z., *Performance of submersible Pv solar pumping systems under conditions in the Sudan*. *Renewable Energy*, 1995. **6**(5-6): p. 491-495.
30. Ng, C. W.; Wang, Y. H.; Zhang, L. M., *Physical modelling in geotechnics*. in *Proceedings of the Sixth International Conference on Physical Modelling in Geotechnics*. 2006.
31. Crittenden, J. C.; Trussell, R. R.; Hand, D. W.; Howe, K. J.;

- Tchobanoglous, G., *Water treatment - principles and design* 2nd ed. 2005, New Jersey: John Wiley & Sons. Chapter 9.
32. Chen, X.; Costeux, C.; Larson, R. G., *Characterization and prediction of long-chain branching in commercial polyethylenes by a combination of rheology and modeling methods*. *Journal of Rheology*, 2010. **54**(6): p. 1185-1205.
 33. Blanco, A.; Fuente, E.; Monte, M. C.; Corts, N.; Negro, C., *Polymeric branched flocculant effect on the flocculation process of pulp suspensions in the papermaking industry*. *Ind. Eng. Chem. Res.*, 2009. **48**(10): p. 4826-4836.
 34. Kim, O. K.; Little, R. C.; Patterso. R.; Ting, R. Y., *Polymer structures and turbulent shear stability of drag reducing solutions*. *Nature*, 1974. **250**(5465): p. 408-410.
 35. Wang, X. Y.; Feng, X. H.; Xu, Z. H.; Masliyah, J. H., *Polymer aids for settling and filtration of oil sands tailings*. *Canadian Journal of Chemical Engineering*, 2009. **88**(3): p. 403-410.

Chapter 2 Literature Review

Fine solids in oil sands tailings take long time to settle in the tailings ponds. To accelerate the settling of fine solids, flocculants and/or coagulants are usually used. These chemicals are able to induce aggregation of particles. With increase in particle size, settling is accelerated. Filtration is a quick and effective method to release water from suspensions. The application, definition and mechanisms of coagulation, flocculation and filtration as well as polymer properties and mixing conditions in the context of flocculation are introduced in the following sections.

2.1 Basics of particle aggregation

2.1.1 Electrical double layer

The charge on the surface of particles and charge in the solution form a system of charges called electrical double layer [1]. Interaction of charged species in an electrolyte solution is usually explained by the formation of electrical double layer. In such a system, the charged surface attracts oppositely charged ions, forming electrical double layer (stern plane and shear plane in Stern-model [2, 3] describing the profile of charge

distribution as shown in Figure 2.1) near the charged surface with whole system being electrically neutral [4]. Figure 2.1 shows schematically the distribution of ions in Stern model of electrical double layer system.

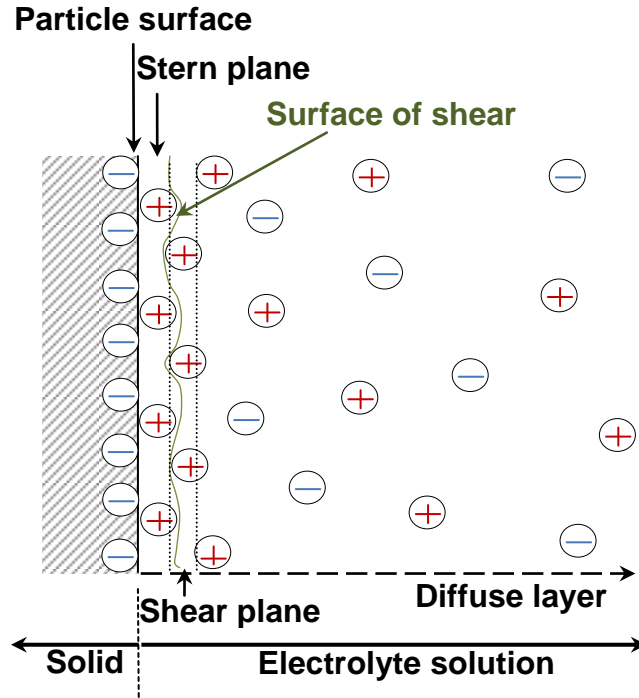


Figure 2.1 Distribution of ions in Stern-model of electrical double layer system [1].

2.1.2 DLVO theory

DLVO is the first successful theory describing colloid stability. It was named after scientists Derjaguin, Landau, Verwey and Overbreek in 1941 [1]. The basic assumption of DLVO theory is that the energy of a colloidal system E is treated as the sum of attractive van der Waals energy E_{vdw} and repulsive

double layer overlapping energy E_{DL} [1], presented in equation 2.1 and shown in Figure 2.2.

$$E = E_{vdw} + E_{DL} \quad (2.1)$$

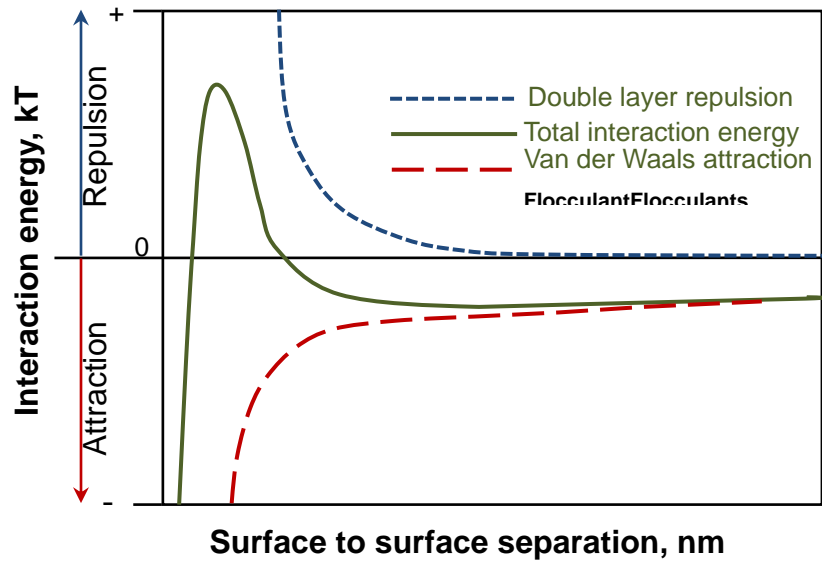


Figure 2.2 General illustration of interaction energy profile of particle surface in electrolyte solution (DLVO) [1].

2.1.3 Coagulation and flocculation

Coagulation process is defined as the addition of chemical coagulant for the purpose of destabilizing the suspended particles due to repulse forces (long range electrostatic, steric, electrosteric and/or short range hydration forces) [5]. Coagulation occurs when the surface charge of particles is

substantially reduced through the addition of inorganic multivalent cations known as coagulant, reducing particle charges and/or compressing electrical double layers to destroy the repulsive forces to an extent that the attractive van der Waals forces become predominant (see Figure 2.2) and are able to bring and hold particles together [1], forming microflocs upon collision driven by Brownian motion [6].

Coagulants are usually inorganic salts such as aluminum sulphate ($\text{Al}(\text{SO}_4)_3 \cdot 14\text{H}_2\text{O}$), potassium alum ($\text{KAl}(\text{SO}_4)_2 \cdot 12\text{H}_2\text{O}$), gypsum ($\text{CaSO}_4 \cdot 2\text{H}_2\text{O}$) [5], lime (80% Calcium hydroxide), sulfuric acid, fly ash and carbon dioxide, while flocculants are usually organic polyelectrolytes (e.g., Percol LT27A, Allied Colloids) [7].

According to DLVO theory, the critical coagulation concentration (CCC) is inversely proportional to the sixth power of the charges on the electrolyte ions [5]. Therefore, trivalent ions can compress electrical double layer more effectively than monovalent and divalent ions.

Aggregates formed by coagulation are normally more compact and smaller in size than those formed by flocculation. In contrast to coagulation, which relies on the reduction of repulsive forces between aggregating particles,

flocculation involves the addition of a polymer to bridge particles into large flocs, as shown in Figure 2.3 (b). In flocculation, it is not necessary to reduce the repulsive forces between aggregating particles, as the polymer bridge can extend beyond the range of electrical double layer repulsion.

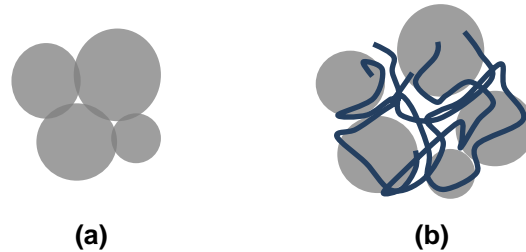
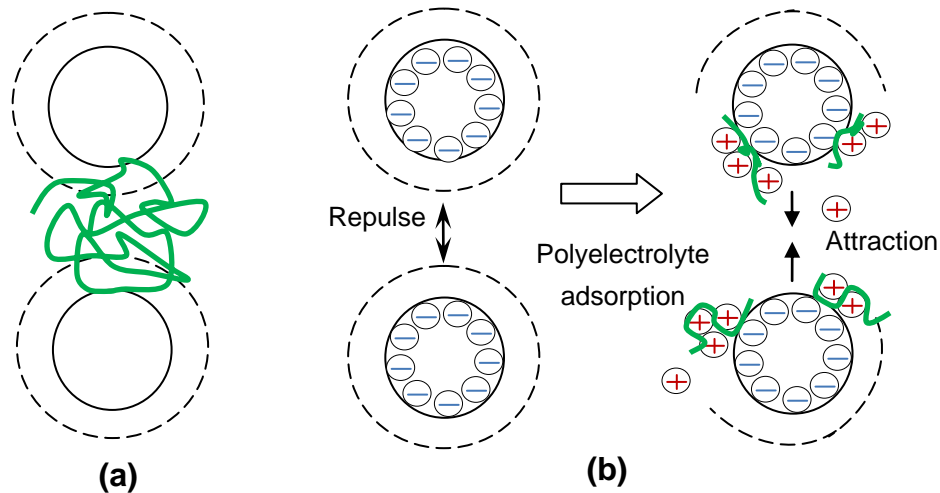


Figure 2.3 Schematic aggregates by (a) coagulation; and (b) flocculation [1].

The term flocculation is derived from the Latin, “flocculus,” literally a small tuft of wool, or a loosely fibrous structure. Those particles united into a random, three-dimensional structure are referred as “floc”, which is loose and porous. Flocculation process refers to the macroscopic aggregation of suspended particles into loosely packed flocs by addition of polymeric flocculant [5, 6]. The mechanisms of polymer flocculation mainly include bridging through polymer-particle surface complex formation [8], depletion flocculation or the combination of all of the afore-mentioned mechanisms [9, 10]. The main flocculation mechanisms of polymers can be schematically represented by Figure 2.4. For bridging mechanism, polymers with higher

molecular weight have stronger ability to bridge more particles, forming larger aggregates or flocs [11].



The dashed line represents the range of electric double layer.

Figure 2.4 Schematic flocculation mechanisms of particles: (a) bridging; and (b) charge neutralization [8, 11].

Under a certain range of pH, temperature, salinity and other appropriate conditions, some flocculants react with water to form insoluble hydroxides, linking together to form long chains or meshes, physically catching small particles and forming larger flocs [12].

2.2 Properties of polymer flocculants

Polymers are often used as flocculation aids to produce large and stable flocs [5]. The application of polymer flocculants depends on many factors.

Their properties such as charge and polymer structure are discussed in the following sections.

2.2.1 Charge of polymers

Most flocculants in use today are synthetic polymers based on repeating units of acrylamide and its derivatives. These polymers may contain either cationic or anionic charges and are available in a wide range of molecular weights and ionic charge density [13, 14]. For example, polyacrylamide (PAM) products are available in non-ionic, cationic or anionic forms. Non-ionic PAM has molecules with no charge. They are used in very rare instances and special circumstances only, and mostly in mining [15]. Anionic PAMs are negatively charged, and they are toxic [15, 16]. Due to a high affinity for solids and low concentration in the treated water, these polymers are universally used in industries including raw water clarification, thickening and dewatering of wastewater and sludge. Cationic PAMs are positively charged and are generally used in pre-settlement for many municipal wastewater treatment plants [15].

The adsorption of polymer chains on suspended particles at one or more sites is mainly by electrostatic interactions and hydrogen bonding [5]. For a

dispersion system with negatively charged particles, cationic polymer can be used more effectively because the electrostatic attraction increases the chance of polymer adsorption on particle surfaces [5].

2.2.2 Structure of polymers

Properties of polymer flocculants are also affected by their architecture [9]c. The simplest polymer structure is a linear chain, i.e., a single backbone with no branches. Figure 2.5 shows images of real linear PAM chains detected with an atomic force microscope on a solid surface in aqueous medium. The contour length of the polymer chain is about 204 nm and the chain thickness is about 0.4 nm [17].

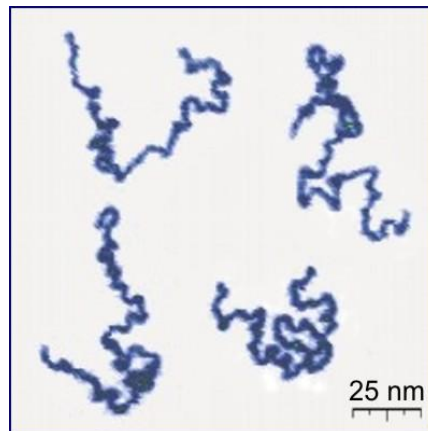


Figure 2.5 Image of PAM, a linear polymer with long chain [17].

A branched polymer molecule is composed of a main chain with one or more side chains or branches. The branched polymers of medium charge density are more capable to flocculate small size particles due to an open structure, mainly at the secondary aggregating stage [18, 19]. Special types of branched polymers include star-like polymers in which small core molecules have branches extending from the core [9]. Figure 2.6 shows the structure features of branched polymers.

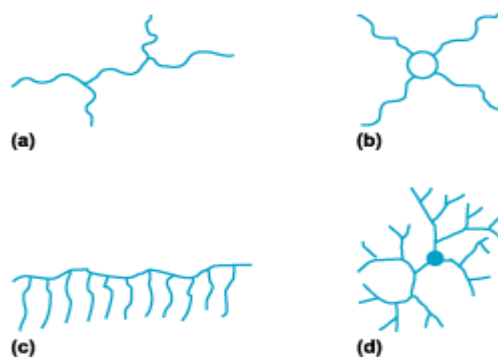


Figure 2.6 Examples of branched polymers: (a) branched polymer with arms of the composition similar to backbones or graft polymer with compositions of branches being different from backbones; (b) star polymer; (c) comb polymer; and (d) dendritic polymer.

Kim et al. [20] found that some star-like polymers are more shear resistant than other polymers. There are also various types of inorganic–organic hybrid polymers belonging to star-like polymers [21]. The bonds between

inorganic and organic phases consist of van-der-Waals interaction, hydrogen bonds, and covalent bonds [22].

2.3 Flocculation application in oil sands tailings treatment

The research by Yuan and Shaw [23] showed that the conventional processes based simply on a single flocculant/coagulant were ineffective for treating higher fines tailings in a thickener. They often produce an overflow containing 1–4 wt% solids, which is much higher than the target solids content of <0.5 wt%. The clarified water containing such high level of fines content would interfere with bitumen recovery, particularly when excess amount of divalent cations are present in the process water [24].

New processes including coagulation–flocculation–coagulation (CFC), flocculation–coagulation (FC) and flocculation–coagulation–flocculation (FCF) have been developed for the tailings treatment. The FCF process performed better than the others as it produced larger flocs, leading to fast initial settling rates. The choice of chemicals and their sequence of addition are important. The anionic flocculant of high molecular weight ($12\text{-}24 \times 10^6$ Da) was first added at a dosage of 250-300 g/t (based on slurry properties) to bridge comparatively large particles together, forming large flocs with

fines being left dispersed. Then cationic coagulant of low molecular weight (5000-50000 Da) with high charge density (90-100%) was added at a dosage of 250 g/t to compress electrical double layer of dispersed fine particles, forming small aggregates. Finally a small amount of flocculant with high molecular weight at a dosage of 60 g/t was added to flocculate large flocs formed in the first stage with small aggregates formed in the second stage by coagulation. With these chemicals and their sequences of addition, almost all submicron clay minerals were aggregated together and settled as a whole, resulting in an overflow of <0.13 wt% solids and an underflow stream of >20 wt% solids. The only drawback of the above process was that the sediments could not be self-contained, i.e., low solids content [25].

2.3.1 Combination of flocculation and filtration in oil sands tailings treatment

While remarkable effort has been devoted to developing solutions for oil sands tailings treatment, it has to be recognized that there is no single mature commercial solution to resolving fluid fine tailings challenges. Filtration appears to be a promising solution, at least at a laboratory scale, as it not only produces dry tailings for rapid land reclamation, but also offers solutions for recycled water chemistry issues in bitumen recovery

due to the addition of flocculants with low concentration [26]. Fast water drainage is a critical step for the filtration process. It has been found that after the fines are flocculated with the coarse particles to form uniformed flocs, the filterability is improved by several orders of magnitude. The results demonstrate that filtration of the flocculated coarse tailings to produce “dry” stackable tailings can be a viable solution to tailings problem [27].

The dewatering method with combination of flocculation and filtration has been used in the kaolin suspensions treatment. Applications of anionic polyacrylamide as a flocculant used to dewatering kaolin suspension have been studied [28].

References

1. Masliyah, J. H.; Czarnecki, J.; Xu, Z. H., *Handbook on theory and practice of bitumen recovery from Athabasca oil sands*. Vol. Volume I: Theoretical Basis. 2011: Kingsley Knowledge Publishing.
2. Henderson, D., *Recent progress in the theory of the electric double-layer*. Progress in Surface Science, 1983. **13**(3): p. 197-224.
3. Masliyah, J. H.; Bhattacharjee, S., *Electrokinetic and colloid*

- transport phenomena*. Wiley-Interscience, 2006. Chapter 1, 5, 11.
4. King, R. P., *Principles of flotation*. Chapter 2. 1982: Johannesburg : South African Institute of Mining and Metallurgy.
 5. Crittenden, J. C.; Trussell, R. R.; Hand, D. W.; Howe, K. J.; Tchobanoglous, G., *Water Treatment - Principles and Design* 2nd ed. 2005, New Jersey: John Wiley & Sons. Chapter 9.
 6. Hunter, R. J., *Foundations of colloid science*. 2nd ed. 2001, New York: Oxford University Press. Chapter 1, 7, 8 and 12.
 7. Wang, X. Y.; Feng, X. H.; Xu, Z. H.; Masliyah, J. H., *Polymer aids for settling and filtration of oil sands tailings*. Canadian Journal of Chemical Engineering, 2010. **88**(3): p. 403-410.
 8. Adachi, Y.; Kobayashi, A.; Kobayashi, M., *Structure of colloidal flocs in relation to the dynamic properties of unstable suspension*. International Journal of Colloid Science, 2011.
 9. Mporu, P.; Addai-Mensah, J.; Ralston, J., *Flocculation and dewatering behaviour of smectite dispersions: effect of polymer structure type*. Minerals Engineering, 2004. **17**(3): p. 411-423.
 10. Sworska, A.; Laskowski, J. S.; Cymerman, G., *Flocculation of the Syncrude fine tailings Part I. Effect of pH, polymer dosage and Mg²⁺ and Ca²⁺ cations*. International Journal of Mineral Processing, 2000. **60**(2): p. 143-152.

11. Nasser, M. S.; James, A. E., *The effect of polyacrylamide charge density and molecular weight on the flocculation and sedimentation behaviour of kaolinite suspensions*. Separation and Purification Technology, 2006. **52**(2): p. 241-252.
12. Chesters, S. P.; Darton, E. G.; Silvia, G., *The safe use of cationic flocculants with reverse osmosis membranes*. Desalination and Water Treatment, 2009. **6**(1-3): p. 144-151.
13. Forbes, D. L., *Theory of Flocculation*, WET USA Inc, 2000.
14. *Studies in interface science*. Vol 20. 2005. p. 354-414.
15. Sojka, R. E.; Bjorneberg, D. L.; Entry, J. A.; Lentz, R. D.; Orts, W. J., *Polyacrylamide in agriculture and environmental land management*, in Advances in Agronomy, Vol 92. 2007. p. 75.
16. Weston, D. P.; Lentz, R. D.; Cahn, M. D.; Ogle, R. S.; Rothert, A. K.; Lydy, M. J., *Toxicity of anionic polyacrylamide formulations when used for erosion control in agriculture*. Journal of Environmental Quality, 2009. **38**(1): p. 238-247.
17. Roiter, Y.; Minko, S., *AFM single molecule experiments at the solid-liquid interface: In situ conformation of adsorbed flexible polyelectrolyte chains*. Journal of the American Chemical Society, 2005. **127**(45): p. 15688-15689.
18. Chen, X. C., C.; Larson, R. G., *Characterization and prediction of*

- long-chain branching in commercial polyethylenes by a combination of rheology and modeling methods.* Journal of Rheology, 2010. **54**(6): p. 1185-1205.
19. Blanco, A.; Fuente, E.; Monte, M. C. ; Corts, N.; Negro, C., *Polymeric branched flocculant effect on the flocculation process of pulp suspensions in the papermaking industry.* Ind. Eng. Chem. Res., 2009. **48**(10): p. 4826-4836.
 20. Kim, O. K.; Little, R. C.; Patterso, R. I.; Ting, R. Y., *Polymer structures and turbulent shear stability of drag reducing solutions.* Nature, 1974. **250**(5465): p. 408-410.
 21. Yang, W. Y.; Qian, J. W.; Shen, Z. Q., *A novel flocculant of Al(OH)(3)-polyacrylamide ionic hybrid.* Journal of Colloid and Interface Science, 2004. **273**(2): p. 400-405.
 22. Hass, K.; Rose, K., *Hybrid inorganic organic polymers with nanoscale building blocks precursors processing properties and applications.* Rev. Adv. Mater. Sci.5 2003: p. 47-52.
 23. Yuan, X. S.; Shaw, W., *Novel processes for treatment of syncrude fine transition and marine ore tailings.* Canadian Metallurgical Quarterly, 2007. **46**(3): p. 265-272.
 24. Wik, S.; Sparks, B. D.; Ng, S.; Tu, Y.; Li, Z.; Chung, K. H.; Kotlyar, L. S., *Effect of process water chemistry and particulate mineralogy on*

- model oilsands separation using a warm slurry extraction process simulation*. Fuel, 2008. **87**(7): p. 1394-1412.
25. Yuan, X. S.; Shaw, W., *Novel processes for treatment of Syncrude fine transition and marine ore tailings*. Canadian Metallurgical Quarterly, 2007. **46**(3): p. 265-272.
26. Li, H. H., Long, J.; Xu, Z. H.; Masliyah, J. H., *Novel polymer aids for low-grade oil sand ore processing*. Canadian Journal of Chemical Engineering, 2008. **86**(2): p. 168-176.
27. Xu, Y. M.; Dabros, T.; Kan, J. M., *Filterability of oil sands tailings*. Process Safety and Environmental Protection, 2008. **86**(B4): p. 268-276.
28. Besra, L.; Sengupta, D. K.; Roy, S. K.; Ay, P., *Influence of polymer adsorption and conformation on flocculation and dewatering of kaolin suspension*. Separation and Purification Technology, 2004. **37**(3): p. 231-246.

Chapter 3 Materials and Experiments

3.1 Materials

3.1.1 Polymers

The polymers used in this study are listed in Table 3-1 and are classified in two categories:

- a. Magnafloc1011 (MF1011), a partially hydrolyzed polyacrylamide with a high molecular weight of about 17.5 million Daltons and of a medium charge density of around 27 % [1]. Its commercial name is previously known as Percol 727, which is produced by Ciba Specialty Chemicals. This polymer is used as flocculants in settling and filtration tests.

- b. In-house synthesized organic-inorganic hybrid polymer, aluminum polyacrylamide (Al-PAM). Al-PAM is $\text{Al}(\text{OH})_3$ -polyacrylamide, with ionic bond between $\text{Al}(\text{OH})_3$ colloids and polyacrylamide chains [2]. They are of star-like structure. Al-PAMs with low, medium, and high molecular weight were synthesized to contain both higher and lower Al content. In Table 3-1, numbers of 4, 6 and 8 represent low, medium and high

molecular weight, respectively. Letter R refers to a regular or relatively lower Al content and letter H refers to a higher Al content. For example, AIPAM6R is the Al-PAM with medium molecular weight and low Al content. Molecular weight of Al-PAM can be adjusted by changing the concentration of acrylamide and initiator [3].

Table 3-1 Physical properties of polymer flocculants used in this study

Polymer	$[\eta]^*$ (g/mL) ⁻¹	MW 10 ⁶ Da	Al content wt%	Zeta potential mV
MF1011	13968	17.5	0	anionic
AIPAM4R	437.0	1.5	0.10%	+0.18 ± 0.05
AIPAM6R	675.2	2.0	0.10%	+0.20 ± 0.05
AIPAM6H	650.0	2.0	0.24%	+0.16 ± 0.05
AIPAM8R	834.6	2.5	0.11%	+0.17 ± 0.05

* Intrinsic viscosity

** Zeta potential of polymer solutions

In this study, Huggins equation [4] given below was used to calculate the intrinsic viscosity of polymers.

$$\eta_{sp} / c = [\eta] + k_h [\eta]^2 c \quad (3.1)$$

Where η_{sp} is specific viscosity given by $\eta_{sp} = \frac{\eta - \eta_0}{\eta_0}$, η_0 is the viscosity of the pure solvent and η is the viscosity of solution. Symbol c in equation 3.1

is the concentration of polymer in grams per litre of solution (g/L). k_h is the Huggins coefficient, and $[\eta]$ stands for intrinsic viscosity, which can be experimentally determined from the y-intercept by plotting η_{sp}/c against c [5, 6]. The intrinsic viscosity of Al-PAM in water was measured by Ubbelohde viscometer ($\Phi 75$, CANNON® Instrument Company, PA, USA) at 25 ± 0.5 °C. All the Al-PAM solutions were adjusted to pH 5.6-6.2 using hydrogen chloride and the pH was determined by an Accumet Basic pH meter (Fisher Scientific). The Al content of Al-PAM polymers was analyzed using Atomic Absorption (AA880, Varian, USA). In these analyses, the analyzer gave the concentration of elemental aluminum (Al). The calculated Al content in Table 3-2 was given by weight percentage of Al added in the process of making colloid to the total solution (mixture of colloid solution and acrylamide). According to the chemical formula (see 3.1.2.2), for example, there is 0.384 g Al in each 25.5 g colloid solution, after adding 4.5 g monomer acrylamide, the total solution becomes 30 g. So the calculated Al content is $0.384/30 * 100\% = 1.28\%$. Al content could be expressed by weight ratio of $\text{Al}(\text{OH})_3$ in polymer Al-PAM. However, since the inorganic core of the Al colloid is a mixture of Al^{3+} , $\text{Al}(\text{OH})^{2+}$, $\text{Al}(\text{OH})_2^+$ and $\text{Al}(\text{OH})_3$, it is more accurate to represent Al content ratio by elemental Al than by $\text{Al}(\text{OH})_3$.

3.1.2 Al-PAM preparation and measurement

3.1.2.1 Materials and instrument

All the chemicals including acrylamide (monomer), aluminum chloride anhydrous (>99%), ammonium carbonate, ammonium persulfate (98%), sodium hydrogen sulfite (95%), acetone (>99.5%) by weight and nitrogen (gas) which was used to keep air away from reaction, were from Fisher Scientific. Milli-Q water was used for solution preparation.

3.1.2.2 Colloid preparation

a. Principle of colloid preparation

The preparation of $\text{Al}(\text{OH})_3$ colloid is shown by the following reaction. The production of different aluminum ion species depends on the pH of the solution as shown in Table 3-2 [7].



Table 3-2 Relationship between pH and aluminum ion species

pH range	Aluminum ion species
pH < 5	Al^{3+}
$5 < \text{pH} < 6.2$	Al^{3+} , $\text{Al}(\text{OH})^{2+}$, and colloid $\text{Al}(\text{OH})_3$
pH > 6.2	$\text{Al}(\text{OH})_3$, $\text{Al}(\text{OH})_4^-$



Figure 3.1 Set-up for colloid preparation.

b. Procedure

A given amount (0.33 g) of AlCl_3 was dissolved in water in a 250-mL beaker to make 25 g of 0.1 M AlCl_3 solution. In a separate 250-mL beaker, 0.48 g $(\text{NH}_4)_2\text{CO}_3$ was dissolved in water to make 50 g of 0.1 M $(\text{NH}_4)_2\text{CO}_3$ solution. The prepared $(\text{NH}_4)_2\text{CO}_3$ solution was added to AlCl_3 solution at a rate of 0.5-0.6 g/min by a mini pump (Master FLEX C/L) through a plastic tube (TYGON tubing, R-3603). The two solutions were mixed by a

mechanical stirrer (IKA RW20) at 500 rpm. The addition rate of $(\text{NH}_4)_2\text{CO}_3$ solution was monitored by an electronic balance. A home-made baffle was installed in the beaker containing AlCl_3 solutions to ensure a satisfactory mixing. The pH of the mixture was monitored during the synthesis. Addition of $(\text{NH}_4)_2\text{CO}_3$ solution was stopped when the mole ratio of $(\text{NH}_4)_2\text{CO}_3$ to AlCl_3 in the mixture reached 1.41-1.43, corresponding to 36-37 g of $(\text{NH}_4)_2\text{CO}_3$ solution added to 25 g of AlCl_3 solution. A gentle stir at about 300 rpm of the mixture continued for 30 minutes to complete the reaction.

The particle size of the colloid in suspension was measured using Zeta PALS immediately after completion of reaction and after overnight storage, respectively. The average size of the above prepared colloids was 30-50 nm, and pH was 5.0-5.6. The particle size after overnight storage increased by about $25 \pm 5\%$ in diameter, but it remained constant for a month. Based on thermodynamic equilibrium constant at 25 °C and ionic strength of 0.16, Martin et al. [8, 9] reported the distribution of soluble mononuclear Al species in aqueous solutions at various pH values, Al^{3+} is prevailing species below pH 5.0. In the pH range between 5.0 and 6.2, there is a mixture of Al^{3+} , $\text{Al}(\text{OH})^{2+}$, $\text{Al}(\text{OH})_2^+$ and colloidal $\text{Al}(\text{OH})_3$ species. When pH is higher than 6.2, the dominant species is $\text{Al}(\text{OH})_4^-$.

An increase in the pH of an acidic Al solution resulted in an increase in Al hydrolysis, leading to polymerization of aluminum hydrolysis species [8]. Thus the formation of Al colloid is sensitive to pH change. The characteristics of the colloidal particles, such as ratio of Al to Al-PAM, pH, particle size (nm), and zeta potential (mV) immediately after preparation and storage overnight, formed at varying $(\text{NH}_4)_2\text{CO}_3$ to AlCl_3 molar ratio and pH are shown in Table 3-3. The particle size increased after overnight storage for all the cases although to different degrees. For this reason, fresh colloid suspensions were used in Al-PAM synthesis.

Table 3-3 Colloid characteristics of Al-PAMs freshly prepared and after one night storage

Ratio*	pH	size(nm)	ζ (mV)	time
1.40:1	4.99	5	0.016	immediate
	4.96	20	39.02	1 night
1.41:1	4.61	10	19.43	immediate
	4.55	23	4.64	1 night
1.42:1	5.40	20	37.02	immediate
	5.13	28	39.39	1night
1.43:1	5.68	69	38.63	immediate
	6.02	1000	43.10	1night
1.44:1	5.58	198	14.98	immediate
	6.15	1660	46.55	1night
1.45:1	6.19	1000	44.58	immediate
	6.40	50000	37.94	1night

Note: *mole ratio of $(\text{NH}_4)_2\text{CO}_3$ to AlCl_3

3.1.2.3 Preparation of Al-PAM hybrid

a. Principle of Al-PAM synthesis

The following mechanism (Figure 3.2) was proposed for the synthesis of Al-PAM [2].

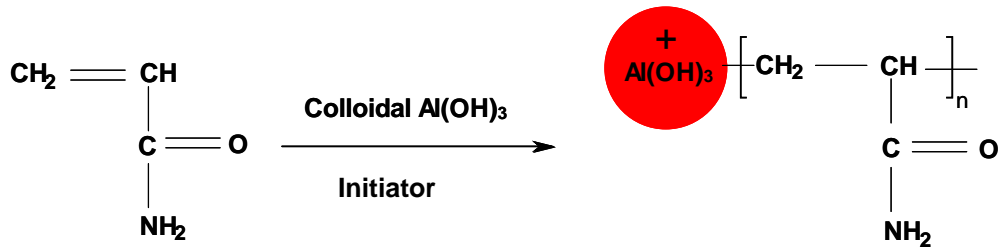
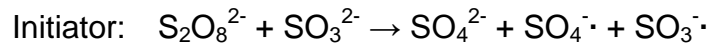


Figure 3.2 Schematics of Al-PAM synthesis.



It takes three main steps to prepare the Al-PAM, namely, aluminum hydroxide colloid preparation, synthesis of Al-PAM hybrid, and purification and drying of Al-PAM. Since the monomer acrylamide is initiated on the surface of the positively charged $\text{Al}(\text{OH})_3$ colloid particles, Al-PAM polymer has a star-like structure [2] as shown in Figure 3.3.

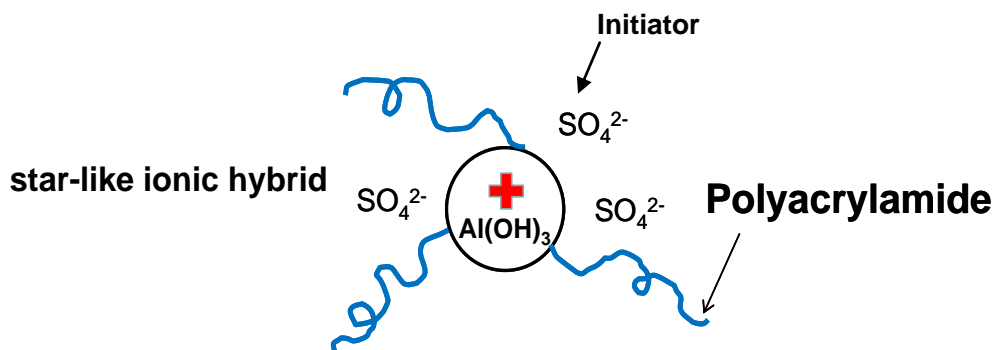


Figure 3.3 Schematics of Al-PAM structure.

b. Procedure

4.5 g of acrylamide were added to 25.5 g of fresh colloidal suspension (in a 100-mL flask) under magnetic stirring (Fisher brand stir bar, 1" l × 5/16" d) at 250 rpm. Nitrogen was introduced to the mixture from the beginning to the end of reaction to avoid any oxidation. The whole process was maintained at a constant temperature of 40 °C by an oil bath. Flask was protected from exposure to light. After 0.5 h, initiators (1 mL of 2 g/L $(\text{NH}_4)_2\text{S}_2\text{O}_8$ and 1 mL of 1 g/L NaHSO_3) were added within 30 minutes through a 10-mL glass funnel. The reaction was kept for 4 to 8 h until the formation of a transparent gel.

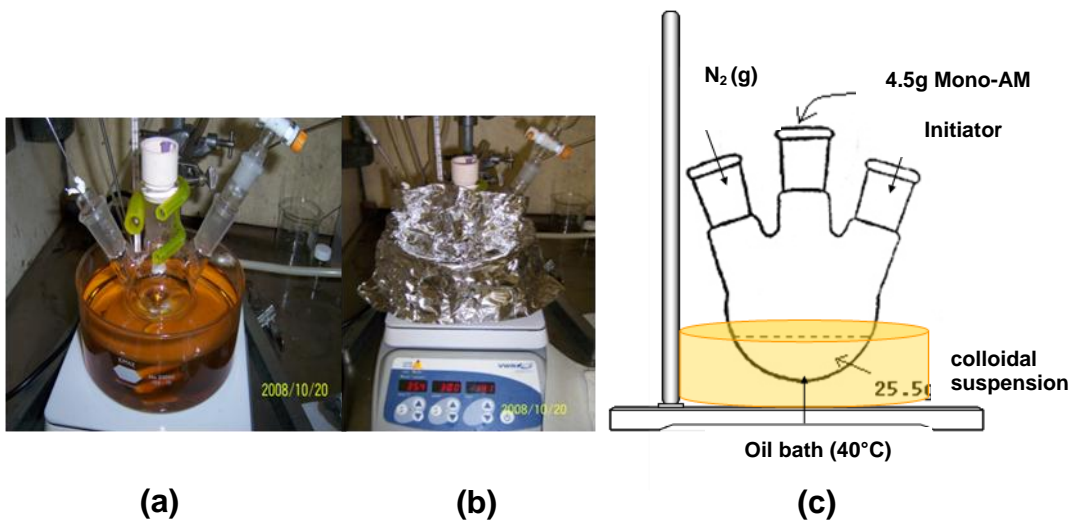


Figure 3.4 Setup for synthesis of Al-PAM (a) before put on protection from exposure to light; (b) with protection from exposure to light; and (c) schematics of Al-PAM synthesis setup.

Molecular weight of Al-PAM was controlled by changing the concentration of acrylamide and initiators [3]. For example, Al-PAM4R was synthesized following the above procedure at a given initiator concentration, whereas AIPAM8R was synthesized using 1/8 of this initiator concentration. Al content in polymer, on the other hand, is related to mole ratio of Al to acrylamide.

3.1.2.4 Purification and viscosity measurement

To remove un-reacted monomer and initiators, the polymer gel product was purified. For purification, the gel was first diluted with distilled water and shaken in a mechanical shaker for 2 to 3 days. The polymer solution was

then added drop-wise to acetone (the volume ratio of acetone to polymer was about 5) during which polymer precipitated out. Finally, the purified polymer was transferred to a Teflon dish and the dish was put in a vacuum oven for drying under vacuum overnight at 60°C.

To measure intrinsic viscosity of the polymer, 1.2-1.5 g/L polymer solutions were prepared. The viscosity measurements were carried out with an Ubbelohde viscometer (CANNON 75-J953). The intrinsic viscosity of the polymer was calculated using Huggins equation shown in 3.1.1. The highest intrinsic viscosity of the polymer is 834.6 L/g.

Table 3-4 Aluminum content of Al-PAMs

Polymer	Al Content, wt%	
	Calculated	Measured
AIPAM4R	1.28	0.10
AIPAM6R	1.28	0.10
AIPAM8R	1.28	0.11
AIPAM6H	5.10	0.24

The results listed in Table 3-4 are for polymers after purification. The measured Al content is much less than the calculated Al content indicating that only a part of the added Al participated in the reaction. In this study,

Al content is referred to the measured Al content after purification process given in section 3.1.2.4.

3.1.3 Model fine tailings

Model fine tailings were used to help understand flocculation characteristics of the polymers and the effect of fines. Model fine tailings slurry was prepared using kaolinite (K2-500, Fisher Scientific). The particle size distribution of the kaolinite was determined using Mastersizer Hydro2000SM, (Malven, MA, USA).

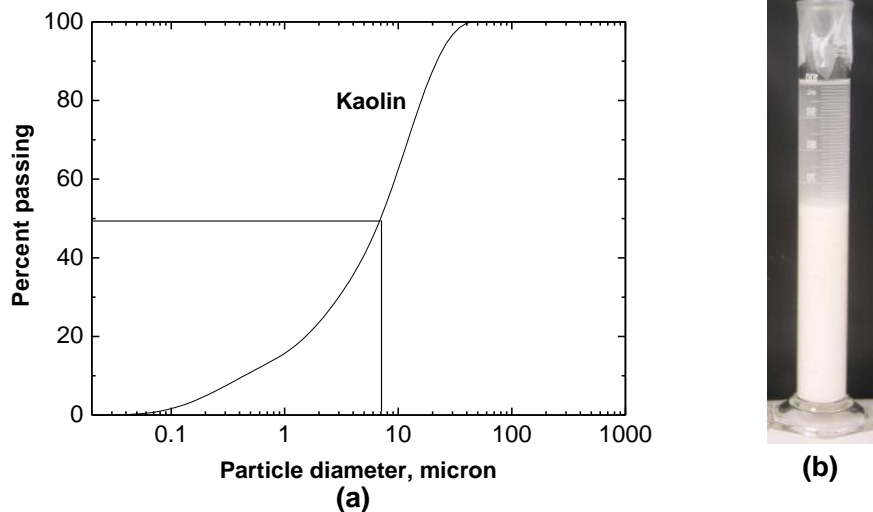


Figure 3.5 (a) Particle size distribution of kaolinite in model fine tailings; and (b) photograph of model fine tailings in the process of settling.

As shown in Figure 3.5, D_{50} as an average or mean particle size of 50%

volume or weight fraction of kaolinite was 7.0 μm . The solid content of model fine tailings was made to 5 wt%. Kaolinite was mixed in 95 wt% Aurora process water (Aurora 2008) at pH 8.4. The composition of Aurora process water is given in Table 3-5.

Table 3-5 Ion concentration of Aurora process water (mg/L)

K^+	Na^+	Mg^{2+}	Ca^{2+}	Cl^-	NO_3^-	SO_4^{2-}	HCO_3^-	pH
20.2	612.1	16.2	22.3	405.0	5.70	113.5	741.9	7.8

3.1.4 Laboratory extraction tailings

Two types of tailings were generated from laboratory extraction tests, one from good processing ore SYN704 with medium fines content, (fines are defined as mineral solids smaller than 44 microns), and the other one from poor processing ore with high fines content-POSYN. Aurora plant process water (2008) was used for bitumen extraction. Similar flotation procedures as described by Wang (2009) were used for this study. The composition of the tailings produced from laboratory extraction tests was determined using the standard industrial procedures. The particle size distribution of the solids in the tailings was analyzed using Mastersizer Hydro2000SM (Malven, MA, USA). Bitumen content in the tailings was derived by

controlling bitumen recovery during extraction at different temperatures and using different flotation time as shown in Table 3-6 and Table 3-7.

Table 3-6 Composition of laboratory extraction tailings (wt%)

Tailings type	Bitumen	Solids	Fines in solids
SYN704HB	3.4	11.0	26
SYN704LB	0.8	11.2	26
POYSYN-HB	3.8	22	26
POYSYN-LB	1.9	23	26

Tailings SYN704HB and SYN704LB were both extracted from SYN704 ore containing 82% solids (with 25.5% fines) and 9.6 % bitumen by weight. Tailings POSYN-HB and PONSYN-LB were both extracted from POSYN ore containing 85.9% solids (with 37.2% fines) and 5.5% bitumen by weight.

Table 3-7 Experimental conditions of laboratory extraction tests

(pH=8.4)

Tailings type	Extraction method	Temperature, °C	Air, ml/min	Flotation time, min	Agitation speed, rpm	Recovery, %
SYN704HB	LHES*	45	500	30	1160	62.2±0.5
SYN704LB	Denver Cell	80	120	60	1500	91.7±0.5
POYSYN-HB	Denver Cell	35	80	5	1500	49.5±0.5
POYSYN-LB		35	80	25	1500	65.5±0.5

* Laboratory hydrotransport extraction system

Laboratory extraction tailings (e.g. SYN704LB, POSYN-LB) with lower bitumen content were produced by additional removal of bitumen using longer flotation time and/or higher extraction temperature.

3.2 Procedures for settling and filtration experiment

3.2.1 Isokinetic sampling

Since tailings are stocked in a 20-L container, it is important to make sure that the tailings slurry is homogeneous and the samples taken have the same composition. Figure 3.6 shows the impeller and mechanical stirrer used to mix the tailings generated from laboratory extraction. The stirring rate was controlled so that fewer solids settled on the bottom, and the time

is set usually from 1 to 2 hours, depending on the solids content and density of the tailings. A heavy duty pump (Figure 3.7 (a)) was used to pump the well-mixed tailings out of the 20-L container into 4-L bottles, while maintaining continuous mixing.

The sub-samples were prepared using a disposable pipette (Figure 3.7 (b)) to transfer 95 g of tailings from the 4-L bottles into the beakers of 250 mL under mechanical mixing at 650 rpm. After sampling, all the beakers were sealed with paraffin film.

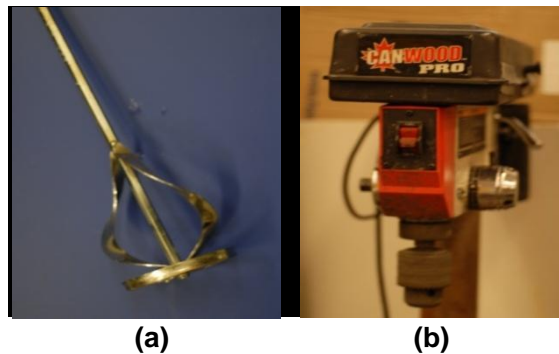


Figure 3.6 (a) Impeller fit for a 20-L pail; and b) mechanical stirrer suitable for a 20-L pail.

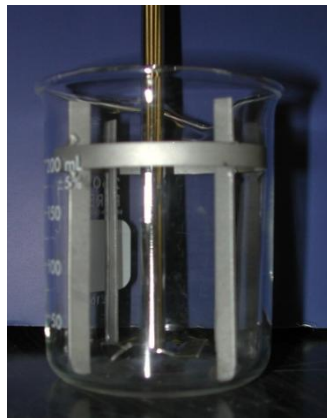


(a)



(b)

Figure 3.7 (a) Masterflex® heavy duty pump; and (b) disposable plastic pipette of 23 mL in volume.



(a)



(b)

Figure 3.8 (a) Home-made baffle and customized impeller for 250-mL beakers; and (b) mechanical stirrer used for mixing tailings in 250-mL beakers.

3.2.2 Settling tests

Samples were stirred at 500 rpm for 2 minutes using the setup as shown in Figures 3.8 (a) and 3.8 (b). The polymers were then added drop-wise (10

seconds altogether) at a rate of 0.1 second using an auto-pipette while the sample was under agitation at 350 rpm. Since flocculation by polymers was sensitive to mixing conditions such as mixing rate (detail see Chapter 4), the mixing was stopped right away when the addition of polymer solutions was completed. The flocculated tailings were transferred into a 100-mL graduated cylinder (use spatula if necessary to grab the residue out). After inverting the cylinder for several times, it was placed on a bench. The suspension mud-line was recorded as volume graduation with time during the settling period (Figure 3.9). Two methods could be applied: either record the time in second for every 5-mL volume of the mud-line going down, or record the volume of the mud-line for every 5 seconds of settling.

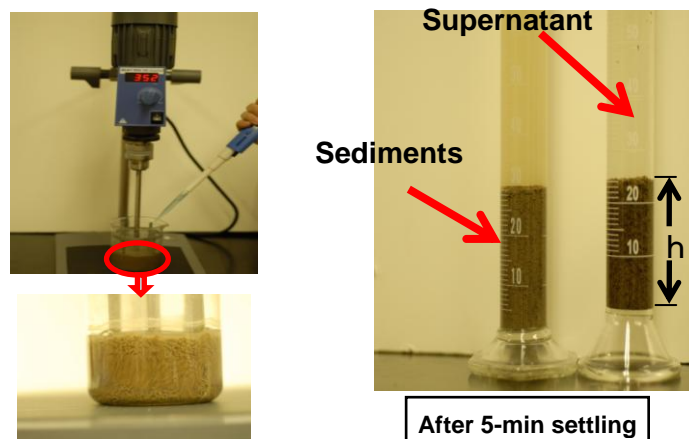


Figure 3.9 Setup for settling experiment

3.2.3 Filtration tests

Figure 3.10 shows the set-up for filtration experiment.

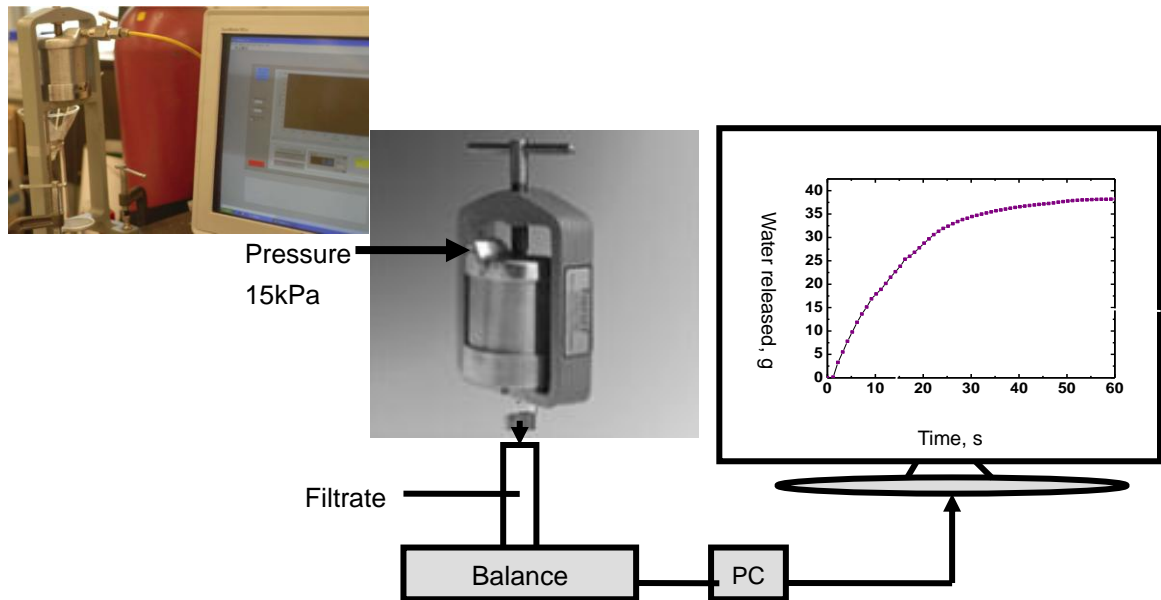


Figure 3.10 Setup for the filtration experiment

All the filtration experiments were carried out using a laboratory filter press which was described elsewhere (see Figure 3.10) [10]. Briefly, it consists of a stainless steel cylinder of 9 cm inner-diameter and 11.5 cm height. The base of the filter press is a perforated stainless mesh with a rubber gasket to fix the filter paper between them. A special hardened filter paper of 2-5 μm pore sizes (N87000, Fann Instrument Company, USA) was used as the filter medium throughout the filtration tests. The flocculated tailings were poured into the filter press for filtration tests under a selected pressure

(15kPa) applied by a nitrogen gas cylinder. The filtrate was collected in a customized container placed on an electronic balance. The electronic balance was connected to a computer with LABVIEW software. The weight of released filtrate registered by the electronic balance was recorded continuously by a computer data acquisition system. The data recorded every half a second were used to make filtration curves. A filtration time of 3 minutes was chosen since there was no more water released as indicated by little change in the mass of filtrate collected. The filtration was considered to be completed over 3 minutes. The filter cake was then carefully removed, weighed and dried in a vacuum oven at 50 °C until it attained a constant weight (usually overnight). Moisture content of the cake (in weight percent) was determined from the difference in weight before and after drying of the filter cake. The Al content in the filtrate was analyzed using AA (AA880, Varian, USA).

References

1. Li, H. H.; Long, J.; Xu, Z. H.; Masliyah, J. H., *Synergetic role of polymer flocculant in low-temperature bitumen extraction and tailings treatment*. Energy & Fuels, 2005. **19**(3): p. 936-943.
2. Yang, W. Y.; Qian, J. W.; Shen, Z. Q., *A Novel flocculant of*

- Al(OH)₃-polyacrylamide ionic hybrid*. Journal of Colloid and Interface Science, 2004. **273**(2): p. 400-405.
3. Flory, P. L., *Principles of polymer chemistry*. 1953, New York: Cornell University Press.
 4. Staszewska, D.; Kovar, J.; Bohdanecky, M., *A note on the viscosity of dilute-solutions of polymer mixtures*. Colloid and Polymer Science, 1980. **258**(5): p. 600-604.
 5. Li, H. H., Long, J.; Xu, Z. H.; Masliyah, J. H., *Novel polymer aids for low-grade oil sand ore processing*. Canadian Journal of Chemical Engineering, 2008. **86**(2): p. 168-176.
 6. Li, H. J.; Long, J.; Xu, Z. H.; Masliyah, J. H., *Flocculation of kaolinite clay suspensions using a temperature-sensitive polymer*. American Institute of Chemical Engineering Journal, 2007. **53**(2): p. 479-488.
 7. Cornelis, R., *Handbook of Elemental Speciation II Species in the Environment, Food, Medicine and Occupational Health* 2003: John Wiley & Sons.
 8. Martin, R. B., *Citrate binding of Al³⁺ and Fe³⁺*. Journal of Inorganic Biochemistry, 1986. **28**(2-3): p. 181-187.
 9. Martin, R. B., *The chemistry of aluminum as related to biology and medicine*. Clinical Chemistry, 1986. **32**(10): p. 1797-1806.
 10. Wang, X. Y.; Feng, X. H.; Xu, Z. H.; Masliyah, J. H., *Polymer aids for*

settling and filtration of oil Sands tailings. Canadian Journal of Chemical Engineering, 2010. **88**(3): p. 403-410.

11. Dean, E. W.; Stark, D. D., *A convenient method for the determination of water in petroleum and other organic emulsions.* Journal of Industrial and Engineering Chemistry-Us, 1920. **12**: p. 486-490.

Chapter 4 Settling and Filtration

In this study, most results were from settling and filtration tests. Therefore, more details including data processing, basic principles and example discussion for settling and filtration are stated in this chapter.

4.1 Settling

In the settling tests, the following parameters are used to evaluate the performance of polymer flocculants on settling of tailings. They are:

1. Initial settling rate (ISR). ISR is evaluated by calculating the initial slope of the settling curve. The unit of ISR is meter per hour (m/h).
2. Turbidity of supernatant. After settling, the liquid on the top of sediment is supernatant. Turbidity is used to measure the clarity of supernatant. The unit of turbidity is NTU.
3. Sediment height. After settling, the sediment volume was recorded as milliliter (mL) (see appendices).
4. Zeta potential of the surface of particles in supernatant. The unit of zeta potential is millivolt (mV). (see effect of Al content in Chapter 5)

4.1.1 Settling curve and ISR

Figure 4.1 shows a schematic diagram of a typical settling curve. The suspension mud-line is the interface between supernatant and hindered settling flocculated flocs. The mud-line descends with time during settling. h is the mud-line height at time t and H is the initial mud-line height or whole suspension height at time $zero$. The initial slopes are taken as initial settling rate.

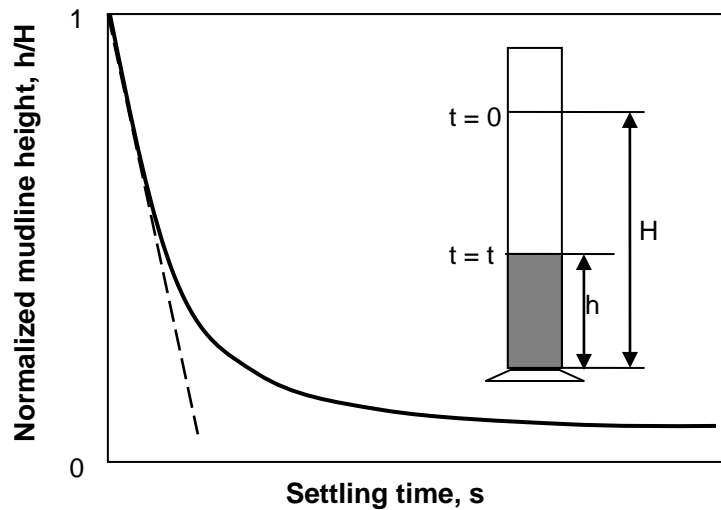


Figure 4.1 Schematic of a typical settling curve.

Polymer dosages in this study are represented in ppm (part-per-million, i.e., milligrams of polymer flocculant per kilogram of model fine tailings or laboratory extraction tailings suspension or slurry). It can be converted to

ppm on dry solids basis from known solids content of tailings.

For example, 2 ppm of MF1011 was added to the laboratory extraction tailings, the settling curve of normalized mudline against settling time is plotted in Figure 4.2. A dosage of 2 ppm on tailing basis is equivalent to 18 ppm polymer dosage on dry solids basis and 70 ppm polymer dosage on dry fines basis.

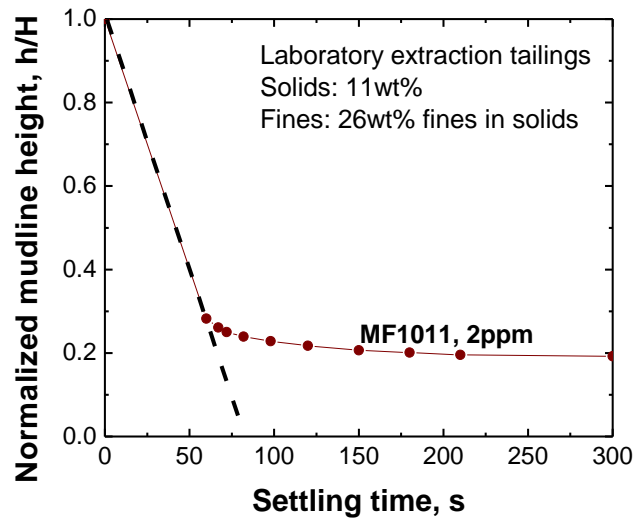


Figure 4.2 Settling curve of flocculated laboratory extraction tailings by 2ppm MF1011.

Other settling curves were plotted as the same way, and the ISRs were calculated accordingly. The results are shown in Figure 4.3.

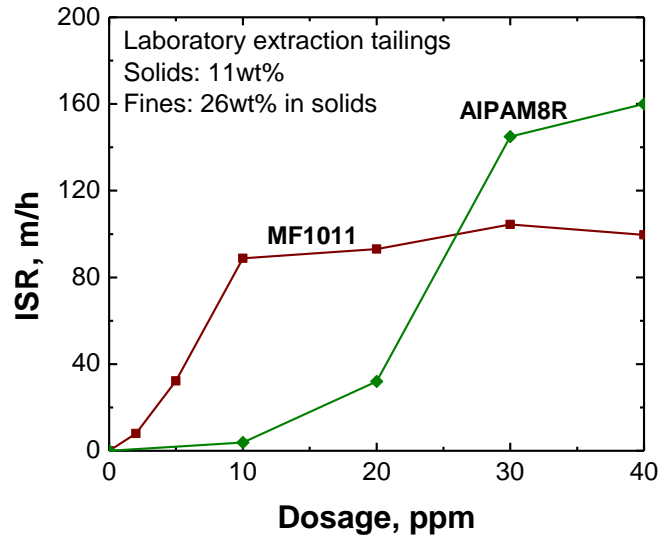


Figure 4.3 Initial settling rates of flocculated laboratory extraction tailings by MF1011 and Al-PAMs at different dosages.

4.1.2 Discussion

Michaels and Bolger [1] suggested that the hindered-settling rate can be expressed by the following equation.

$$Q_0 = \frac{g(\rho_A - \rho_w)d_A^2}{18\mu_w} (1 - \phi_A)^{4.65} \quad (4.1)$$

where Q_0 is hindered-settling rate, ρ_A is density of aggregate, ρ_w is density of water, d_A is the aggregate diameter, μ_w is viscosity of water at a given temperature, ϕ_A is volume fraction of aggregates, and g is acceleration of gravity. From equation 4.1, we can see that the

hindered-settling rate for uniform spherical particles is proportional to square of the aggregate diameter, namely, $Q_0 \propto d_A^2$. In general, for a certain type of flocs with similar components in aggregates, the larger size results in faster settling rate.

The above equation has its limitations that, the aggregate diameter d_A is relatively independent of the concentration of suspension over the “dilute” range, and d_A does not change once settling has begun. The Reynolds number must be less than 0.3 here to use Stokes law [2].

a. Mixing rate

Mixing and agitation rates are important factors to aggregation of particles. When shear rate increases, fractal dimension decreases [3] due to the domination of the disruption process during agitation [4]. Size and properties of the flocs would be affected under different shear forces [5], and all these would result in decreasing flocculation efficiency with increasing agitation speed. Figures 4.4 (a) and (b) show the different flocculation stages under correct or excessive mixing.

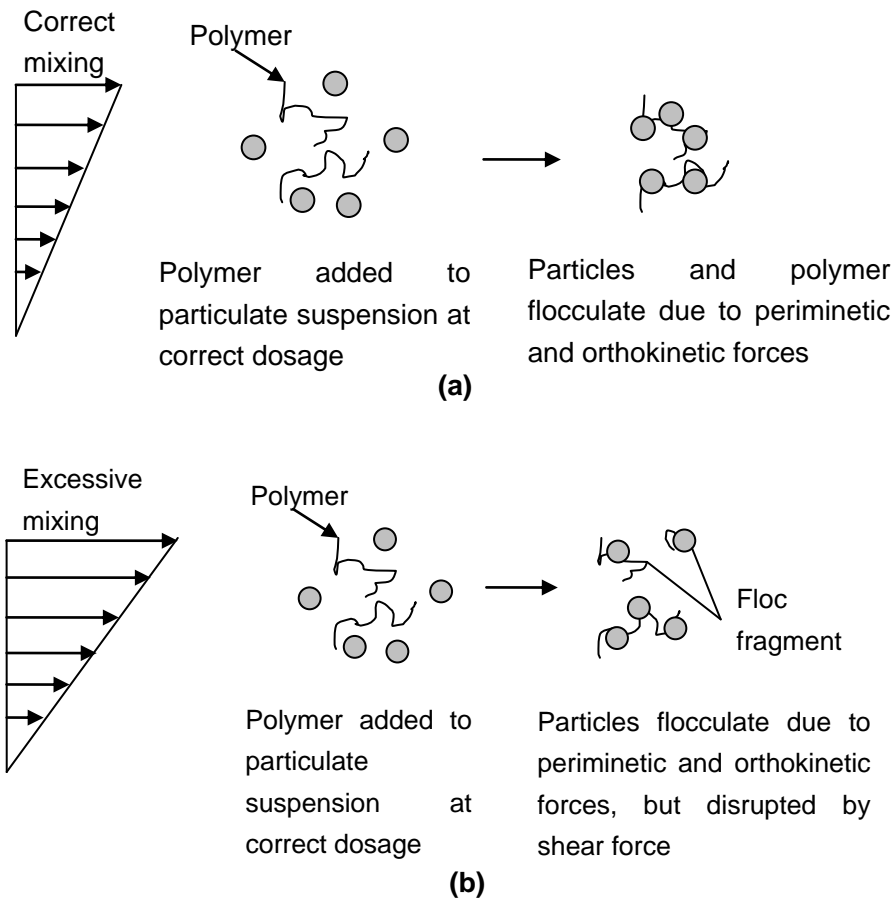


Figure 4.4 Schematic representation of the bridging model under (a) a correct mixing; and (b) an excessive mixing [6].

Wang et al. [7] has performed a series of tests to compare different mixing rates on flocculation and found that for maganofloc1011 (MF1011), the desirable mixing rate ranges from 250 to 350 rpm for mixing system used, and the higher mixing rate is not good for flocculation. For Al-PAM, mixing rate ranges roughly from 300 to 700 rpm. To compromise and to be consistent with previous work, the mixing rate in this study was fixed at 350 rpm.

Negro et al. [8] suggested that under a constant stirring intensity, the average energy dissipation rate (ε_a) can be calculated by the equation

$$\varepsilon_a = \frac{\pi n_s \tau}{30 \rho V} \quad (4.2)$$

Where n_s is impeller speed (rpm), τ is stirring torque (Nm), V (m^3) is the volume of the beaker and ρ is the density of the fluid (kg/m^3).

Equation 4.2 indicates that energy dissipation rate is indirectly proportional to impeller speed. The length scale of the smallest eddies [8] in turbulent flow is given by the Kolmogorov microscale (η), which can be represented by:

$$\eta = \left(\frac{\nu^3}{\varepsilon} \right)^{1/4} \quad (4.3)$$

where ν is the kinematic viscosity of the fluid, and ε is the average rate of energy dissipation per unit mass. Equation 4.3 shows that the Kolmogorov microscales decrease with increasing impeller stirring speed [5]. Therefore, the Kolmogorov microscale can be assumed to be constant at a given stirring rate. In this case, when adding extra polymer, the floc size increases to be larger than the Kolmogorov microscale, at which point the microscale will be fractured, suggesting that the flocs are ready to be broken [9].

b. Polymer dosage

When polymer was introduced to a suspension at 350 rpm, it was rapidly adsorbed on the particles. These particles were flocculated by polymer bridging between them. Increasing dosage of polymer is advantageous to enlarge the floc size and porosity of fractal-like flocs, which will affect the collision efficiency [10] and also collision frequency among particles [11]. Growing floc size, on the other hand, would increase the possibility of weak bonds in the agglomerated structure. Chance of flocs fracture increases due to floc size larger than the Kolmogorov microscale [12]. Overall, these long chain polymers are very susceptible to destabilization (e.g. precipitation), resulting in a decrease in the overall efficiency of flocculation and dewatering [13-16]. Large flocs highly resistant to shear can lead to an increase in permeate flux because flocs were not easily broken. As a consequence, an ideal balance needs to be quantified for flocs size and enough resistance to shear stress between aggregates [17]. The structure of Al-PAMs satisfies this balance to some level. But Al-PAMs have their own overdose problem, although their chains are much shorter [21] as compared to MF1011. They are also not as sensitive to mixing speed and dosage as MF1011 [7]. More water entrapped in the flocs by extra amount of polymer, which lead to lower sediment densification, would result in lower settling rate [18].

4.2 Filtration

In the filtration test, three parameters were used to evaluate the performance of polymer flocculants on filtration of flocculated tailings. They are:

1. The specific resistance to filtration (SRF). The unit of SRF is meter per kilogram (m/kg).
2. Filtration rate, which is much dependent on SRF.
3. Moisture content in filter cake. The unit is weight percent (wt.%).

The filtration can be divided into three regions:

1. Filtration: the initial drainage of the liquid in the suspension through the porous medium, which gives a very fast drainage. Particles are accumulated on the top of the filter medium and a filter cake forms during this stage and becomes part of filtration medium.
2. Dewatering: in permeation period, the breakdown of the water film and drainage of the water from particle surface. The process is slow. The liquid is removed by applying desaturation forces [19].
3. The flushing of air through the pores of the cake; at this step almost no more water was drained out, as shown by near vertical line (an example of AIPAM8R at 30 ppm shown in Figure 4.10). In this study,

only the initial linear part of the curve was used to derive the slope for the calculation of specific resistance to filtration.

For one type of tailings in this study (11% solids with 26% fines in tailings suspension), most water released in a short period. After that, only a small fraction of water dripped out.

4.2.1 Specific resistance to filtration

The specific resistance to filtration (SRF) is a measure of the resistance of the cake to the flow of the filtrate. It is therefore a measure of the filterability [20]. The higher the resistance, the lower is the filterability [21]. The specific resistance is inversely related to the permeability of the incompressible filter cake [20]. The general filtration is given by:

$$\frac{t}{V} = \frac{\mu r \phi}{2PA^2} V + \frac{\mu r L_m}{PA} \quad (4.4)$$

where:

t : filtration time (s)

V : filtrate volume (m³)

μ : viscosity of filtrate (Pa·s)

P : the pressure difference applied on the top of the filter cake (Pa)

r : specific resistance to filtration (m/kg)

A : filter area (m²)

L_m : the thickness of filter medium (m)

ϕ : the mass of solids in suspension (kg/m³)

Equation 4.4 shows a linear relationship between t/V and V with the intercept a given by $\frac{\mu r L_m}{PA}$ and the slope b given by $\frac{\mu r \phi}{2PA^2}$. A larger slope leads to a longer time to get a certain volume to filtrate. In other words, a larger slope corresponds to a lower filtration rate as shown in Figure 4.5.

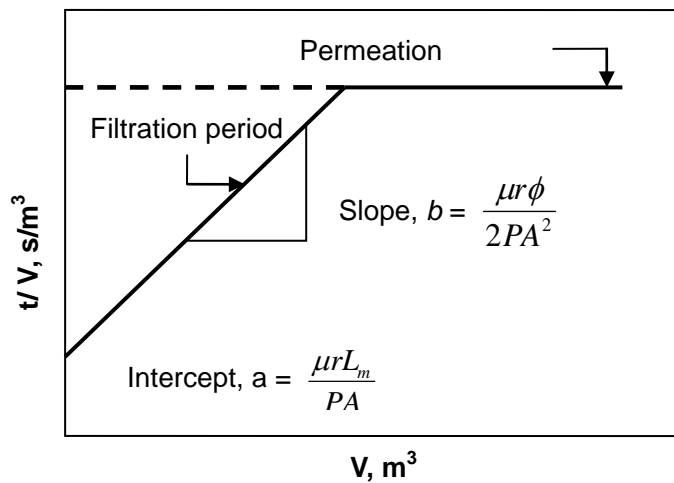


Figure 4.5 Theoretical results of a filtration experiment.

Therefore equation 4.4 can be modified to equation 4.5 and resistance of

filtration (r is SRF) can be calculated by equation 4.5.

$$\frac{t}{V} = a + bV \quad (4.5)$$

$$r = \frac{2PA^2}{\mu\phi} b \quad (4.6)$$

Detailed derivation of the filtration equations can be found in many publications or chemical engineering text books [18]. During the filtration, the flow rate of the filtrate depends on pressure difference across the filter cake and resistance from the filter medium and the filter cake. In this study, the filtration tests were conducted using a bench-scale pressure filtration unit at a constant filtration pressure of 15kPa throughout the entire filtration period. The filter area A was 45.8 cm² and viscosity μ of filtrate was considered the same as pure water at room temperature.

4.2.2 Filtration curves and data processing

An original filtration curve is derived from filtrate weight (recorded by a balance connect to a computer) against filtration time as shown in Figure 4.6 (a). $Water_{left}$ is defined as the mass of water left at filtration time t divided by the mass of water in the original slurry at filtration time “zero”. This filtration curve is shown in Figure 4.6 (b). The water content is given

by:

$$Water_{left} = \frac{M_w - W_{ft} + W_f}{M_w + W_f} \times 100\% \quad (4.7)$$

where M_w (g) is the mass of water in the total slurry at time zero, W_{ft} (g) is the mass of filtrate collected up to filtration time t , and W_f (g) is the mass of water in the flocculant solution added in the slurry.

Moisture is defined as weight of water left in the slurry at a given filtration time t divided by weight of total slurry at a given filtration time t . This filtration curve is shown in Figure 4.6 (c). The moisture content is given by:

$$Moisture = \frac{\text{Mass of water in filter press at time } t}{\text{Mass of total slurry at time } t} \quad (4.8)$$

$$Moisture = \frac{M_w - W_{ft} + W_f}{M_{slurry} - W_{ft} + W_f} \times 100\% \quad (4.9)$$

where, M_{slurry} (g) is the mass of total slurry at filtration time “zero”. The final cake moisture $\frac{M_{wet} - M_{dry}}{M_{wet}}$ was checked as well, where M_{wet} and M_{dry} are the mass of the cake before and after drying in the oven at 100 °C for 12 hours, respectively.

A general flow for filtration data processing and corresponding plotting is shown in Figure 4.6.

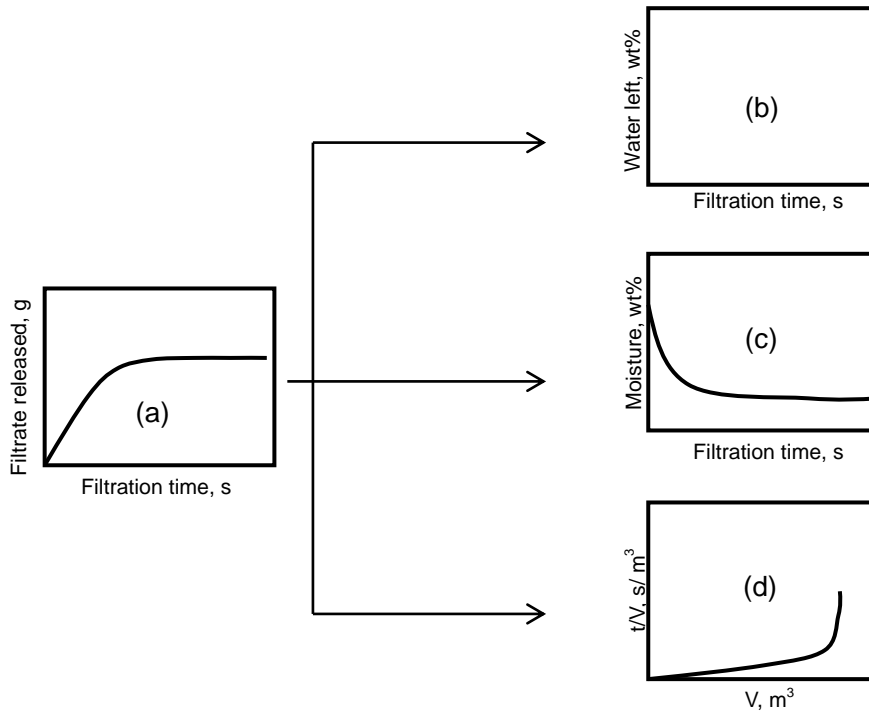


Figure 4.6 A general flow for filtration data processing and corresponding plotting.

For example, for the flocculated laboratory tailings (11 wt% solids with 26% fines) by 30 ppm MF1011 or 30 ppm Al-PAM (in terms of the whole tailings suspension or slurry), different filtration curves are shown in Figure 4.7, Figure 4.8, Figure 4.9 and Figure 4.10, respectively.

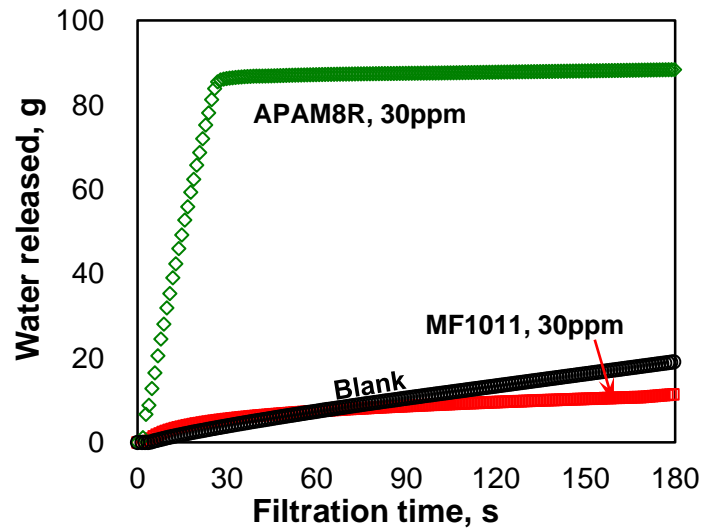


Figure 4.7 Original filtration curve plotted according to released filtrate against filtration time.

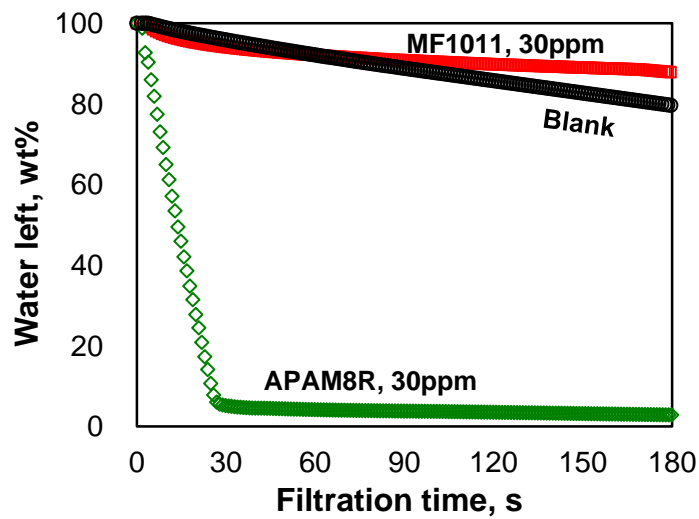


Figure 4.8 Derived filtration curve plotted as percent water left in the slurry against filtration time.

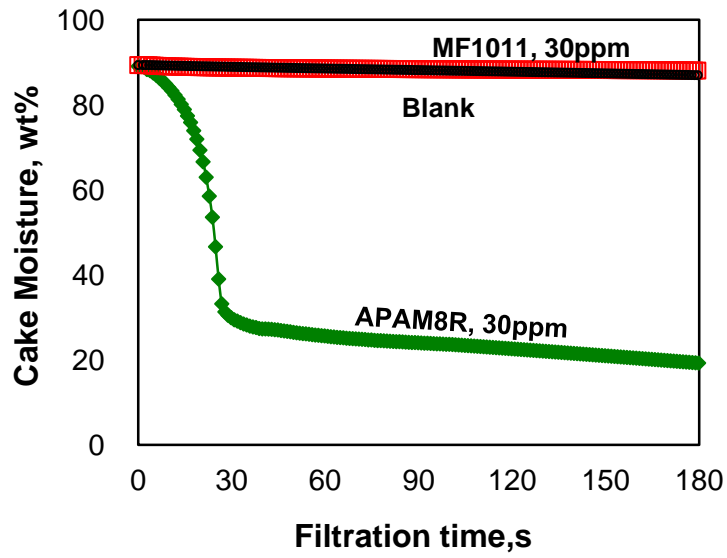


Figure 4.9 Derived filtration curve plotted as moisture content in filter cake against filtration time.

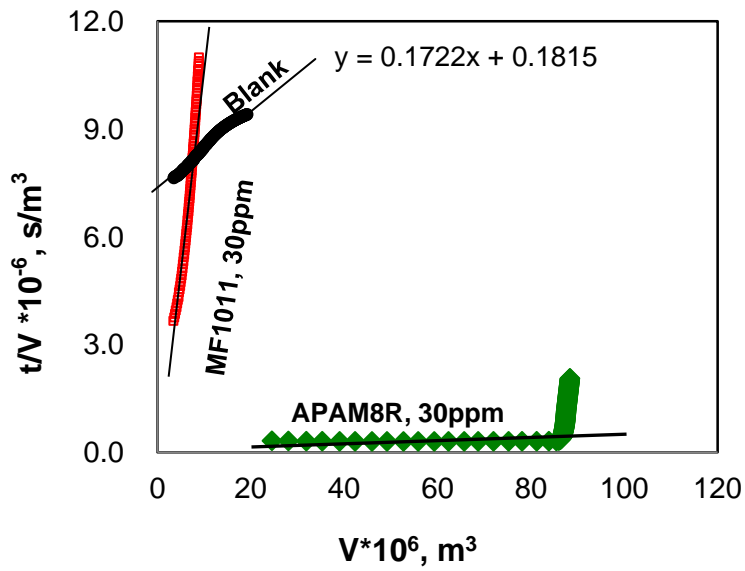


Figure 4.10 Derived filtration curve plotted as t/V against filtrate volume.

SRF is calculated based on t/V against V curves. In Figure 4.10, for example, the slope of blank is $0.1722 \cdot 10^{12}$ s/m⁶, $P = 15 \cdot 10^3$ Pa, $A = 45.8$

$\times 10^{-4} \text{ m}^2$, $\mu = 1 \times 10^{-3} \text{ pa}\cdot\text{s}$, and $\phi = 110 \text{ kg/m}^3$. Therefore $r = 9.85 \times 10^{11} \text{ m/kg}$.

The rest results are listed in Table 4-1.

Table 4-1 List of linear fit of $t/V-V$ and SRF for laboratory extraction tailings: 11 wt% solids with 25 wt% fines at pH=8.4

Polymer	Linear fit of $t/V-V$	SRF, m/kg
Blank	$y = 0.1722x + 0.1815$	9.85×10^{11}
MF1011, 30 ppm	$y = 1.4416x + 0.1354$	8.25×10^{12}
AIPAM8R, 30 ppm	$y = 0.0009x - 0.0987$	4.86×10^9

For this specific tailings, 30 ppm Al-PAM addition dramatically enhanced filtration and the slope of t/V vs. V was much lower than the case without polymer addition (“Blank” in Figure 4.10). The corresponding SRF was $4.86 \times 10^9 \text{ m/kg}$, which was more than two orders of magnitude lower than that of blank and three orders of magnitude lower than that with 30 ppm MF1011 addition. The results were comparable to the cases of Wang [7] (SRF was from 10^9 to 10^{12}) and Xu [18]. The same method was used for plotting filtration curves and data processing in other chapters.

References

1. Michaels, A. S.; Bolger, J. C., *Settling rate and sedimentation*

- volumes of flocculated kaolin suspensions*. Ind. Eng. Chem. Fund. , 1962. **1**: p. 24-33.
2. Perry, R. H., *Perry's chemical engineers' handbook*. 1984, Toronto: McGraw-Hill.
 3. Flesch, J. C.; Spicer, P. T.; Pratsinis, S. E., *Laminar and turbulent shear-induced flocculation of fractal aggregates*. AIChE Journal, 1999. **45**(5): p. 1114-1124.
 4. Lu, S. C.; Ding, Y. Q.; Guo, J. Y., *Kinetics of fine particle aggregation in turbulence*. Advances in Colloid and Interface Science, 1998. **78**(3): p. 197-235.
 5. Negro, C.; Sanchez, L. M.; Fuente, E.; Blanco, A.; Tijero, J., *Polyacrylamide induced flocculation of a cement suspension*. Chemical Engineering Science, 2006. **61**(8): p. 2522-2532.
 6. Crittenden, J. C.; Trussell, R. R.; Hand, D. W.; Howe, K. J.; Tchobanoglous, G., *Water treatment - principles and design* 2nd ed. 2005, New Jersey: John Wiley & Sons. Chapter 9.
 7. Wang, X. Y.; Feng, X. H.; Xu, Z. H.; Masliyah, J. H., *Polymer aids for settling and filtration of oil sands tailings*. Canadian Journal of Chemical Engineering, 2010. **88**(3): p. 403-410.
 8. Landahl, M.T.; Mollo-Christensen, E., *Turbulence and random processes in fluid mechanics*. 2nd ed. 1992, Cambridge,UK:

Cambridge University Press.

9. Ducoste, J., *A two-scale PBM for modeling turbulent flocculation in water treatment processes*. Chemical Engineering Science, 2002. **57**(12): p. 2157-2168.
10. Kusters, K. A.; Wijers, J. G.; Thoenes, D., *Aggregation kinetics of small particles in agitated vessels*. Chemical Engineering Science, 1997. **52**(1): p. 107-121.
11. Lee, D. G.; Bonner, J. S.; Garton, L. S.; Ernest, A. N. S.; Autenrieth, R. L., *Modeling coagulation kinetics incorporating fractal theories: A fractal rectilinear approach*. Water Research, 2000. **34**(7): p. 1987-2000.
12. Lu, C. F.; Spielman, L. A., *Kinetics of floc breakage and Aggregation in agitated liquid suspensions*. Journal of Colloid and Interface Science, 1985. **103**(1): p. 95-105.
13. Peng, F. F.; Di, P. K., *Effect of multivalent salts calcium and aluminum on the flocculation of kaolin suspension with anionic polyacrylamide*. Journal of Colloid and Interface Science, 1994. **164**(1): p. 229-237.
14. Somasundaran, P.; Chia, Y. H.; Gorelik, R., *Adsorption of polyacrylamides on kaolinite and its flocculation and stabilization*. Acs Symposium Series, 1984. **240**: p. 393-410.

15. Taylor, M. L.; Morris, G. E.; Self, P. G.; Smart, R. S., *Kinetics of adsorption of high molecular weight anionic polyacrylamide onto kaolinite: The flocculation process*. Journal of Colloid and Interface Science, 2002. **250**(1): p. 28-36.
16. Mporfu, P.; Addai-Mensah, J.; Ralston, J., *Investigation of the effect of polymer structure type on flocculation, rheology and dewatering behaviour of kaolinite dispersions*. International Journal of Mineral Processing, 2003. **71**(1-4): p. 247-268.
17. Zhao, B. Q.; Wang, D. S.; Li, T.; Chow, C. W. K.; Huang, C., *Influence of floc structure on coagulation-microfiltration performance: Effect of Al speciation characteristics of PACls*. Separation and Purification Technology, 2010. **72**(1): p. 22-27.
18. Xu, Y. M.; Dabros, T.; Kan, J. M., *Filterability of oil sands tailings*. Process Safety and Environmental Protection, 2008. **86**(B4): p. 268-276.
19. Wakeman, R. J., *Filtration post-treatment processes*. 1975, New York: American Elsevier Publishing Company. Chapter 1-3.
20. Wakeman, R., *The influence of particle properties on filtration*. Separation and Purification Technology, 2007. **58**(2): p. 234-241.
21. FTFC (Fine Tailings Fundamentals Consortium), *Advances in oil sands tailings research*. 1995, Alberta Department of Energy. Oil

Sands and Research Division.

Chapter 5 Effect of Polymer Properties on Oil Sands Tailings Treatment

5.1 Effect of molecular weight

A series of Al-PAM with different molecular weights were tested as flocculants for both settling and filtration of model fine tailings prepared from 5 wt% kaolinite and laboratory extraction tailings prepared from extraction of SYN704 ore.

5.1.1 Settling behaviour

Standard settling tests were used to the kaolinite model fine tailings and laboratory extraction tailings obtained from oil sands extraction tests. The initial settling rates as a function of polymer dosage are based on changing interface (mudline) of settling over time. Turbidities and zeta potential of the supernatant were also measured and used to understand the settling behaviour.

5.1.1.1 Model fine tailings

Suspensions of 5 wt% kaolinite were used as model tailings to investigate the flocculation characteristics of Al-PAM. Figure 5.1 (a) shows initial

settling rate (ISR) as a function of polymer dosage at pH 8.4. Figure 5.1 (b) is the settling curve of normalized mudline height, h/H , against settling time after adding 10 ppm AIPAM8R to the model fine tailings.

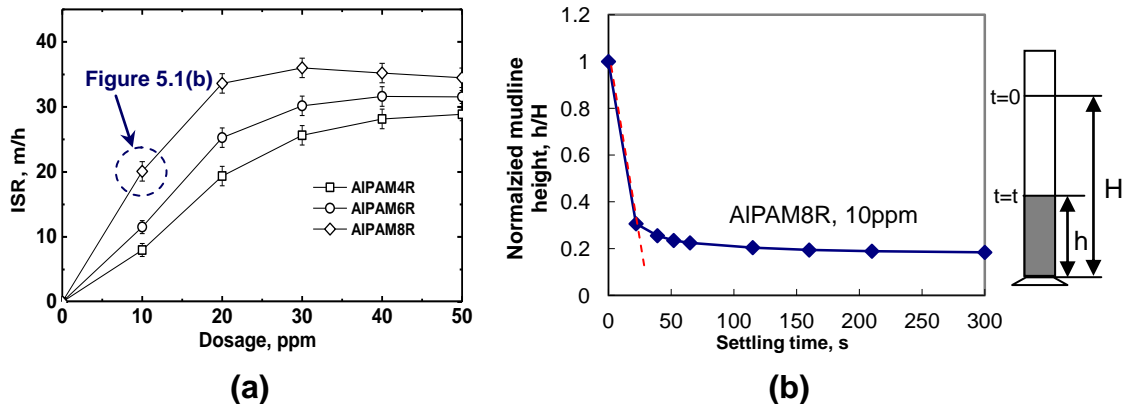


Figure 5.1 (a) Initial settling rate of 5 wt% kaolinite suspensions as a function of Al-PAM dosage; and (b) settling of flocculated model fine tailings with 10 ppm AIPAM8R (Al-PAM dosage ppm is expressed in terms of tailings slurry).

The results shown in Figure 5.1 (a) indicate that all the Al-PAMs with different molecular weights enhance settling of model fine tailings. The settling rate without flocculant addition was lower than 0.5 m/h. With increasing Al-PAM dosage, the ISR increases initially and eventually reach a plateau. For AIPAM8R, AIPAM6R, and AIPAM4R, the optimum dosages were 30 ppm, 40 ppm and 50 ppm, respectively. Figure 5.1 (a) also shows that at a given dosage, Al-PAM with higher molecular weight (e.g. AIPAM8R) produces higher ISR than Al-PAM with lower molecular weight (e.g. AIPAM4R and AIPAM6R).

Turbidity measurement was conducted to examine the clarity of supernatant of flocculated tailings after settling. Figure 5.2 shows the turbidities of the supernatant of model fine tailings with addition of Al-PAMs. For all the Al-PAMs, supernatant turbidities were improved significantly. The turbidity of supernatant without polymer was 320 NTU. With increasing polymer dosage, supernatant turbidities decreased from about 100 NTU at 10 ppm to about 10 NTU at 40 ppm.

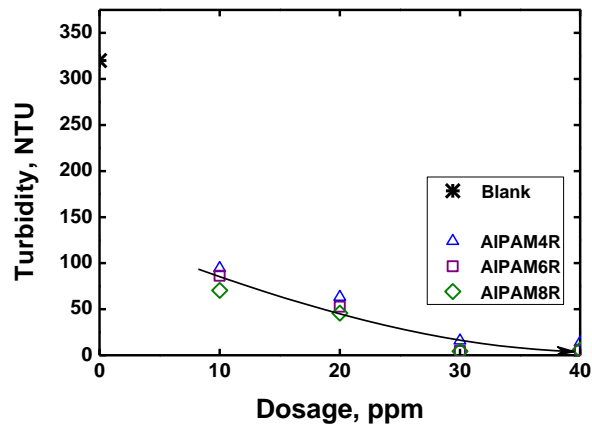


Figure 5.2 Supernatant turbidities of model fine tailings with 5 wt% kaolinite at different dosages of Al-PAMs.

5.1.1.2 Laboratory extraction tailings

The ability of Al-PAM and MF1011 to flocculate actual oil sands tailings was investigated using laboratory generated tailings (11 wt% solids with 26 wt% fines). The setting test results are shown in Figure 5.3. Dosage ppm is

part-per-million, i.e., milligrams of polymer flocculant per kilogram of the whole tailings suspension or slurry.

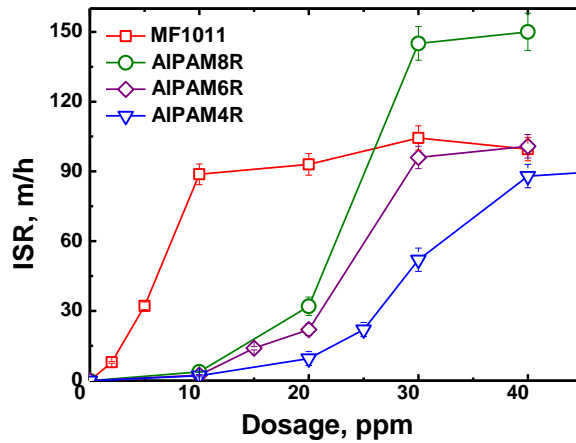


Figure 5.3 Initial settling rates of flocculated laboratory extraction tailings by MF1011 and Al-PAMs (pH=8.4).

It can be seen from Figure 5.3 that all the Al-PAM polymers improved settling rates, indicating that they are efficient flocculants for fresh tailings. In the absence of flocculants, a typical low settling rate (less than 0.5 m/h) was observed. With lower dosages of polymer, the similar results were obtained as in the case of kaolinite model fine tailings given in Figure 5.1. All Al-PAMs improved settling rates at a dosage of 30 ppm. The results also show that Al-PAM with higher molecular weight produced higher ISR at a given dosage. Al-PAMs with different molecular weight exhibited different optimum dosages. Higher molecular weight Al-PAM required a lower dosage to achieve a given settling rate.

Although Figure 5.4 illustrates that both MF1011 and Al-PAM are effective flocculants for oil sands laboratory extraction tailings, when the dosage was lower than 20 ppm, the settling rate with MF1011 was obviously higher than that with Al-PAM. Part of the reasons is that polymer chains of Al-PAM, even AIPAM8R of the longest polymer chains compared to other Al-PAMs, are much shorter than those of MF1011.

The supernatant turbidity results in Figure 5.4 show that MF1011 did not improve turbidity of supernatant, while all Al-PAMs improved supernatant turbidity significantly.

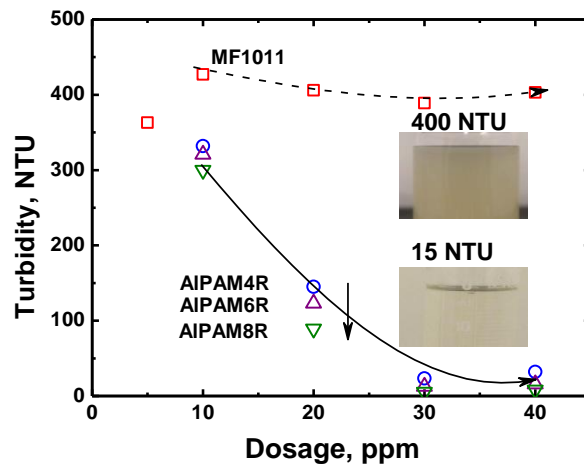


Figure 5.4 Supernatant turbidities of laboratory extraction tailings (11 wt% solids with 26 wt% fines) at different dosages of MF1011 and Al-PAMs (pH=8.4).

For example, when 30 ppm of MF1011, the optimum dosage for settling

rate, was added to the laboratory extraction tailings, the supernatant was observed unclear with the turbidity around 400 NTU. For all AI-PAMs, regardless of their molecular weight, a higher dosage of AI-PAM produced clearer supernatants. The turbidities of supernatant with all AI-PAMs were lower than those with MF1011. Furthermore, at a given dosage, the higher the molecular weight of AI-PAM, the lower is the supernatant turbidity. For example, at 30 ppm dosage, the supernatant turbidity of AIPAM4R, 6R and 8R was 35, 20 and 15 NTU, respectively.

5.1.2 Filtration performance

5.1.2.1 Model fine tailings

Figure 5.5 shows the filtration performance – moisture content change in filter cake with time of flocculated model fine tailings with MF1011 and AI-PAMs.

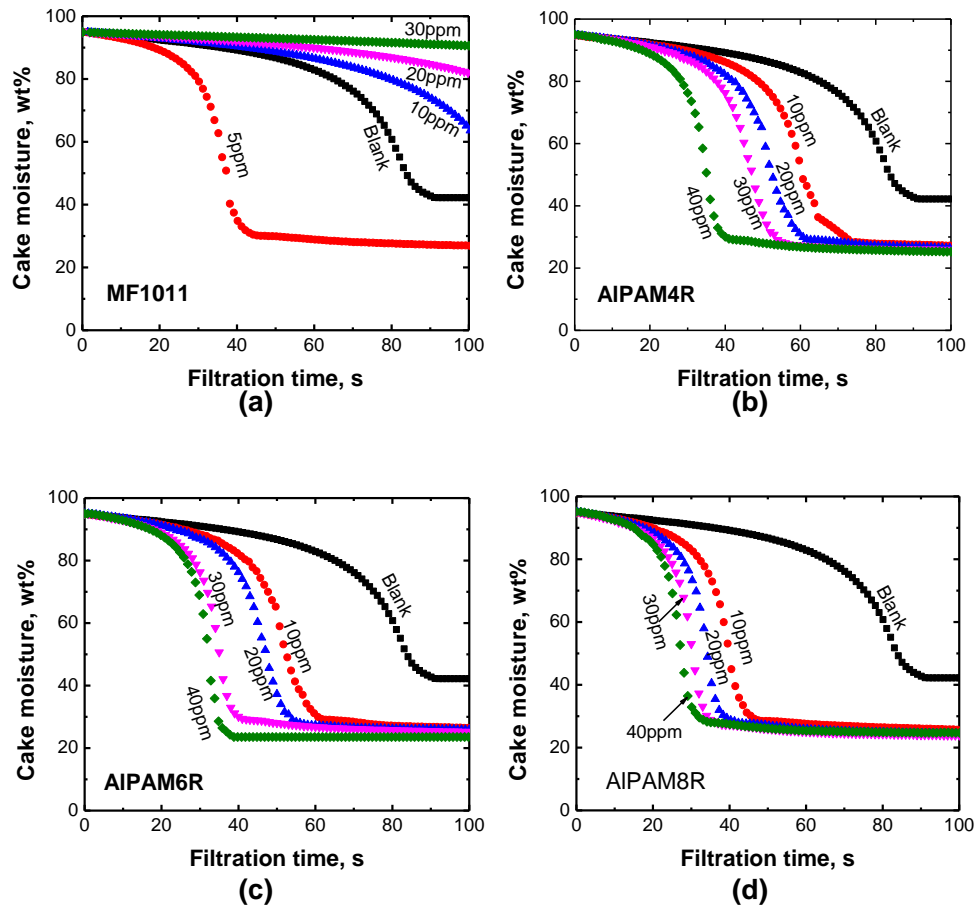


Figure 5.5 Filtration of flocculated model fine tailings by (a) MF1011; (b) AIPAM4R; (c) AIPAM6R; and (d) AIPAM8R (pH=8.4, flocculant dosage is shown in reference to mass of tailings).

Figure 5.5 (a) shows that filtration rate (the mass of released filtrate from flocculated tailings per unit time) of flocculated model fine tailings with 5 ppm MF1011 was almost as good as that with 40 ppm AIPAM4R, but increasing dosage reduced the filtration rate to be lower than that of samples without polymer addition (blank). Figures 5.5 (b), (c) and (d) show that the filtration of flocculated model fine tailings with higher molecular

weight Al-PAMs addition was better.

Taking Figure 5.5 (a) for MF1011 as an example, t/V against V was plotted as shown in Figure 5.6.

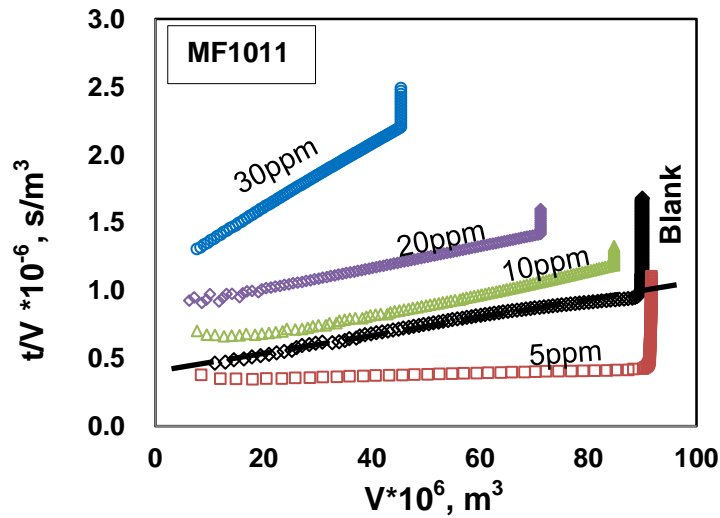


Figure 5.6 SRFs of flocculated model fine tailings with 5 wt% kaolinite by MF1011.

In Figure 5.6, for example, the slope of blank is $0.062 * 10^{12} \text{ s/m}^6$, $P=15*10^3 \text{ Pa}$, $A=45.8 * 10^{-4} \text{ m}^2$, $\mu=1 * 10^{-3} \text{ pa}\cdot\text{s}$, and $\phi = 50 \text{ kg/m}^3$ (2% by volume).

$$r = \frac{2PA^2}{\mu\phi} = \frac{2 * 15 * 10^{-3} \text{ Pa} * (45.8 * 10^{-4} \text{ m}^2)^2}{1 * 10^{-3} \text{ Pa s} * 50 \text{ kg/m}^3} * 0.062 * 10^{12} \text{ s/m}^6$$

$$r = 7.80 * 10^{11} \text{ m/kg}$$

The SRFs for the filtration of flocculated laboratory extraction tailings are listed in Table 5-1.

Table 5-1 Effect of molecular weight on SFR of flocculated model fine tailings

Polymer	Dosage, ppm	SRF, m/kg
Blank	0	7.80×10^{11}
MF1011	5	3.53×10^9
	10	2.01×10^{11}
	20	9.82×10^{11}
	30	8.31×10^{11}
	40	3.36×10^{12}
AIPAM4R	10	3.02×10^9
	20	2.39×10^9
	30	1.89×10^9
	40	1.76×10^9
AIPAM6R	10	3.02×10^9
	20	2.27×10^9
	30	1.76×10^9
	40	1.64×10^9
AIPAM8R	10	2.27×10^9
	20	1.76×10^9
	30	1.51×10^9
	40	1.38×10^9

Generally speaking, AI-PAMs have much lower SRF than MF1011. The SRFs of AI-PAMs were more than two orders of magnitude lower than that

of blank and three orders of magnitude lower than that of MF1011 at 30 ppm. Higher molecular weight Al-PAMs gave a slightly better result. For example, when 40 ppm AIPAM8R was applied, the SRF was 1.38×10^9 m/kg and the filtration rate was 3.4 g/s, whereas at the same dosage of AIPAM6R, SRF was 1.64×10^9 m/kg and filtration rate was 2.8 g/s. For each Al-PAM, increasing the dosage of polymer slightly improved the filtration rate and SRF.

5.1.2.2 Laboratory extraction tailings

The filtration tests were conducted on the laboratory extraction tailings derived from ore SYN704 (11 wt% solids with 26 wt% fines). Water released over time was recorded. Moisture in filter cake as a function of time is shown in Figure 5.7.

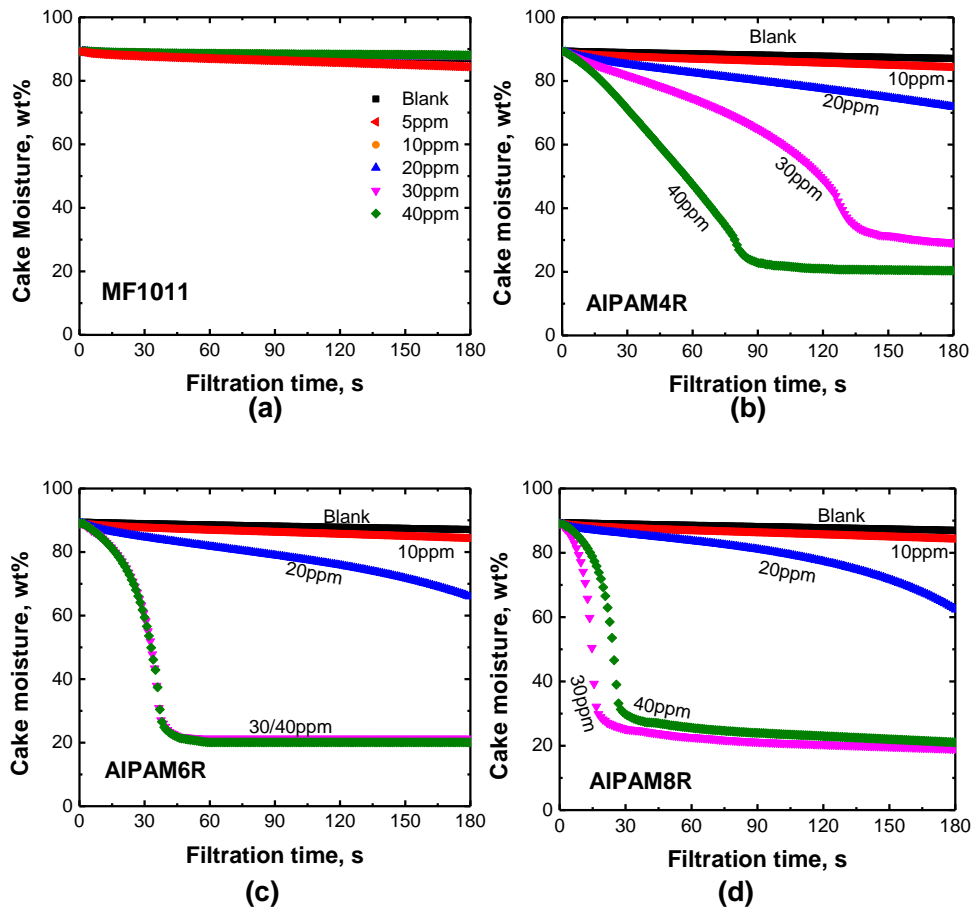


Figure 5.7 Filtration of flocculated laboratory extraction tailings by (a) MF1011; (b) AIPAM4R; (c) AIPAM6R; and (d) AIPAM8R.

Figure 5.7 (a) shows that there was slight effect on filtration of flocculated tailings by adding MF1011 compared to absence of polymers. The rest of Figure 5.7 shows that addition of Al-PAMs improved the filtration of flocculated laboratory extraction tailings significantly. For each Al-PAM, the filtration rate increased with increasing dosage. At a given dosage, Al-PAM with a higher molecular weight led to a faster filtration rate.

Filtration performance was further compared at the optimum dosages of these polymers as shown in Figure 5.8. Filtration rate increased with increasing molecular weight of Al-PAMs, while the moisture content of the final filter cake reduced slightly with increasing molecular weight of Al-PAMs.

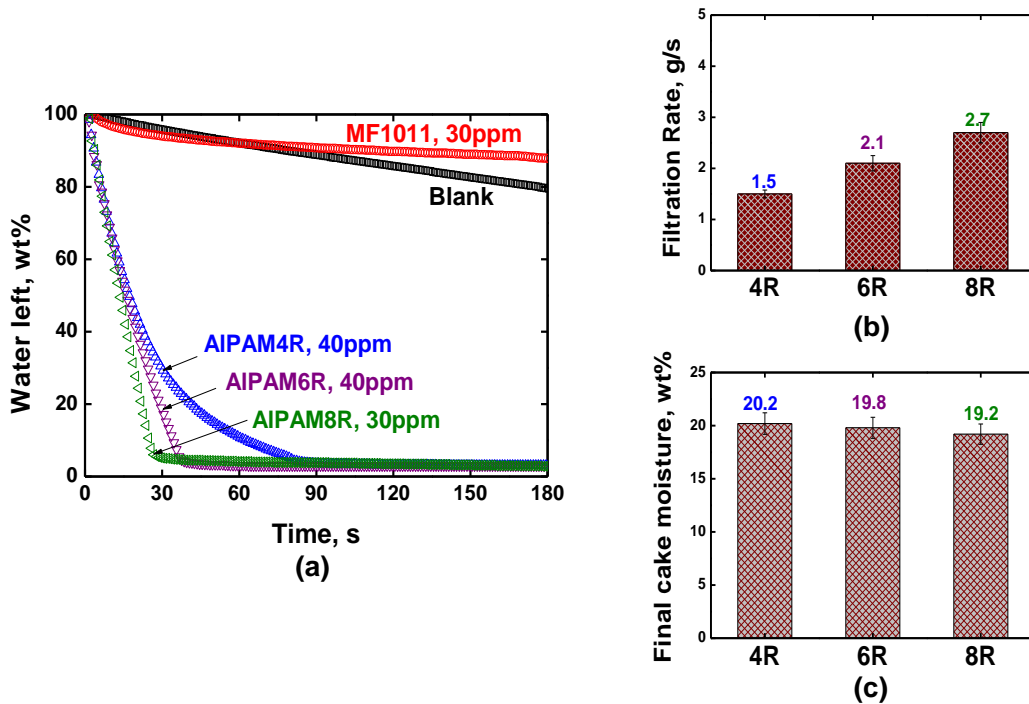


Figure 5.8 Effect of molecular weight on (a) filtration performance; (b) filtration rate; and (c) final filter cake moisture of tailings SYN704HB at optimum dosage of each polymer.

Figure 5.9 shows the SRF for different polymers at selected dosages. SRF of Al-PAMs was more than two orders of magnitude lower than that of blank. All the SRFs for the flocculated laboratory extraction tailings by different polymers are listed in Table 5-2.

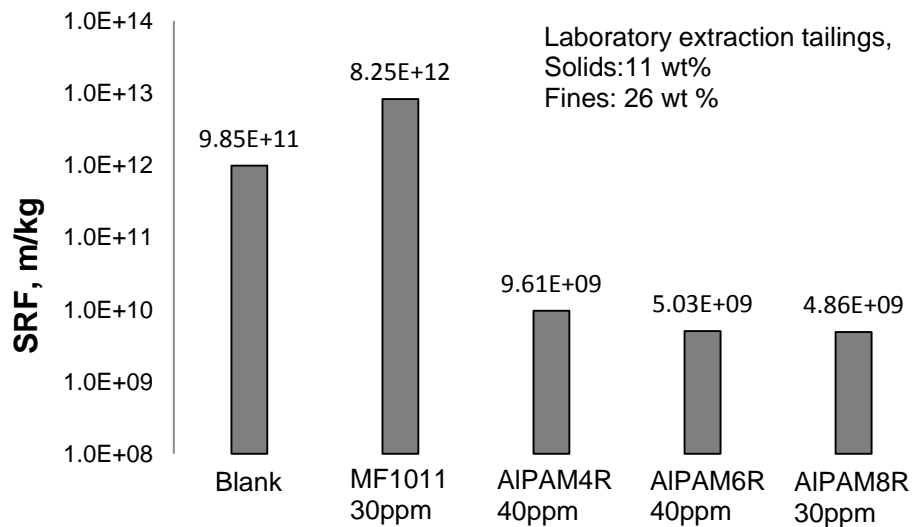


Figure 5.9 Comparison of SRF at selected dosages of different polymers.

Table 5-2 Effect of molecular weight on SRF of flocculated laboratory extraction tailings

Polymer	Dosage, ppm	SRF, m/kg
Blank	0	9.85*10 ¹¹
MF1011	5	9.66*10 ¹⁰
	10	5.04*10 ¹¹
	20	8.18*10 ¹¹
	30	8.25*10 ¹¹
	40	8.33*10 ¹¹
AIPAM4R	10	9.78*10 ¹¹
	20	2.57*10 ¹⁰
	30	1.11*10 ¹⁰
	40	9.61*10 ⁹
AIPAM6R	10	9.73*10 ¹¹
	20	2.18*10 ¹⁰
	30	5.95*10 ⁹
	40	5.03*10 ⁹
AIPAM8R	10	9.71*10 ¹¹
	20	1.58*10 ¹⁰
	30	4.86*10 ⁹
	40	4.92*10 ⁹

SRFs of Al-PAMs were more than two orders of magnitude lower than that of blank. In general, Al-PAMs had much better filtration performance than MF1011. For Al-PAMs, SRFs decreased with increasing molecular weight, filtration rate increased and the final filter cake moisture decreased slightly with increasing molecular weight.

5.1.3 Summary

Higher molecular weight Al-PAMs result in lower SRF, faster filtration rate and lower moisture content for filtration.

A modified Carman–Kozeny relationship [1] which incorporated fractal dimension and related the specific resistance with both floc size and fractal is expressed as below:

$$r = \frac{180(1 - \varepsilon)}{\rho_p d_p^2 \varepsilon^3} \quad (4.4)$$

where r is the specific resistance of filtration (SRF), which is a hydrodynamic character used for measuring dewater ability [2], ε is the void volume of the filter cake, ρ_p is the density of the particles and d_p is the mean diameter of the particles. As indicated by the modified

Carman–Kozeny relationship [3] , for a filtration system of constant μ (dynamic viscosity), P (constant pressure difference applied on the top of filter cake), A (filter area) and ϵ , specific resistance would increase with decreasing floc sizes. Cho et al. [4] reported that coagulated flocs of lower fractal dimension can improve permeability due to its higher porosity and relatively loose aggregation. Higher molecular weight Al-PAM produced larger flocs, consequently better filtration performance was achieved due to the reduced specific resistance to filtration.

5.2 Effect of aluminum content

Al-PAMs are positively charged mainly due to Al colloid core, leading to the hypothesis that aluminum content (Al content) in the Al-PAM is a critical parameter. Settling and filtration tests were conducted by applying two Al-PAMs (see Table 5-3) of similar molecular weight but different aluminum content. In this study, model fine tailings and laboratory extraction tailings were used.

Table 5-3 Physical properties of AIPAM6R and AIPAM6H

Polymer	$[\eta]$ (g/mL) ⁻¹	MW Da	Al wt%	Zeta Potential mV
AIPAM6R	675.2	2.0x10 ⁶	0.10%	+0.20
AIPAM6H	650.0	2.0x10 ⁶	0.24%	+0.16

5.2.1 Settling behaviour

5.2.1.1 Model fine tailings

Al-PAMs with similar molecular weight but different aluminum content (0.09 wt% for AIPAM6R and 0.24 wt% for AIPAM6H) were used in the setting tests of model fine tailings. Initial setting rates against dosages are plotted in Figure 5.10.

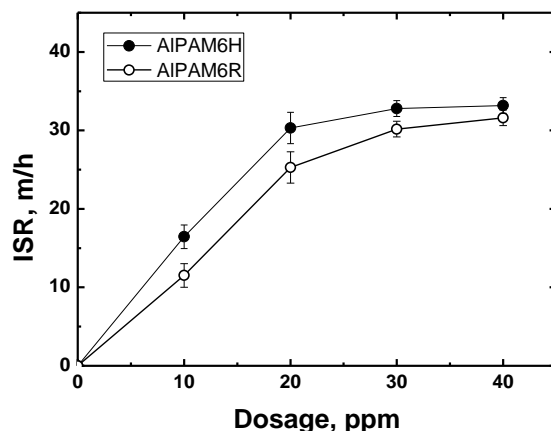


Figure 5.10 Initial settling rates of flocculated model fine tailings with 5 wt% kaolinite by Al-PAM with different Al content at room temperature 22°C, pH=8.4.

AIPAM6R and AIPAM6H, with similar molecular weight, were applied to the model fine tailings; initial settling rates at various dosages were estimated. Figure 5.10 shows that at a given molecular weight and dosage, Al-PAM with higher Al content made tailings to settle slightly faster.

5.2.1.2 Laboratory extraction tailings

AIPAM6R and AIPAM6H were used in the setting tests of laboratory extraction tailings. Initial setting rate was plotted against dosage of polymers as shown in Figure 5.11.

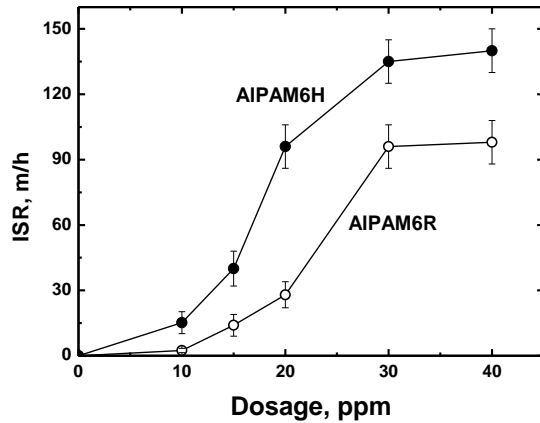


Figure 5.11 Initial settling rates of flocculated laboratory extraction tailings (11 wt% solids with 26 wt% fines) by Al-PAM with different Al content at room temperature 22°C, pH=8.4.

Figure 5.11 shows that for both types of tailings, the Al-PAMs with higher Al content made the tailings settle faster. In particular, the initial settling rate increased rapidly with 20 ppm Al-PAM of higher Al content as compared to the Al-PAM of lower Al content. The supernatant turbidity and zeta potential of particles in supernatant are shown in Figure 5.12, confirming the similar trends as in Figure 5.11.

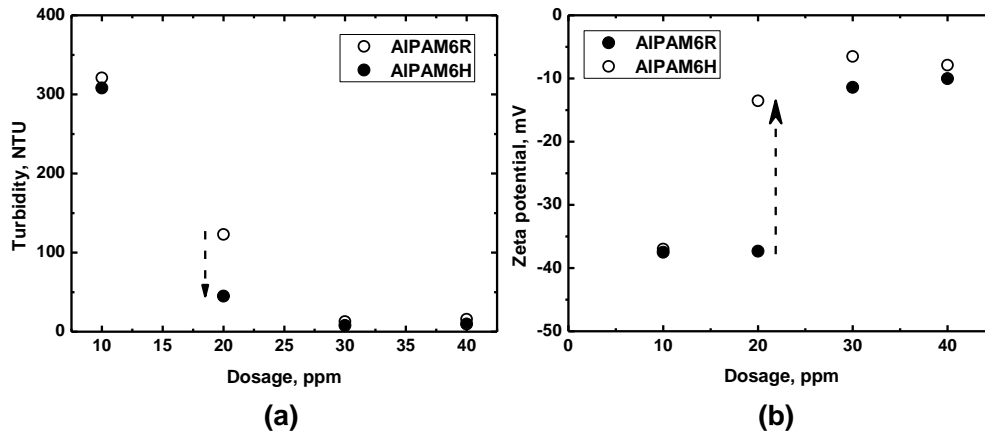


Figure 5.12 (a) supernatant turbidities of flocculated laboratory extraction tailings; and (b) zeta potential of particles in supernatant of flocculated laboratory extraction tailings by Al-PAMs with different Al content.

Figure 5.12 (a) shows that for both Al-PAMs, supernatant turbidity decreased with increasing dosage. At a given dosage, the clearer supernatant was produced by Al-PAM with higher Al-content. For example, when 20 ppm of AIPAM6H was added, the supernatant turbidity (45 NTU) was more significantly improved as compared to the case of AIPAM6R (120 NTU). It is known that Al-PAM is positively charged [5], while particles in supernatant were negatively charged [6]. Increasing the dosage of Al-PAM brings more positive charges to solid surfaces and leads to reducing more negative charges, which is consistent with the results shown in Figure 5.12 (b). At a given dosage, zeta potential of supernatant became less negative by addition of higher Al-content Al-PAMs. For example, at 20 ppm, the zeta potential of particles in supernatant with AIPAM6H was -12 mV, less

negative than -38mV of AIPAM6R.

5.2.2 Filtration performance

5.2.2.1 Model fine tailings

Effect of Al content on filtration of model fine tailings with 5 wt% kaolinite (pH=8.4) is shown in Figure 5.13.

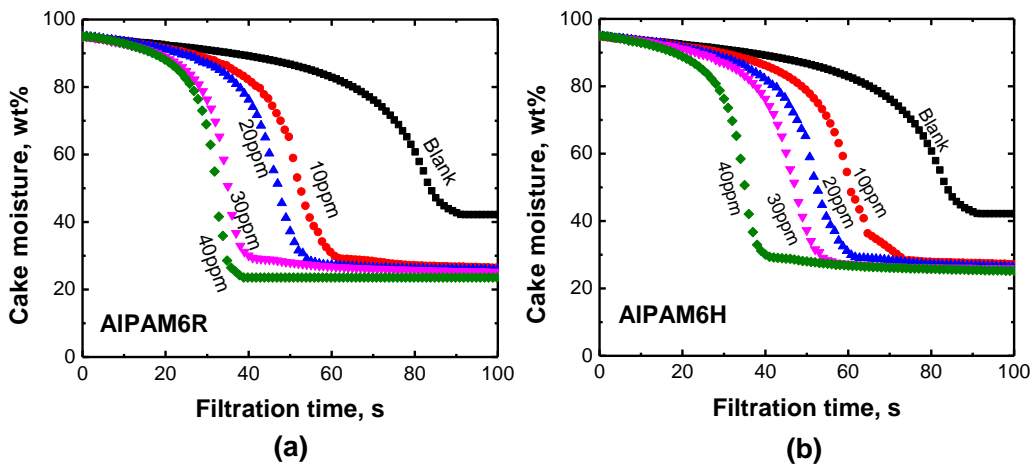


Figure 5.13 Filtration of flocculated model fine tailings by (a) AIPAM6R with lower Al content; and (b) AIPAM6H with higher Al content.

In general, at each dosage, the filtration rate of AIPAM6R was slightly higher than that of AIPAM6H, but at a given dosage, the final cake moisture of both Al-PAMs was similar. SRFs were derived from t/V vs. V based on

original filtration curves which are mass of filtrate with time, and listed in Table 5-4.

Table 5-4 Effect of Al content on SRF of flocculated model fine tailings

SRF, m/kg	Dosage, ppm	AIPAM6R	AIPAM6H
		Blank	7.80*10 ¹¹
	10	3.02*10 ⁹	3.15*10 ¹⁰
	20	2.27*10 ⁹	2.39*10 ¹⁰
	30	1.76*10 ⁹	2.01*10 ⁹
	40	1.64*10 ⁹	1.76*10 ⁹

Overall, Al content has little effect on filtration of flocculated model fine tailings.

5.2.2.2 Laboratory extraction tailings

Al-PAMs with similar molecular weight but different Al content (AIPAM6R and AIPAM6H) were also used for filtration of Laboratory extraction tailings (11 wt% solids with 26 wt% fines, pH=8.4). Filtration curves are shown in Figure 5.14.

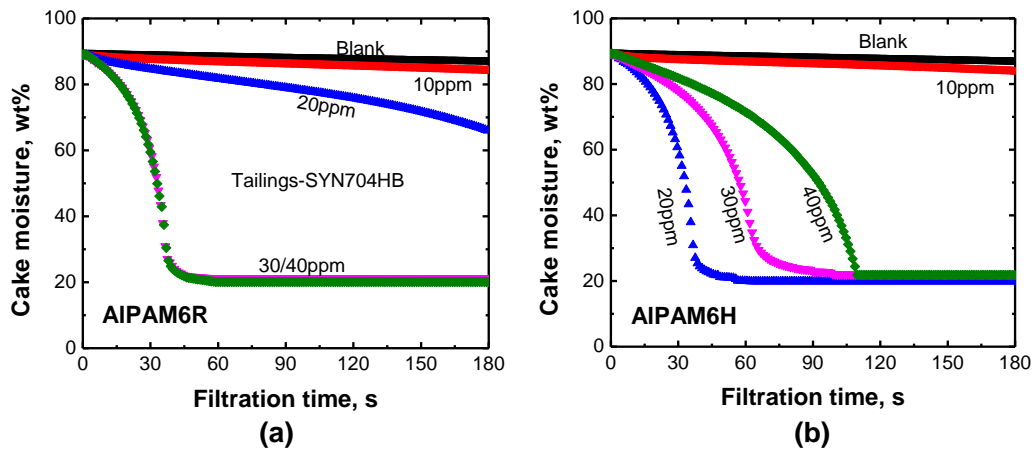


Figure 5.14 Filtration of flocculated laboratory extraction tailings by (a) AIPAM6R with lower Al content; and (b) AIPAM6H with higher Al content.

Figure 5.14 shows that all Al-PAMs improved the filtration performance of flocculated laboratory extraction tailings. The corresponding SRFs were calculated and list in Table 5-5.

Table 5-5 Effect of Al content on SRF of flocculated laboratory extraction tailings

SRF, m/kg	Dosage, ppm	AIPAM6R	AIPAM6H
		Blank	9.85*10 ¹¹
	10	9.73*10 ¹¹	6.63*10 ¹¹
	20	2.18*10 ¹⁰	5.12*10 ⁹
	30	5.95*10 ⁹	2.80*10 ¹⁰
	40	5.03*10 ⁹	4.98*10 ¹⁰

For laboratory extraction tailings, the SRF was 2.18×10^{10} m/kg and filtration rate was 1.7 g/s at 20 ppm of Al-PAM with lower Al content (AIPAM6R). At the optimum dosage (20 ppm) of al-PAM, the SRF for the case of higher Al content (AIPAM6H) was 5.12×10^9 m/kg and filtration rate was 1.8 g/s. Compared to AIPAM6R, the optimum dosage for filtration of laboratory extraction tailings by AIPAM6H was reduced from 40 ppm to 20 ppm.

5.2.3 Summary

For different Al-PAM with comparable molecular weight, the neutralization of charge becomes a more dominant factor in flocculation of laboratory extraction tailings. Zhao et al., 2010 [7] concluded that for given species of Al, the size of flocs is related to the amount of Al. The higher the amount of Al, the larger is the size of flocs. At a given dosage, Al-PAM with higher Al content produces larger flocs, which leads to a faster settling.

As the polymer dosage increases, the resistance to filtration decreases until a critical dose has been reached, where the zeta potential of particles' surface in supernatant was close to zero [8]. A further increase in polymer dose conversely raises the resistance to filtration, and this observation is

consistent with that described by Chang et al., 1997 [8]. For Al-PAMs at a given molecular weight, higher Al content is beneficial to settling of oil sands tailings. Addition of Al-PAM with higher Al content leads to a lower optimal dosage.

References

1. Guan, J.; Amal, R.; Waite, T. D., *Effect of aggregate size and structure on specific resistance of biosolids filter cakes*. Water Science and Technology, 2001. **44**(10): p. 215-220.
2. Agerbaek, M. L.; Keiding, K., *On the origin of specific resistance to filtration*. Water Science and Technology, 1993. **28**(1): p. 159-168.
3. Xu, Y. M.; Dabros, T.; Kan, J. M., *Filterability of oil sands tailings*. Process Safety and Environmental Protection, 2008. **86**(B4): p. 268-276.
4. Cho, M. H.; Lee, C. H.; Lee, S., *Influence of floc structure on membrane permeability in the coagulation-MF process*. Water Science and Technology, 2005. **51**(6-7): p. 143-150.
5. Yang, W. Y.; Qian, J. W.; Shen, Z. Q., *A novel flocculant of Al(OH)(3)-polyacrylamide ionic hybrid*. Journal of Colloid and Interface Science, 2004. **273**(2): p. 400-405.

6. Li, H. H.; Long, J.; Xu, Z. H.; Masliyah, J. H., *Novel polymer aids for low-grade oil sand ore processing*. Canadian Journal of Chemical Engineering, 2008. **86**(2): p. 168-176.
7. Zhao, B. Q.; Wang, D. S.; Li, T.; Chow, C. W. K.; Huang, C., *Influence of floc structure on coagulation-microfiltration performance: Effect of Al speciation characteristics of PACls*. Separation and Purification Technology, 2010. **72**(1): p. 22-27.
8. Chang, I. L.; Chu, C. P.; Lee, D. J.; Huang, C., *Polymer dose effects on filtration followed by expression of clay slurries*. Journal of Colloid and Interface Science, 1997. **185**(2): p. 335.

Chapter 6 Effect of Tailings Characteristics

The oil sands tailings produced from oil sands extraction process are a complicated fluid mixture of water, sand, silt clay, unrecovered hydrocarbons and dissolved chemicals [1]. In this chapter, the effect of bitumen content and fines content on tailings treatment is studied. Tailings were treated by polymer flocculants in some pre-determined conditions, such as at room temperature and pH 8.4.

6.1 Effect of bitumen content

In this section, tailings including different types of laboratory extraction tailings and diluted mature fine tailings with either low or high bitumen content were used to study the effect of bitumen content on settling and filtration.

6.1.1 Laboratory extraction tailings

The properties of laboratory extraction tailings prepared from SYN ore (SYN-tailings) are listed in Table 6-1.

Figure 6.1 shows the initial settling rate (ISR) of flocculated laboratory extraction tailings with either low bitumen (LB) or high bitumen (HB) content at different dosages of AIPAM4R, AIPAM6R, AIPAM8R and MF1011.

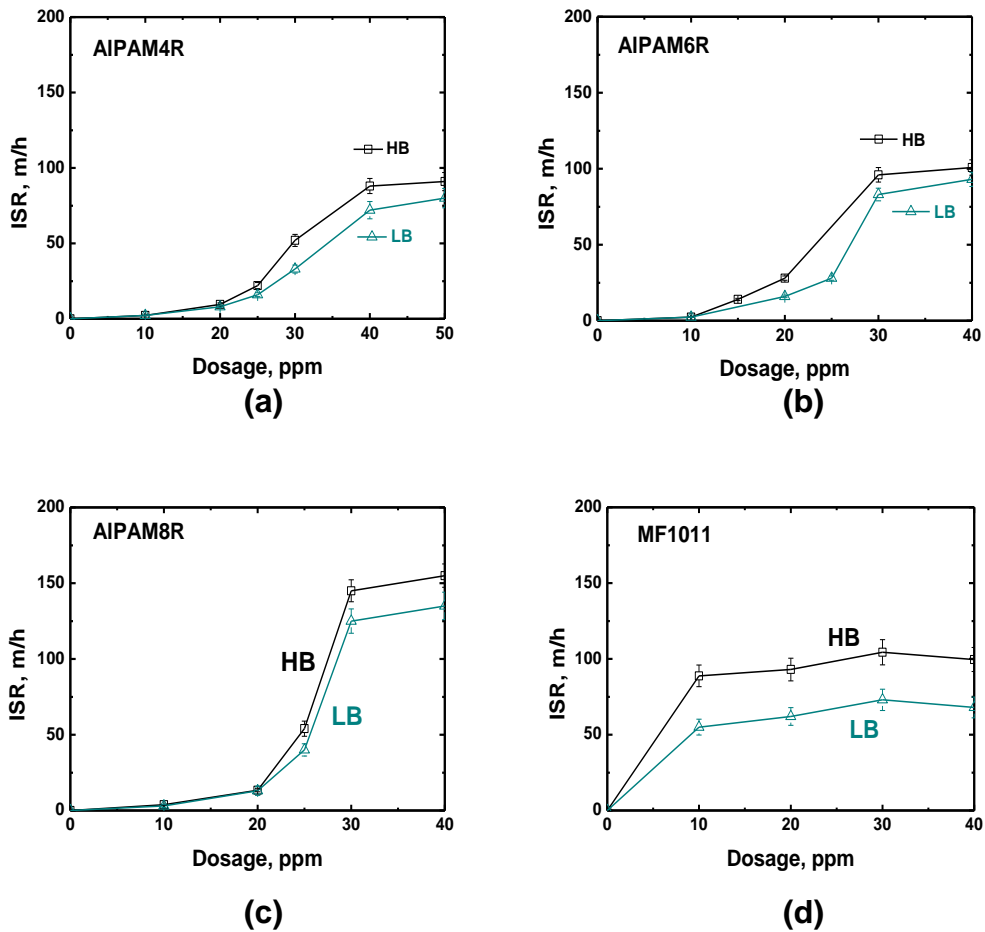


Figure 6.1 Initial settling rates of flocculated laboratory extraction tailings by (a) AIPAM4R; (b) AIPAM6R; (c) AIPAM8R; and (d) MF1011.

Figure 6.1 shows that the ISR of flocculated tailings with low and high

bitumen content by each polymer has the same trend, i.e., the ISR increases with increasing polymer dosage. For AI-PAMs, up to 30 ppm dosage, the settling rate was enhanced significantly, and adding additional AI-PAMs did not change settling rate significantly. For MF1011, 30 ppm was the optimum dosage. Figure 6.1 also shows that at a given dosage, the flocculated tailings with higher bitumen content settled slightly faster than those with lower bitumen content. For example, at 30 ppm dosage, the ISR of flocculated tailings with higher bitumen content was around 50, 90 and 140 m/h; after further removal of bitumen from the tailings, the ISR of corresponding flocculated tailings was around 30, 80, and 125 accordingly for AIPAM4R, AIPAM6R and AIPAM8R, respectively.

Figure 6.2 (a), (b), (c) and (d) show the supernatant turbidity of flocculated SYN-tailings with low bitumen (LB) or high bitumen (HB) content at different dosages of AIPAM4R, AIPAM6R, AIPAM8R and MF1011.

Table 6-1 Composition of laboratory extraction tailings prepared from SYN ore (wt%)

Tailings	Bitumen	Solids	Fines in solids
SYN704HB	3.4	11	26
SYN704LB	0.8	11.2	26

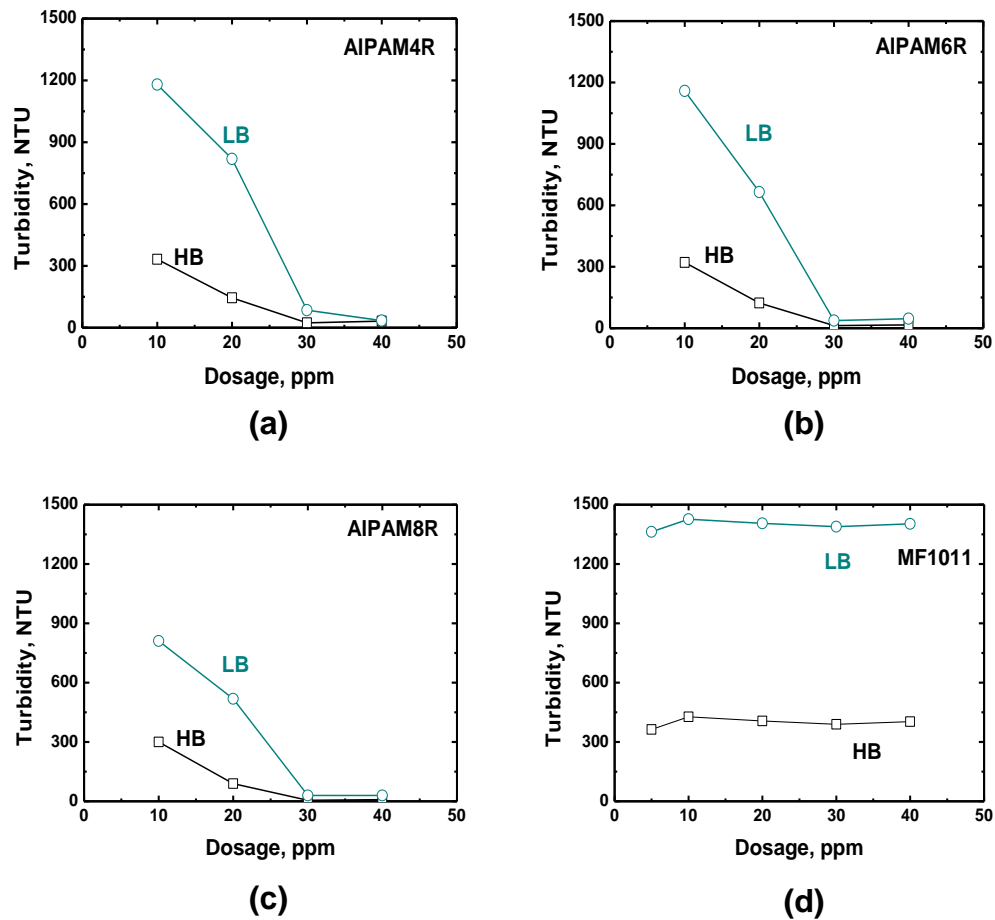


Figure 6.2 Supernatant turbidities of flocculated laboratory extraction tailings by (a) AIPAM4R; (b) AIPAM6R; (c) AIPAM8R; and (d) MF1011.

Figure 6.2 shows that the turbidity of supernatant from all AI-PAMs had the same trend, i.e., the turbidity decreased with increasing polymer dosage, regardless of bitumen content of tailings. With increasing AI-PAMs dosage up to 30 ppm, the supernatant turbidities were improved significantly; further addition of AI-PAMs did not bring significant improvement. Figure 6.2 also shows that at a given dosage, the flocculated SYN-tailings with

higher bitumen content had clearer supernatant than the one with low bitumen content. For example, the supernatant turbidity was 5NTU and 29NTU when 30 ppm AIPAM8R was added to the tailings of higher and lower bitumen contents, respectively. For MF1011, similar trend was observed, higher supernatant turbidities of tailings with lower bitumen content.

In Figure 6.3, the moisture content in the filter cake against time was plotted. The filtration performance of flocculated SYN-tailings with low and high bitumen content at selected dosages of different polymers is compared.

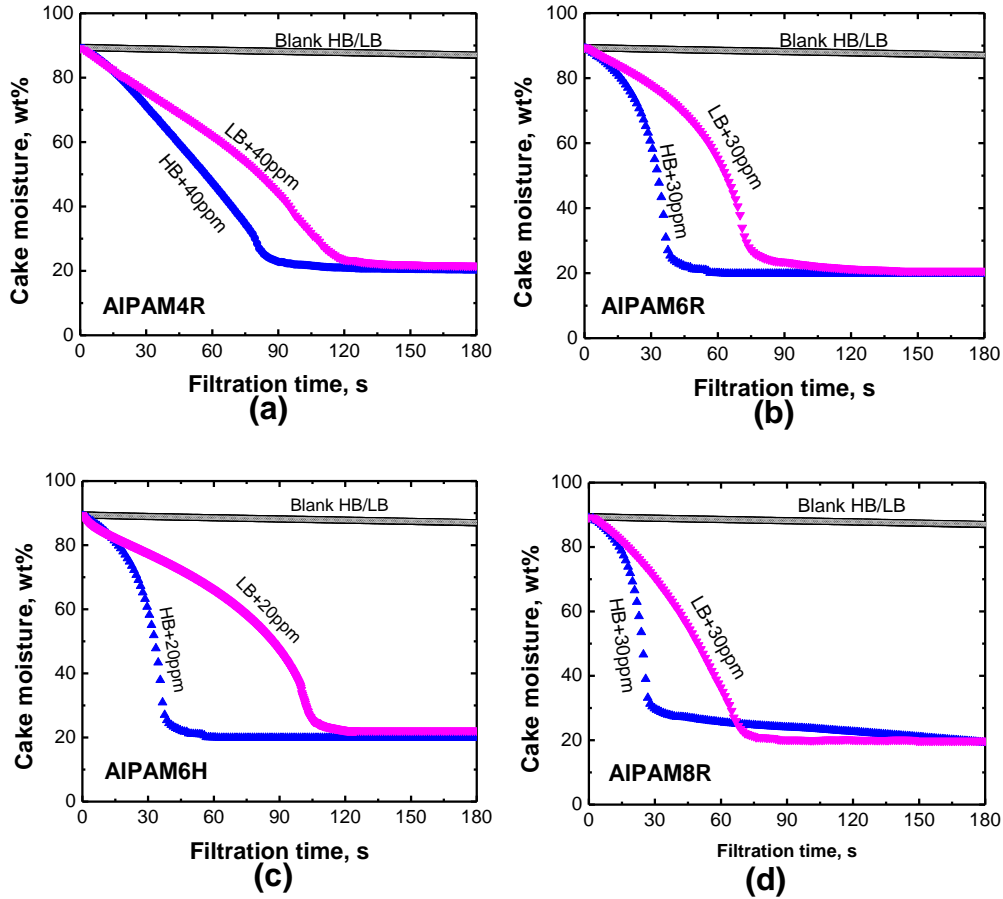


Figure 6.3 Filtration of flocculated laboratory extraction tailings at selected dosages of different polymers.

At a given dosage, the flocculated SYN-tailings with higher bitumen (HB) content were filtered slightly faster than those with lower bitumen (LB) content. For example, at 30 ppm of AIPAM8R, the filtration rate of tailings with lower bitumen content was 2.8 g/s, while the filtration rate of tailings with higher bitumen content was 2.2 g/s. In addition, the final cake moisture at each condition was similar regardless of the bitumen content. SRF of AI-PAMs at selected dosage is listed in Table 6-2.

Table 6-2 SRFs of flocculated laboratory extraction tailings by AI-PAMs at selected dosages

pH=8.4, at room temperature 22°C		Laboratory extraction tailings	
		SYN704HB	SYN704LB
		3.4 wt% bitumen, 11.0 wt% solids with 26 wt % fines	0.8 wt% bitumen, 11.2 wt% solids with 26 wt% fines
Polymer	Dosage, ppm	SRF, m/kg	SRF, m/kg
Blank	0	9.85×10^{11}	9.95×10^{11}
AIPAM4R	40	9.61×10^{09}	1.09×10^{10}
AIPAM6R	40	5.03×10^{09}	1.46×10^{10}
AIPAM8R	30	4.86×10^{09}	7.09×10^{09}

Another type of laboratory extraction tailings prepared from POSYN ore (see Table 6-3) was used to examine effect of bitumen content on the settling and filtration of oil sands extraction tailings. In this section, the tests were conducted with the addition of AIPAM8R at selected dosages.

Table 6.3 Composition of laboratory extraction tailings prepared from POSYN ore (wt%)

Tailings type		Bitumen	Solids	Fines in solids
POYSYN	HB	3.8	22	26
	LB	1.9	23	26

Figure 6.4 shows the results of settling and filtration for flocculated POSYN- tailings by AIPAM8R at selected dosages.

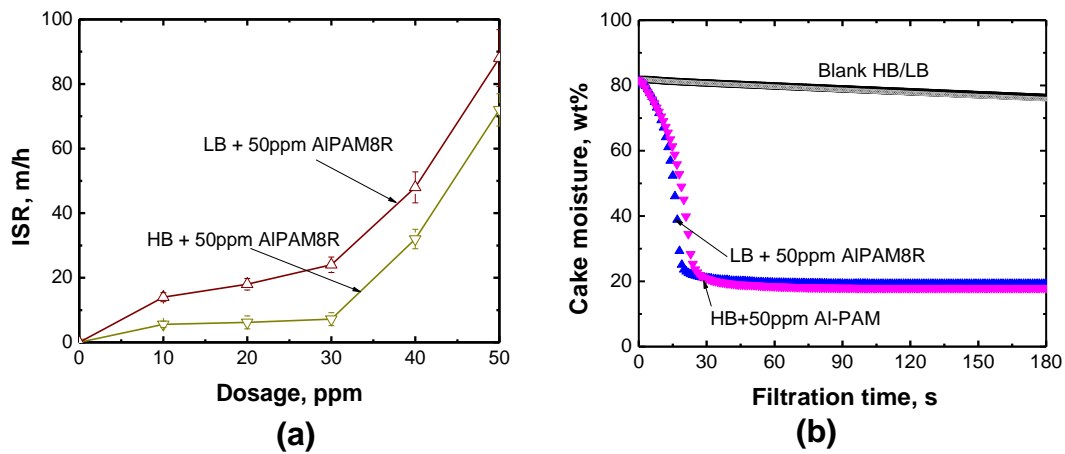


Figure 6.4 Effect of bitumen content on (a) initial settling rate; and (b) moisture content in filter cake of flocculated laboratory extraction tailings (prepared from POSYN ore) by AIPAM8R at selected dosages.

Figure 6.4 (a) shows that at a given dosage of AIPAM8R, the flocculated POSYN-tailings with higher bitumen (HB) content settled faster than those of lower bitumen (LB) content. Figure 6.4 (b) shows there was subtle difference between filtration of flocculated POSYN-tailings with different

bitumen content.

Overall, for laboratory extraction tailings, further removal of bitumen did not improve the performance of settling or filtration.

6.2 Effect of fines in supernatant

In the previous settling tests, the turbidities of supernatant of the flocculated tailings by MF1011 were higher than those of Al-PAMs. In order to confirm the effect of fines in supernatant on filtration of flocculated tailings, two groups of tests were designed and carried out. One was to filter the flocculated tailings directly, and the other to filter the flocculated tailings by Al-PAM first. When most of liquid was released, open the filter press, fill it with supernatant of flocculated tailings by either MF1011 or Al-PAM, which contains varying amount of unflocculated ultra fines, and continue to perform filtration.

6.2.1 Test procedure

Figure 6.5 shows the schematics of supernatant filtration experiment. Model fine tailings and laboratory extraction tailings were used to study the

effect of fines in supernatant on filtration of flocculated tailings.

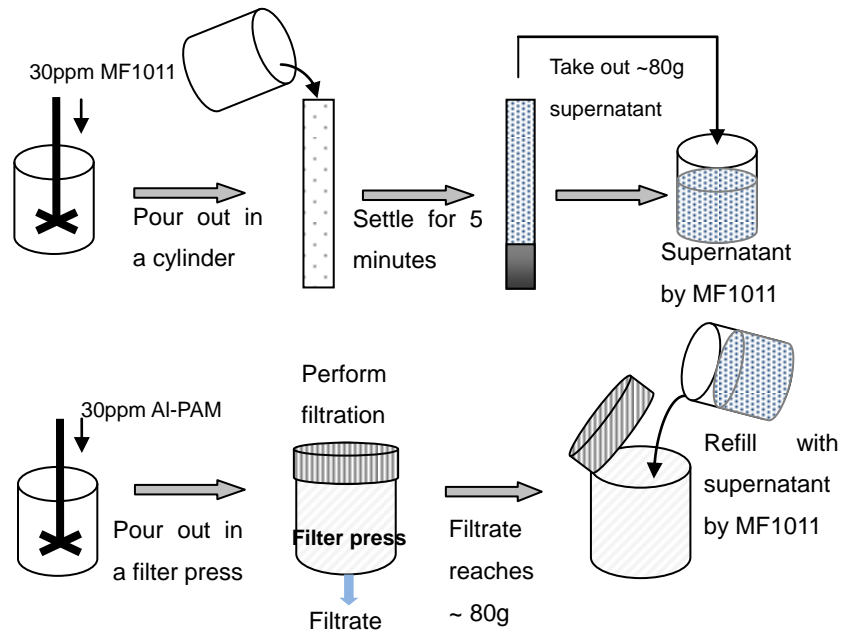


Figure 6.5 Schematics of supernatant-refilling filtration experiment.

The experiment was conducted as following:

1. Flocculate tailings with MF1011 or Al-PAM, and allow the settling for 5 minutes.
2. Decant the majority (80 ml) of the supernatant and leave it aside ready to be used in step 5.
3. Perform a filtration test of flocculated tailings by Al-PAM as a baseline.
4. Perform another group of filtration tests of flocculated tailings by Al-PAM until the released water reaches 80 g, at which point stop filtration immediately.

- Open the filter press and refill it with the prepared supernatant from step 2 right away to continue the filtration experiment.

6.2.2 Supernatant-refilling filtration experiment of model fine tailings

Figure 6.6 shows that the filtration of flocculated tailings refilled by the supernatants from Al-PAM was as efficient as direct filtration of flocculated tailings by Al-PAM. But when the supernatant from flocculated tailings by MF1011 was refilled, the filtration rate became much slower than that of supernatant of flocculated tailings by Al-PAM. The results clearly show the detrimental role of unflocculated fines in hindering filtration of flocculated model fine tailings.

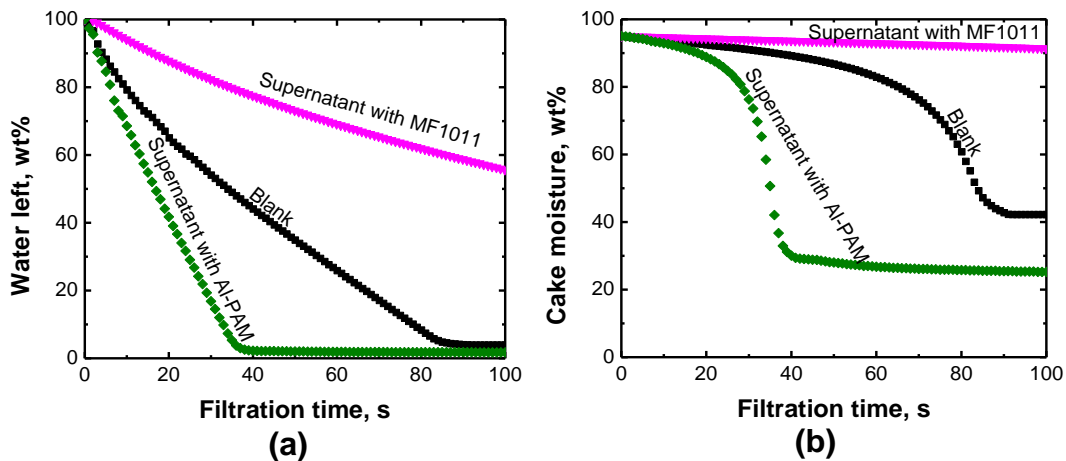


Figure 6.6 Filtration to supernatant of flocculated model fine tailings by MF1011 and Al-PAM as (a) percent of water left in tailings; and (b) moisture content of filter cake as a function of filtration time.

6.2.3 Supernatant-refilling experiment of laboratory extraction tailings

AIPAM8R and MF1011 were used in the flocculation and filtration of laboratory extraction tailings (11 wt% solids with 26 wt% fines). Figure 6.7 shows the results of filtration for flocculated laboratory extraction tailings.

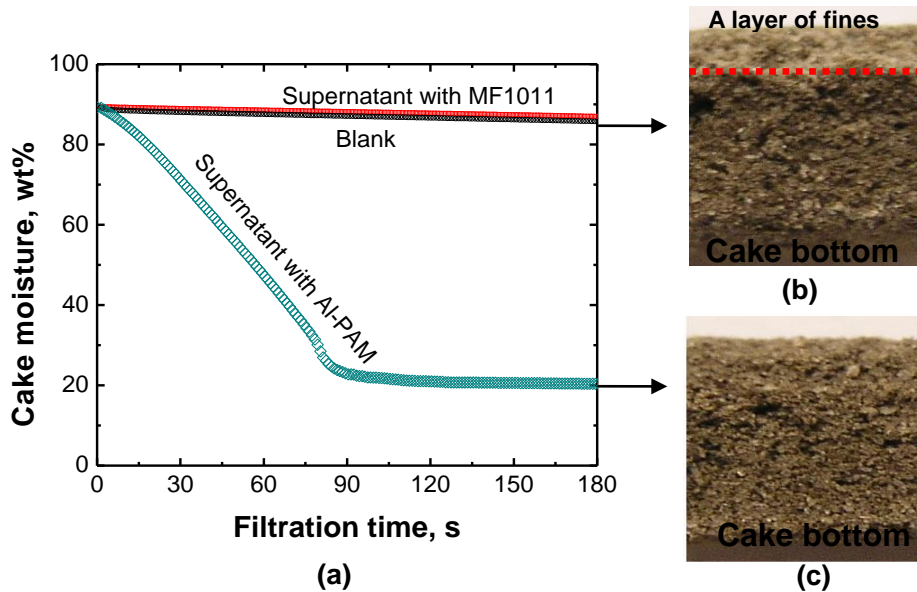


Figure 6.7 (a) filtration to supernatant of flocculated laboratory extraction tailings by Al-PAM and MF1011; (b) photograph of cross section of filter cake from flocculated tailings with refilled supernatant with MF1011; and (c) photograph of cross section of filter cake from flocculated tailings with refilled supernatant with Al-PAM.

Figure 6.7 (a) shows that the filtration of flocculated tailings refilled by the supernatant from Al-PAM was much efficient than that of flocculated tailings refilled by MF1011. In addition, Figure 6.7 (c) shows that filter cake

from flocculated tailings by Al-PAM supernatant was porous across the cake thicken from the top to the bottom, while there was a thin layer of fines exhibiting a light color on the top of filter cake, obtained from flocculated tailings with refilled MF1011 supernatant (see Figure 6.7 (b)). The light thin layer of fines is the non-flocculated fines that block the pore of filter cakes, leading to blockage of liquid flow.

6.2.4 Discussion

Figure 6.8 shows the filter cakes with different permeability. In studying the effect of fines experiments, a uniform slurry mixture of coarse particles or flocs would form a more permeable cake [2, 3] such as the filter cake derived by filtering flocculated tailings with Al-PAM directly. In the filtration of refilling supernatant with MF1011, the filter medium was filter paper and filter cake formed from flocculated tailings by Al-PAM on the top. Un-flocculated fines in the supernatant of flocculated tailings by MF1011 blocked the channels in the filter medium, leading to the filter cake of lower permeability. Fouling refers to the deposition of suspended particles at the pore opening of the filter medium or within the pores of the filter medium [2, 3], as observed in the filter cake of tailings without flocculants addition (blank).

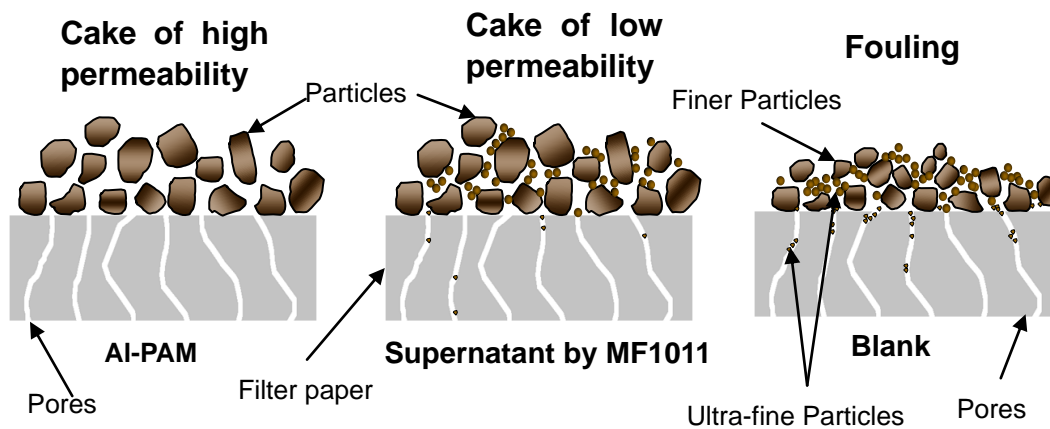


Figure 6.8 A schematic diagram of different filter cake structures.

In this study, P was 15 kPa, filter area of the filter press A was 45.8 cm², and viscosity μ of filtrate was considered as the same as pure water at room temperature. Using the data for Figure 6.6 and Figure 6.7, t/V was plotted against V as shown in Figure 6.9 (a) and (b), from which corresponding SRFs were calculated and the results are given in Table 6-4.

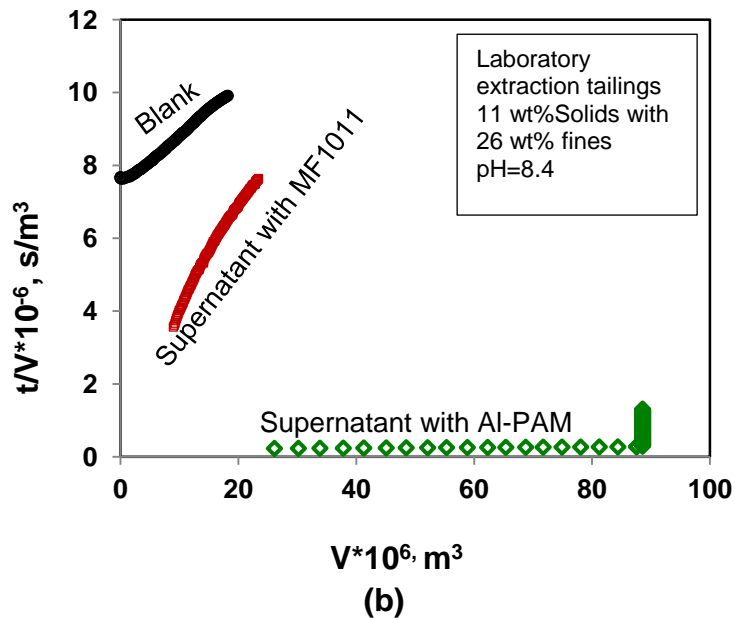
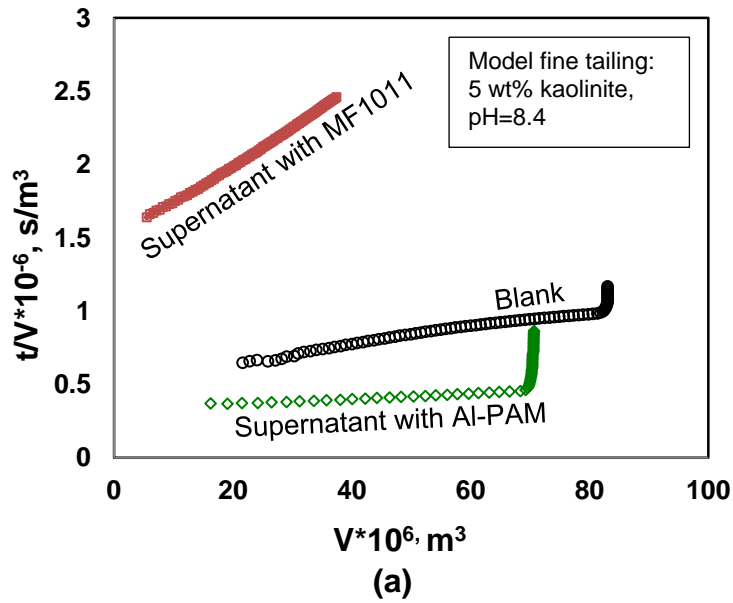


Figure 6.9 Linear fit of t/V - V for (a) model fine tailings; and (b) laboratory extraction tailings (pH=8.4).

For either model fine tailings or laboratory extraction tailings, SRF of filtering flocculated tailings by Al-PAM was much lower than the one by MF1011. Fines can be more effectively flocculated or/and coagulated by

Al-PAM than by MF1011.

Table 6-4 SRFs of the supernatant filtration tests

Tailings	Conditions	SRF, m/kg
Model fine tailings with 5 wt% kaolinite, pH=8.4	Blank	7.80 E+11
	30 ppm MF1011	3.36E+12
	30 ppm Al-PAM	1.51E+09
	supernatant with MF1011	6.48E+11
	supernatant with Al-PAM	2.44E+09
Laboratory extraction tailings, 11wt% solids with 26 wt% fines. pH=8.4	Blank	9.85E+11
	30 ppm MF1011	8.25E+11
	30 ppm Al-PAM	4.86E+09
	supernatant with MF1011	1.55E+11
	supernatant with Al-PAM	5.14E+09

SRFs of filtration for supernatant with Al-PAM through a filter cake were much lower than the one with MF1011, but slightly higher than filtration of flocculated tailings by Al-PAM. In the case of MF1011, fines in supernatant contribute to the poor filtration of tailings. In the case of filtering supernatant of flocculated tailings by Al-PAM, the more compact filter cake seems to contribute to a slightly higher SRF of laboratory extraction

tailings.

References

1. *Backgrounder: Oil sands tailings and directive 074*. 2009.
2. Dickey, G. D., *Filtration*. 1961, New York: Reinhold Pub. Cop. Chapter 3 and 9.
3. Crittenden, J. C.; Trussell, R. R.; Hand, D. W.; Howe, K. J.; Tchobanoglous, G., *Water treatment - principles and design* 2nd ed. 2005, New Jersey: John Wiley & Sons. Chapter 9.

Chapter 7 A Proposal of Al-PAM Assisted Flocculation - Filtration Dewatering System for Oil Sands Tailings Treatment

Tailings treatment and management have been pursued, not only for limiting the size of the tailings ponds, but also for efficient water recycling and energy savings [1]. In general, the temperature of the industrial fresh tailings is around 40-50°C [1]. It is necessary to investigate the settling behaviour and filtration performance at an average temperature (e.g. 45°C) similar to that of real operation temperature in industry. AIPAM8R was applied to the model fine tailings and laboratory extraction tailings in the settling and filtration tests.

7.1 Settling behaviour at different temperatures

Settling of flocculated tailings with Al-PAM at a high temperature (H.T. - 45°C) was compared with the results obtained from room temperature (R.T. - 22°C).

Figure 7.1 shows the set-up for settling of flocculated tailings at a higher temperature, where the major processing (i.e. mixing and settling) was conducted in a water bath of temperature at 45°C

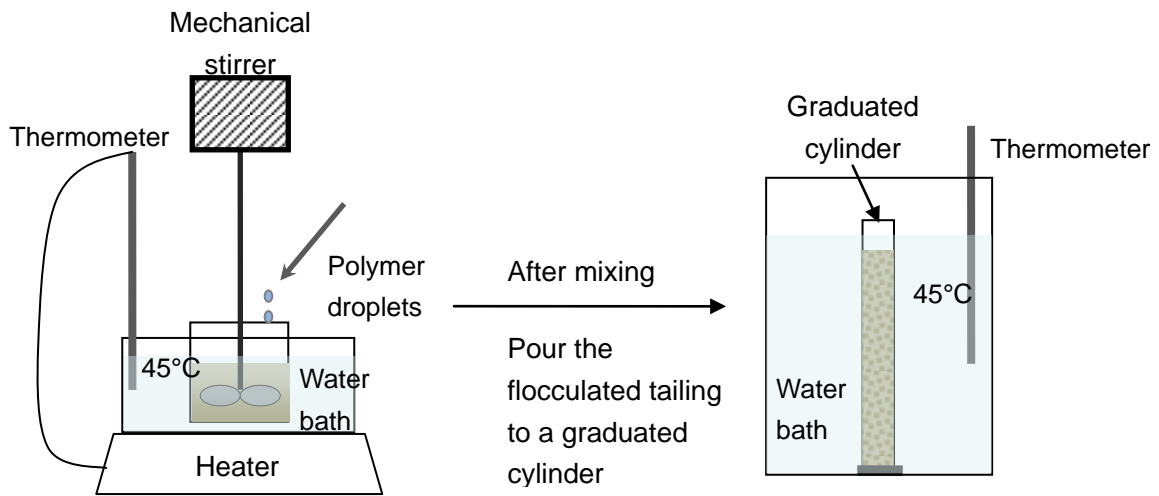


Figure 7.1 Schematics of set-up for settling at 45°C.

7.1.1 Settling tests

Figures 7.2 (a) and (b) show that for model fine tailings, an optimum initial settling rate of 38 ± 2 m/h, was obtained at 40 ppm AIPAM8R addition for both settling temperatures.

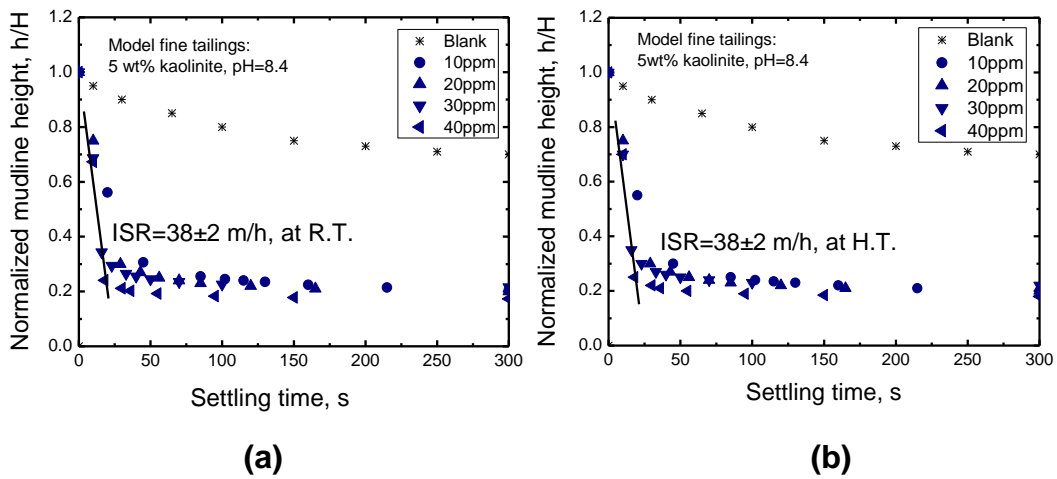


Figure 7.2 Settling behaviour of the flocculated model fine tailings by AIPAM8R at (a) 22 °C (R.T.); and (b) 45°C (H.T.).

Figure 7.3 shows that for laboratory extraction tailings (11.2 wt% solids with 26 wt% fines), an optimum initial settling rate of 100±10 m/h was obtained with the addition of 30 ppm AIPAM8R at 22° C and 45° C.

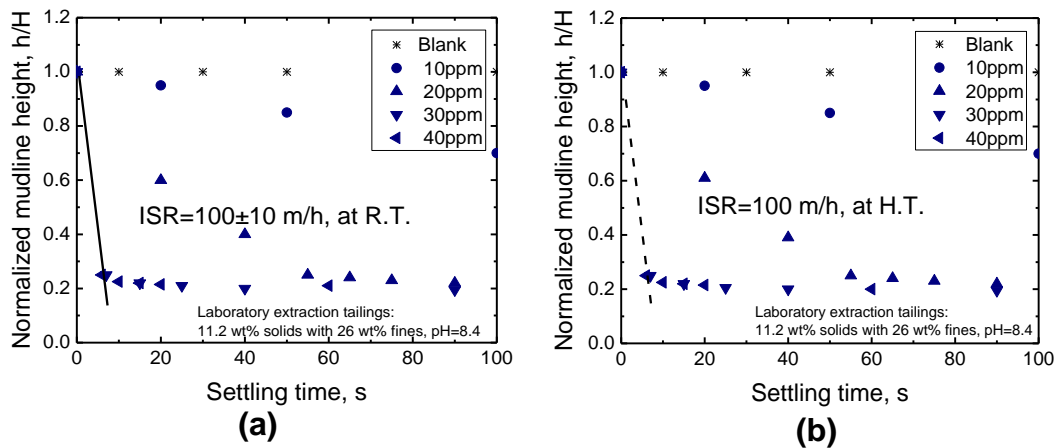


Figure 7.3 Settling behaviour of the flocculated laboratory extraction tailings by AIPAM8R at (a) 22 °C (R.T.); and (b) 45°C (H.T.).

For both model fine tailings and laboratory extraction tailings, Al-PAM can improve settling rates regardless of mixing and settling temperatures. A clear mud line was observed during the settling process. Overall, temperature had very little effect on flocculation and hence settling of flocculated tailings.

7.1.2 Discussion

Changing temperature leads to changes in the polymer chain conformation [2], which is usually defined as dimensions of macromolecules [3]. Here, expansion coefficient, root-mean-square end-to-end distance of the chain and hydrodynamic radius of a polymer coil in the solution are used to describe the polymer conformation. The relationship of expansion coefficient, α_{exp} , can be shown by the following equations.

$$\alpha_{\text{exp}} = \left(\frac{[\eta]}{[\eta_{\theta}]} \right)^{1/3} \quad (7.1)$$

where, $[\eta]$ is intrinsic viscosity of polymer solution at a given temperature, and $[\eta_{\theta}]$ is intrinsic viscosity of polymer solution at θ temperature [2]. From equation 7.1, it can be seen that α_{exp} is proportional to $[\eta]^{1/3}$. Since $[\eta_{\theta}]$

is a constant, the α_{exp} decreases when temperature rises, as $[\eta]$ becomes lower at higher temperatures [2, 4].

$$\left(\overline{r^2}\right)^{1/2} = \left(\frac{[\eta]M}{\phi}\right)^{1/3} \quad (7.2)$$

The root-mean-square end-to-end distance of polymer chain, $\overline{r^2}$, is given by equation 7.2, where $[\eta]$ is intrinsic viscosity (dm^3/g), ϕ is Flory-Fox constant approximately equal to $2.1 \times 10^{21} \text{ mol}^{-1}$, [5]. M is polymer molecular weight (g/mole). Equation 7.2 reveals that $\left(\overline{r^2}\right)^{1/2}$ is proportional to $[\eta]^{1/3}$ as well. When temperature rises, the $\left(\overline{r^2}\right)^{1/2}$ diminishes because the $[\eta]$ becomes lower at higher temperatures [2, 4].

$$R_h = f \frac{\left(\overline{r^2}\right)^{1/2}}{\phi^{1/2}} \quad (7.3)$$

The hydrodynamic radius of a polymer coil in the solution, R_h , is given by equation 7.3, where $\left(\overline{r^2}\right)^{1/2}$ is the root-mean-square end-to-end distance of the chains, and f is a constant irrespective of polymer molecular weight [2]. From equation 7.3, we can see that R_h is proportional to $\left(\overline{r^2}\right)^{1/2}$. Thus when temperature rises, $\left(\overline{r^2}\right)^{1/2}$ decreases, causing R_h to decrease.

Figure 7.4 shows the schematics of polymer conformation at low and high temperatures, respectively.

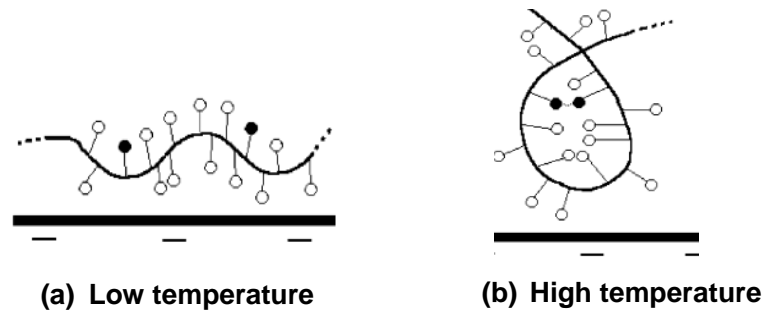


Figure 7.4 Schematics of polymer conformation at different temperatures [4].

From the above equations we know that when temperature increases, α_{exp} , $(\overline{r^2})^{1/2}$, and R_h which represent the polymer stretching situation in solutions, decrease. Such polymer conformation is referred to dimension shrinkage, i.e., the polymer coils tend to curl up at higher temperatures [4]. Compared to the polymer in solution at lower temperatures, the molecule coils at higher temperature have less active surfaces due to curling up (as shown in Figure 7.4(b)) , which results in the association of particles in relatively smaller volumes of flocs, leading to a decrease in the settling rate [6, 7]. It is less effective for bridging particles, forming smaller flocs of less number of particles. On the other hand, the viscosity of water also has impact on the settling behaviour as shown by equation 7.4. generalized for the hindered-settling [8, 9] :

$$V_p = \frac{g(\rho_A - \rho_w)d_A^2}{18\mu_w}(1 - \varphi_A)^{4.65} \quad (7.4)$$

where V_p is hindered-settling velocity, ρ_A is density of aggregate, ρ_w is density of liquid, φ_A is volume fraction of aggregate, g is acceleration of gravity and μ_w is viscosity of water at a given temperature. The viscosity of water, μ , is inversely proportional to the temperature [10]. For example, the viscosity of water at room temperature (22°C) is about $1 \cdot 10^{-3}$ Pa·s and at 45°C, it is about $0.6 \cdot 10^{-3}$ Pa·s [10]. Therefore, when temperature rises, the hindered- settling increases.

Considering the overall effects of floc size and the viscosity of water, temperatures for the given range from 22 °C to 45 °C had little effect on settling of flocculated tailings.

7.2 Filtration performance at different temperatures

Filtration tests of different tailings flocculated at 45°C were conducted to investigate the effect of temperature on filtration of flocculated tailings with Al-PAM.

Figure 7.5 shows the set-up for filtration at a higher temperature, where the filter press was covered an electrical heating band to keep the filtration at 45° C for the entire process.

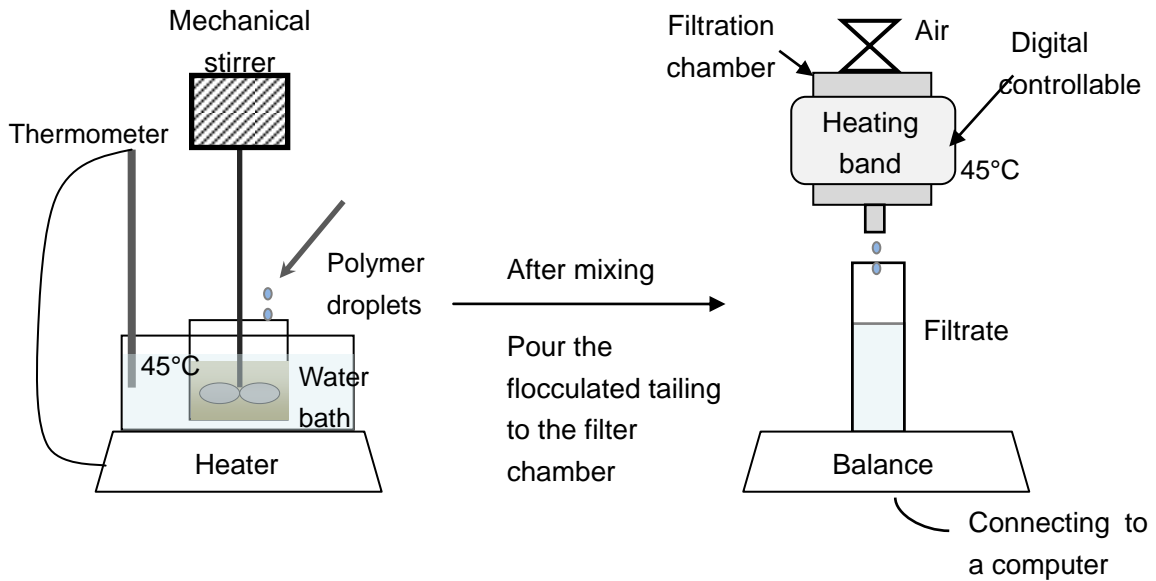


Figure 7.5 Schematics of set-up for filtration at 45°C.

Model fine tailings (5 wt% kaolinite, pH= 8.4) and lab extraction tailings (11.2 wt% solids with 26 wt% fines, pH=8.4) were used in the following filtration tests at different temperatures.

7.2.1 Model fine tailings

Figure 7.6 shows the filtration of flocculated model fine tailings at different

temperatures.

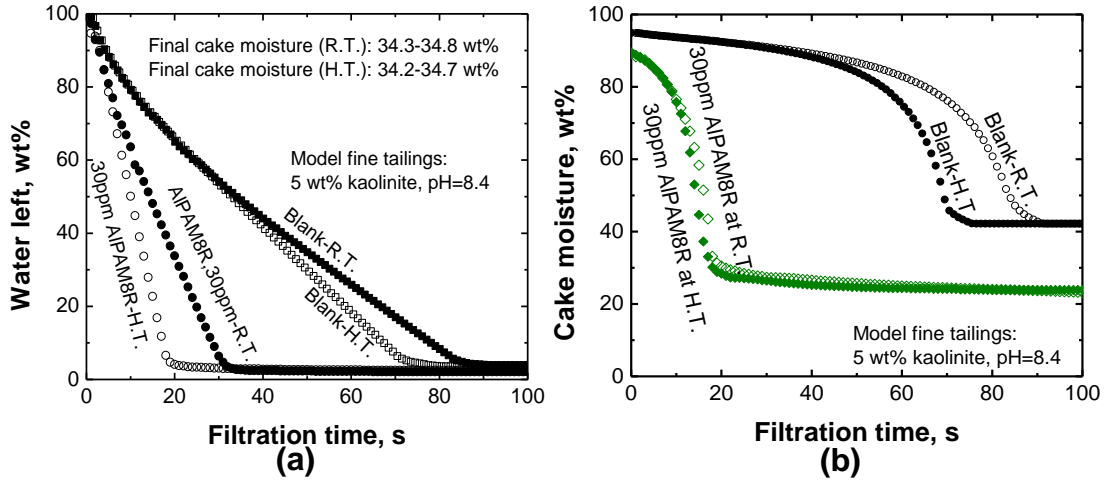


Figure 7.6 Comparison of filtration performance of the flocculated model fine tailings by AIPAM8R at 22 °C (R.T.) to 45 °C (H.T.) as (a) percent of water left in tailings; and (b) moisture content of filter cake as a function of filtration time.

Figure 7.6 shows slight better filtration performances at 45 °C than at 22 °C (room temperature) for model fine tailings. Figure 7.6 (a) shows filtration rate of flocculated model fines tailings with 30 ppm AIPAM8R addition was a little bit faster at 45 °C than at 22 °C. The final moisture content of 34.2-34.8 wt% of the filter cakes was practically the same. Figure 7.6 (b) shows the moisture content in the filter cake as a function of filtration time. At both temperatures, cake moisture was reduced by flocculation with AI-PAM as compared to the case without polymers. However, there is no significant effect of temperature on cake moisture.

The results of SRFs for flocculated model fine tailings with Al-PAM at selected dosages in Table 8-1 show that the SRFs were similar at different temperatures.

Table 7-1 SRFs of flocculated model fine tailings by Al-PAM at different temperatures

Temperature	Dosage, ppm	SRF, m/kg
Room Temperature (RT), 22°C	Blank, 0 ppm	7.80E+11
	AIPAM8R, 30 ppm	1.51E+09
Higher temperature (HT), 45°C	Blank, 0 ppm	5.92E+11
	AIPAM8R, 30 ppm	1.38E+09

7.2.2 Laboratory extraction tailings

Figure 7.7 shows that the filtration performance of the flocculated laboratory extraction tailings by AIPAM8R (11.2 wt% solids with 26 wt% fines) was slight better at 45°C than at room temperature, while the filter cakes achieved at either temperatures had practically the same final cake moisture of 19.5 -20.0 wt%.

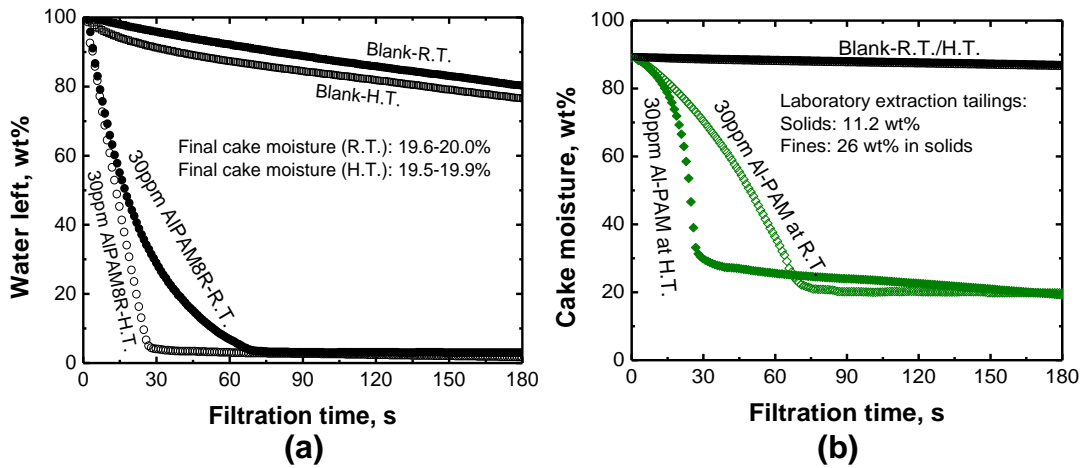


Figure 7.7 Comparison of filtration performance of the flocculated laboratory extraction tailings by AIPAM8R at 22 °C (R.T.) to 45 °C (H.T.) as (a) percent of water left in tailings; and (b) moisture content of filter cake as a function of filtration time.

Here, we can see that the filtration rate of flocculated tailings by Al-PAM is slightly higher at 45 °C than at room temperature, corresponding to a slightly lower SRF (see Table 7-2). 10^{-6}

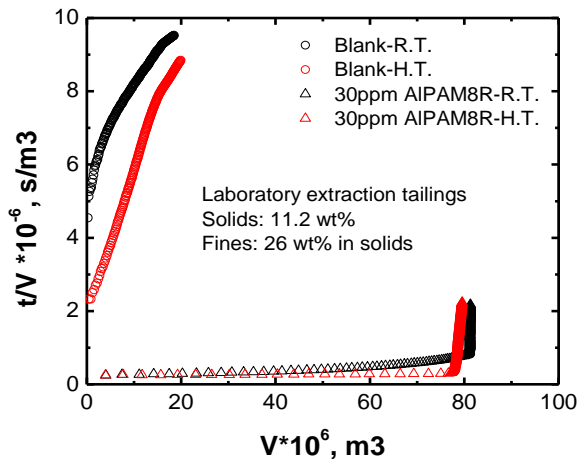


Figure 7.8 Effect of temperature on SRF of flocculated laboratory extraction tailings by Al-PAM.

Table 7-2 SRFs and filtration rates of flocculated laboratory extraction tailings by Al-PAM at different temperatures

Laboratory extraction tailings, 11.2% solids with 26 vol.% fines			
Temperature	Dosage, ppm	SRF, m/kg	Filtration rate, g/s
Room Temperature (RT), 22°C	Blank, 0 ppm	9.95E+11	0.16
	AIPAM8R, 30 ppm	7.09E+09	2.68
Higher temperature (HT), 45°C	Blank, 0 ppm	3.78E+11	0.18
	AIPAM8R, 30 ppm	6.32E+09	2.94

In general, for both model fine tailings and laboratory extraction tailings, temperature had little effect on settling and filtration performances.

7.2.3 Discussion

For a filtration system of constant P and A , but different μ , the filtration rate does depend on both SRF and the suspension viscosity [11]. The higher the temperature, the lower is the viscosity of suspensions [4]. In this study, pressure difference P and filter area A were constant. Viscosity μ of filtrate was higher ($1 \cdot 10^{-3}$ Pa·s) at room temperature than at 45 °C ($0.6 \cdot 10^{-3}$ Pa·s). A smaller value of viscosity results in a smaller value of the slope, leading to a higher filtration rate [11].

7.3 Comparison of direct filtration of whole tailings to filtration of sediments

From chapter 6, we know that fines in supernatant were disadvantage for filtration of flocculated tailings. Removal of supernatant from flocculated tailings after settling to reduce effect of fines became appealing and hence comparison experiments for filtration of whole tailings and sediments were conducted.

7.3.1 Procedure for sediment filtration experiment

First, MF1011 or Al-PAM was added to the tailings while mixing. The flocculated tailings were allowed to settle for 5 minutes in a graduating cylinder until no visible descending of mudline. After settling, 80 ml of the supernatant from the cylinder were taken. Filtration was carried out on the sediment (e.g. the rest of the tailings), and the weight of the released water was recorded as a function of filtration time.

Figure 7.9 shows that direct filtration of sediments of flocculated model fine tailings by polymers was more efficient than filtration without polymers.

7.3.2 Model fine tailings

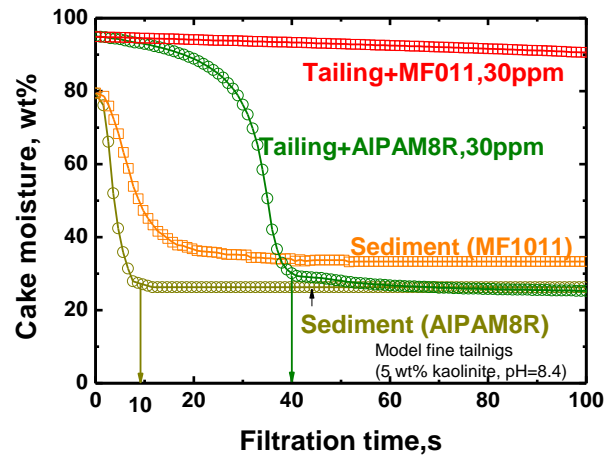


Figure 7.9 Filtration to sediments of flocculated model fine tailings by MF1011 and Al-PAM.

After removal of supernatant, filtration rates were improved by a factor of two. It took about 40 seconds for filtration of whole flocculated tailings to achieve a filter cake with 35 wt% moisture, while 10 seconds were required for filtration of sediment of flocculated tailings after supernatant removal to achieve a filter cake with 35 wt% moisture. For MF1011, since the unflocculated fines remained in the supernatant were removed, there was less fines to block pores of filter cake [12].

7.3.3 Laboratory extraction tailings

Figure 7.10 shows that direct filtration of sediments of flocculated

laboratory extraction tailings by polymer flocculants was also much more efficient than filtration without addition any flocculants. For Al-PAM, after removal of supernatant, filtration efficiency of model fine tailings by AIPAM8R doubled. It took about 30 seconds for filtration of whole flocculated tailings to achieve a filter cake with 20 wt% moisture, whereas it took about 10 seconds for filtration of sediment of flocculated tailings after supernatant removal to achieve a filter cake with 20 wt% moisture. For MF1011, since the unflocculated fines remained in the supernatant were removed, there were fewer fines to block pores of filter cake [12], the filtration performance was improved significantly compared to filtration of whole tailings.

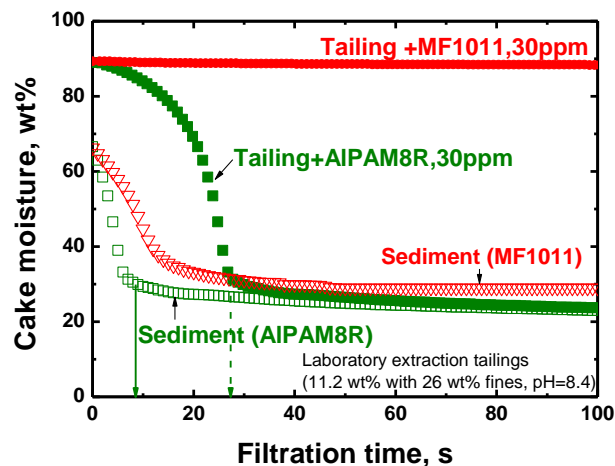


Figure 7.10 Filtration to sediments of flocculated laboratory extraction tailings by MF1011 and Al-PAM.

Figure 7.10 also shows filtration of sediments of Al-PAM was better than of MF1011, although the supernatant containing fines, which would be the key effect to filtration SFR, were removed. Table 7-3 gives the SRFs for filtration of whole tailings and sediments.

Table 7-3 SRFs of flocculated whole tailings and sediments

Tailings	Polymer	SRF, m/kg	
		Whole tailings	Sediments
Model fine tailings	MF1011, 30 ppm	8.31E+11	9.25E+09
	Al-PAM, 30 ppm	1.51E+09	1.30E+09
Laboratory extraction tailings	MF1011, 30 ppm	9.46E+11	9.58E+09
	Al-PAM, 30 ppm	7.09E+09	6.72E+09

Figure 7.11 shows the images of the flocs in sediments of flocculated laboratory tailings by Al-PAM and MF1011. The flocs from flocculated tailings by Al-PAM and MF1011 were taken and observed under the microscope. The size of the flocs of Al-PAM was even and the flocs were more integrated, while the majority of flocs of MF1011 was aggregated, but there were still some unflocculated small particles trapped in the sediment, which may also contribute to the higher turbidity of supernatant after settling and poor filtration performance.

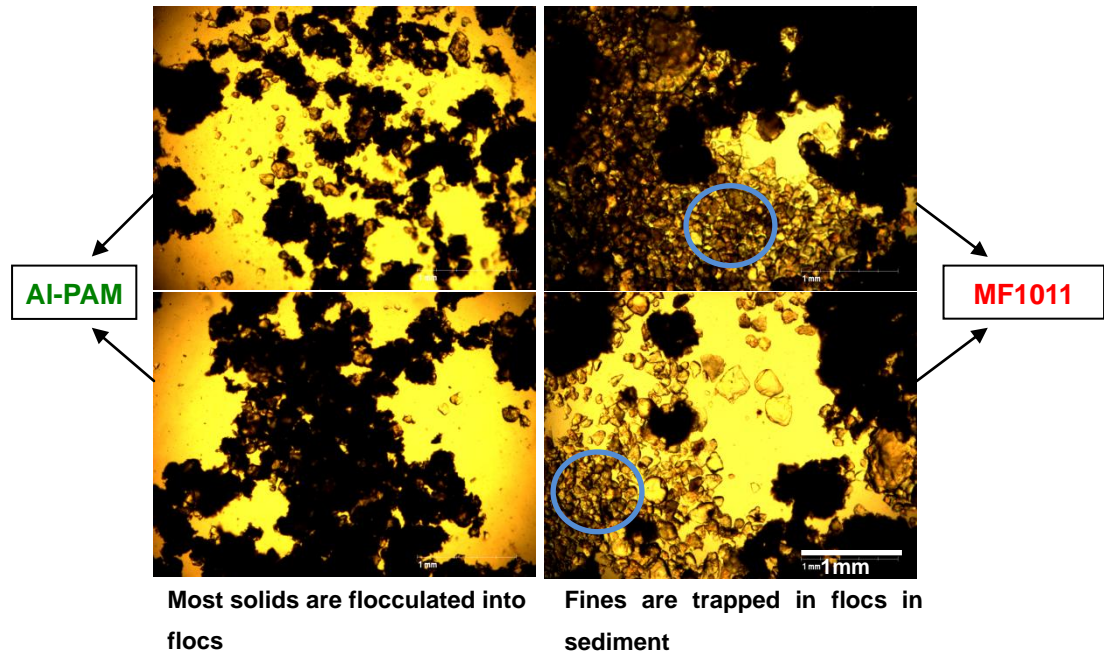


Figure 7.11 Images of flocs in sediment of flocculated laboratory extraction tailings by Al-PAM and MF1011.

7.3.4 Summary

The fines in supernatant contribute to poor filtration of tailings. Filtration of flocculated sediments is more attractive than filtration of whole flocculated tailings. Filtration of sediments of flocculated tailings after settling is more efficient than filtration of whole flocculated tailings. Fines can be more effectively flocculated or/and coagulated by Al-PAM than MF1011.

7.4 A Design of dewatering system

Based on what has been found and discussed above, since temperature

has no major effect on settling and filtration of laboratory oil sands extraction tailings with addition Al-PAM and filtration of sediments of flocculated tailings are much efficient than filtration of whole tailings slurry, a feasible dewatering system is suggested as shown in Figure 7.12.

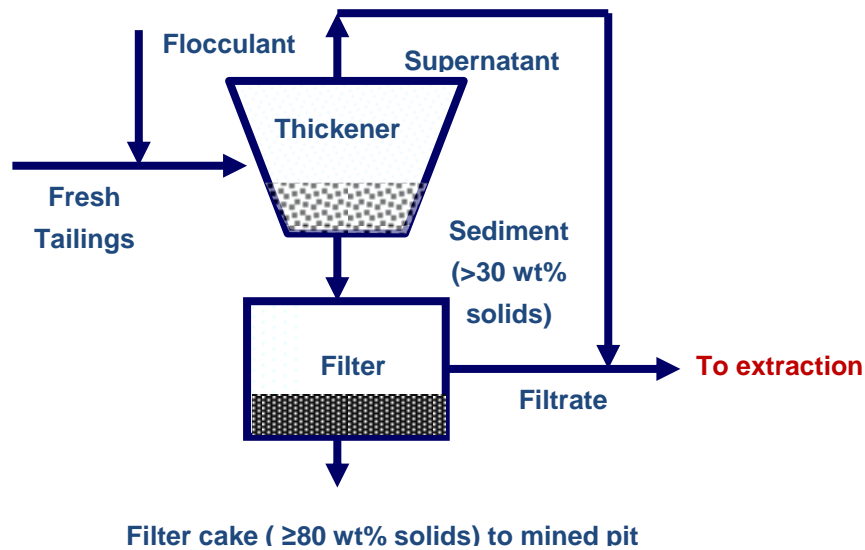


Figure 7.12 Concept of a novel two-step filtration process for treating large volume of oil sands extraction tailings: filtration of sediments after flocculation and thickening.

After extraction process, the fresh tailings (cyclone overflow) with about 10 wt% solids [13] are mixed with Al-PAM solution, and then the flocculated tailings flow into a special thickener, where the tailings can be settled (Solids content can be more than 30 wt%) [13]. The sediments are drained to a filter batch with large volume. Then pressure or vacuum is applied and the drainage water is collected, and it is recycled to other processes, such

as bitumen extraction. The filter cakes are dry enough (solid content ≥ 80 wt%) to be reclaimed directly [1].

Earlier protocol tests were conducted by conducting two sets of experiments (See Figure 7.13).

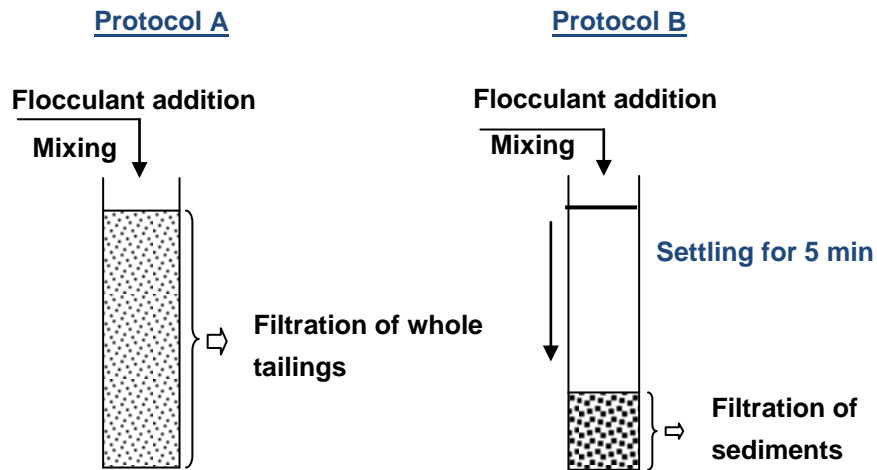


Figure 7.13 Procedure of concept tests.

Protocol A shows that filtration the whole tailings directly right after flocculated by MF1011 or A-PAM. In protocol B, the tailings are flocculated first, after settling for 5minutes and separation of supernatant, do filtration experiment to the rest sediments. Figure 7.14 (a) is for MF1011, the filtration of sediments is more efficient than filtration of whole tailings. Figure 7.14 (b) is of Al-PAM, the filtration efficiency of sediments is improved by about 60% compared to the filtration of whole tailings.

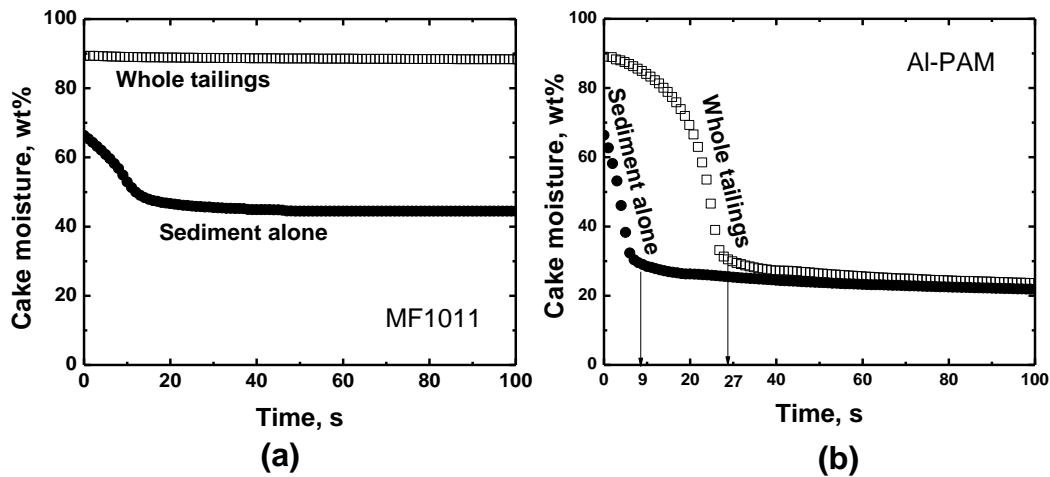


Figure 7.14 Comparison of filtration of whole tailings to sediments flocculated by (a) MF1011; and (b) Al-PAM.

References

1. Masliyah, J. H., *Fundamentals of oil sands extraction*. in Course Pack. 2008: University of Alberta.
2. Wisniewska, M., *Influences of polyacrylic acid adsorption and temperature on the alumina suspension stability*. Powder Technology, 2010. **198**(2): p. 258-266.
3. Wyatt, P. J., *The Size of Macromolecules and Some Observations on Their Mass*. Journal of Liquid Chromatography, 1991. **14**(12): p. 2351-2372.
4. Saadatabadi, A. R.; Nourani, M.; Emadi, M. A., *Rheological*

- behaviour and hydrodynamic diameter of high molecular weight, partially hydrolyzed poly(acrylamide) in high salinity and temperature conditions.* Iranian Polymer Journal. **19**(2): p. 105-113.
5. Bohidar, H. B., *Hydrodynamic properties of gelatin in dilute solutions.* International Journal of Biological Macromolecules, 1998. **23**(1): p. 1-6.
 6. Sabah, E.; Erkan, Z. E., *Interaction mechanism of flocculants with coal waste slurry.* Fuel, 2006. **85**(3): p. 350-359.
 7. Heath, A. R.; Bahri, P. A.; Fawell, P. D.; Farrow, J. B., *Polymer flocculation of calcite: Relating the aggregate size to the settling rate.* AIChE, 2006. **52**(6): p. 1987-1994.
 8. Michaels, A. S.; Bolger, J. C., *Settling rates and sediment volumes of flocculated kaolin suspensions.* Industrial & Engineering Chemistry Fundamentals, 1962. **1**(1): p. 24-33.
 9. Crittenden, J. C.; Trussell, R. R.; Hand, D. W.; Howe, K. J.; Tchobanoglous, G., *Water treatment - principles and design* 2nd ed. 2005, New Jersey: John Wiley & Sons. Chapter 9.
 10. *Handbook of chemistry and physics* 83rd edition. 2002: CRC Press.
 11. Xu, Y. M.; Dabros, T.; Kan, J. M., *Filterability of oil sands tailings.* Process Safety and Environmental Protection, 2008. **86**(B4): p. 268-276.

12. FTFC (Fine Tailings Fundamentals Consortium), *Advances in oil sands tailings research*. 1995, Alberta Department of Energy. Oil Sands and Research Division.
13. Jamasmie, C., *The challenges and potential of Canada's oil sands*, Mining, September-October 2010, p. 7-8.

Chapter 8 Conclusions and Future Work

8.1 Conclusions

Al-PAM is confirmed to be effective in flocculating oil sands extraction tailings for enhanced filtration. Al-PAMs of higher molecular weight and high Al content was identified to be more effective in flocculating fines in oil sands tailings and hence filtration. Removal of bitumen from laboratory extraction tailings did not improve flocculation and filtration of oil sands tailings by Al-PAM. Effective flocculation of ultrafine particles is the key for flocculant to be an effective filtration aid for oil sands extraction tailings. Filtration of sediments after flocculation-assisted thickening reduces filtration time significantly, making filtration more practical. Innovation in design of flocculants will provide a practical solution to management of oil sands tailings.

8.2 Recommendation for future work

Track the water chemistry of Al-PAM addition for the purpose of water recycling; especially watch the effect of residual chemicals on bitumen extraction.

Further effort is considered necessary to explore the effectiveness of Al-PAM at temperatures of oil sand extraction tailings as they are produced,

i.e., treating warm oil sands extraction tailings with AI-PAM and recycling the warm water, which would save more energy and make economic sense. Carry out tests on application of AI-PAM to various commercial tailings from industry, collecting more information and develop a process to apply AI-PAM practically and efficiently.

Appendices

Appendix A - Further investigation of Al-PAM structure

In order to further investigate the structure of Al-PAM, the following experiments of settling and filtration were conducted by comparing Al-PAM to PAM with similar intrinsic viscosity and the mixture of PAM and Al-Colloid (PAM+Colloid).

Synthesized PAM as the same procedure as AIPAM8R but using water instead of colloid solution. Mixture of PAM and Al-Colloid was prepared as follows: add Al-colloid solution (which was used to synthesize AIPAM8R) to 500 ppm PAM solution slowly, while gently mixing until the point at which Al content was 0.1% (the same as Al content in AIPAM8R).

Appendix A-I Settling behaviour

In this part, settling tests were conducted by adding Al-PAM, PAM and mixture of (PAM + Colloid), respectively, to model fine tailings or laboratory extraction tailings. When the mixture of (PAM + Colloid) was added slowly and evenly to the tailings drop wisely, flocs were observed to form gradually. Mixing was stopped at a given dosage of the mixture, and then the flocculated tailings were poured carefully into a cylinder right away. The settling behaviour were then recorded.

Figure A-1 shows that the initial settling rate of (PAM + Colloid) mixture was slightly lower than that of AIPAM8R at a given dosage. Furthermore, the initial settling rate at maximum dosage from mixture of (PAM + Colloid) was 10%-20% lower than that of AIPAM8R.

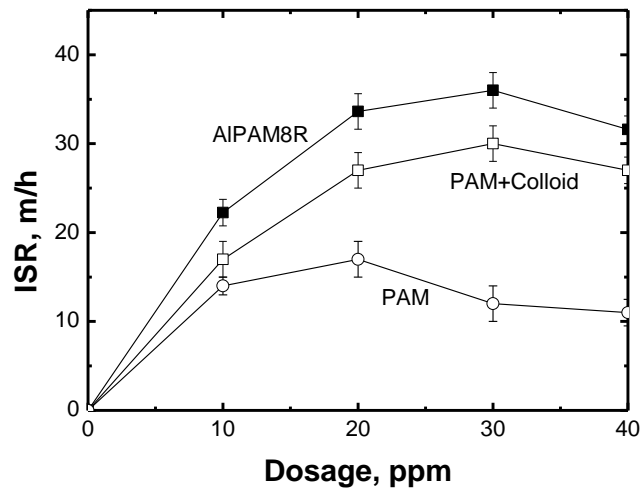


Figure A-1 Settling behaviour of model fine tailings with AIPAM8R, (PAM + Colloid) mixture, PAM, respectively before shaking.

Figure A-2 shows when the flocculated tailings by mixture of (PAM + Colloid) were shaken, the formed flocs were broken-up and settling behaviour became worse, back to the level of original PAM.

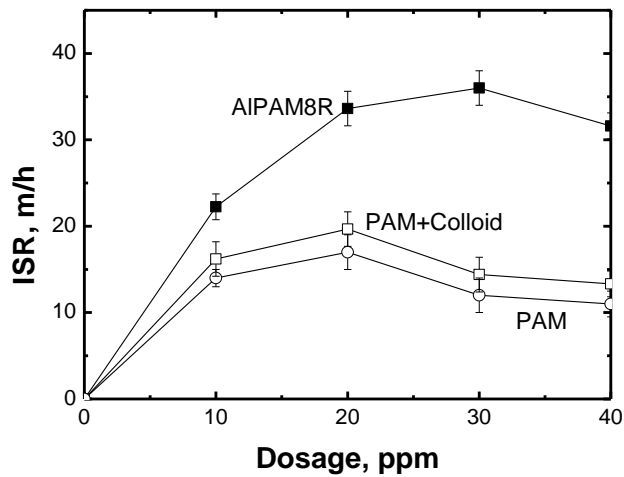


Figure A-2 Settling behaviour of model fine tailings with AIPAM8R, (PAM + Colloid) mixture, PAM, respectively after shaking.

Figure A-3 shows the settling results. Initial settling rate of (PAM + Colloid) mixture was lower than AIPAM8R at a given dosage. When the dosage was at or above 30 ppm, the difference in settling behaviour of Al-PAM and mixture of (PAM + Colloid) became significant. The initial settling rate of mixture ranged from 95 to 120 m/h, while the initial settling rate of Al-PAM ranged from 140 to 155 m/h.

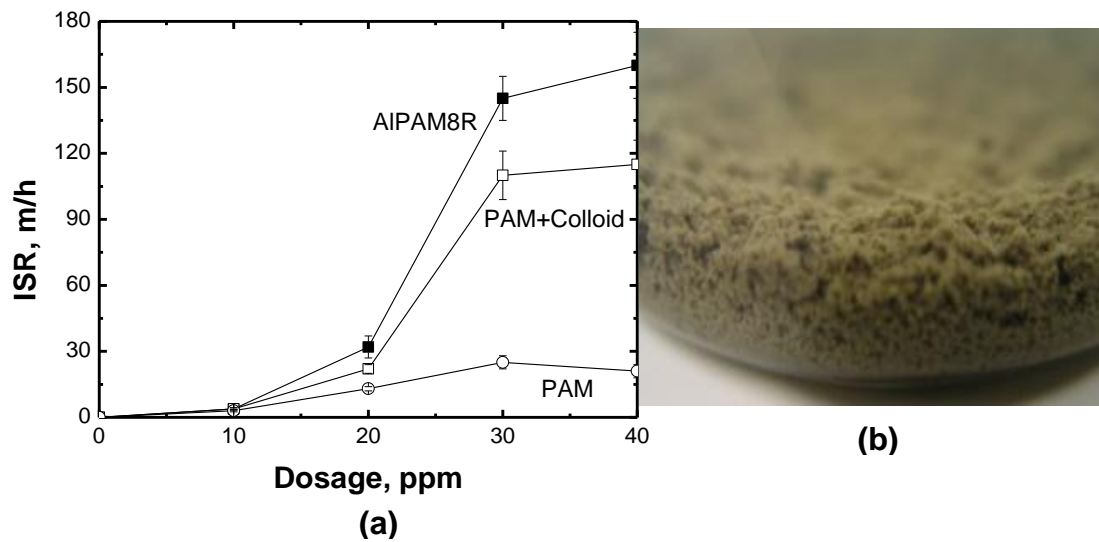


Figure A-3 (a) Settling behaviour of laboratory extraction tailings with AIPAM8R, (PAM + Colloid) mixture, PAM, respectively, before shaking; and (b) photograph of flocs for flocculated tailings by AI-PAM.

Tests of shaking the flocculated tailings by AI-PAM, PAM and mixture of (PAM + Colloid) were conducted subsequently. The settling process was recorded. For the mixture of (PAM+ Colloid), the formed flocs were broken-up partially after shaking and settled slower than before shaking and the settling rate was back to the level of original PAM (Figure A-4(a)). The photograph of flocs from mixture after shaking showed that the flocs were not stable and the ultimate size of flocs was small (See figure A-4(b)).

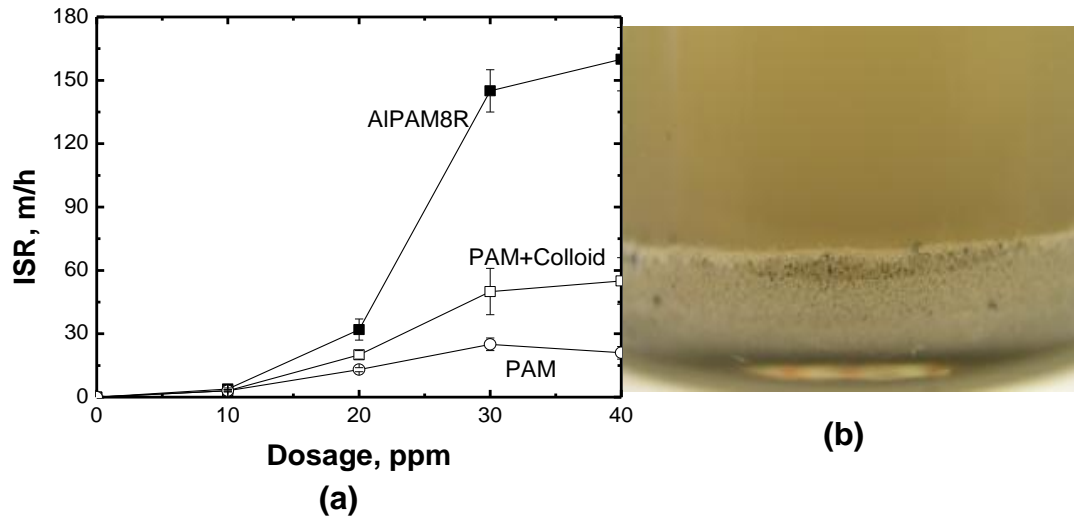


Figure A-4 (a) Settling behaviour of laboratory extraction tailings with AIPAM8R, (PAM + Colloid) mixture, PAM, respectively, after shaking; (b) photograph of released flocs of flocculated tailings by (PAM + Colloid) mixture after shaking.

Appendix A-II Filtration performance

Filtration results of flocculated model fine tailings and laboratory extractions with Al-PAM and mixture of (PAM + Colloid) are shown in Figure A-5.

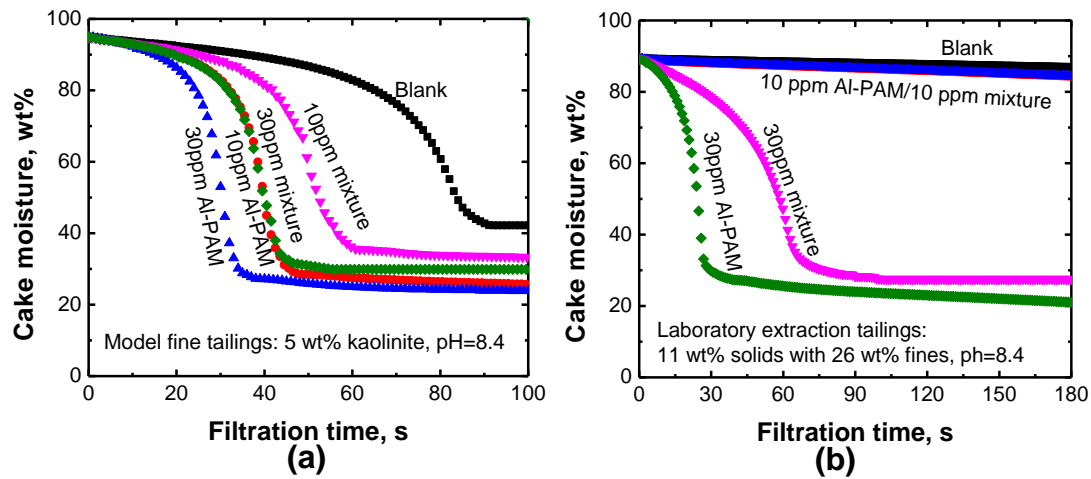


Figure A-5 Filtration performances of flocculated (a) model fine tailings; and (b) laboratory extraction tailings by Al-PAM or mixture of (PAM+Colloid).

For model fine tailings, the filtration rates were improved when either Al-PAM or the mixture of (PAM + Colloid) was added compared to absence of flocculants. In addition, the filtration rates were improved for both flocculants with increasing the dosage of flocculants. For a given dosage, the SRF of Al-PAM was lower than that of mixture of (PAM+Colloid) (see Table A-1), Correspondingly, the filtration rate of flocculated tailings by Al-PAM was higher than that of the mixture of (PAM+Colloid).

For laboratory extraction tailings, the filtration rates were improved when either Al-PAM or (PAM + Colloid) mixture used. In addition, the filtration rates were improved for both flocculants with increasing the dosage of flocculants. At low dosage such as 10 ppm, the filtration rate of flocculated

tailings by Al-PAM was very close to that of (PAM + Colloid) mixture. Both SRFs were similar too (see Table A-1). However, with increasing the dosages, the filtration rate of flocculated tailings by Al-PAM was obviously higher than that of (PAM + Colloid) mixture. SRF of Al-PAM was lower than mixture of (PAM+Colloid) at 30 ppm.

Table A-1 shows the SRFs of flocculated tailings by Al-PAM and mixture of (PAM+Colloid) at selected dosages.

Table A-1 SRFs of flocculated tailings by Al-PAM and mixture of (PAM+Colloid) at selected dosages

pH=8.4		Model fine tailings: 5 wt%	Laboratory extraction tailings: 11.2 wt% solids with 26 wt %
Polymer	Dosage, ppm	SRF, m/kg	SRF, m/kg
Blank	0	7.80E+11	9.95E+11
Mixture	10	2.23E+10	7.45E+11
	30	2.33E+10	1.18E+10
AIPAM8R	10	2.27E+09	7.44E+10
	30	1.51E+09	7.09E+09

Model fine tailings were used to study the mechanism of polymers for settling and filtration. MF1011 and PAM have similar polymer structure, a

single acrylamide chain. Their settling behaviour had the same trend. Figure A-6 (a) shows that for both MF1011 and house made PAM, the optimum dosage was 20 ppm. Due to different polymer chain length, as reflected by different viscosity and molecular weight (See Table A-2), the settling rates of MF1011 were higher than those of PAM at a given dosage. In addition, Figure A-6 (a) also shows that the settling rates of AIPAM8R were better than those of PAM, although they have similar intrinsic viscosity.

Table A-2 Characteristics of polymers

Polymer	Intrinsic viscosity, mL/g	Zeta potential, mV	Al content, wt%
MF1011	13968	anionic	0
PAM	853.5	0	0
AIPAM8R	834.6	+0.17±0.05	0.11

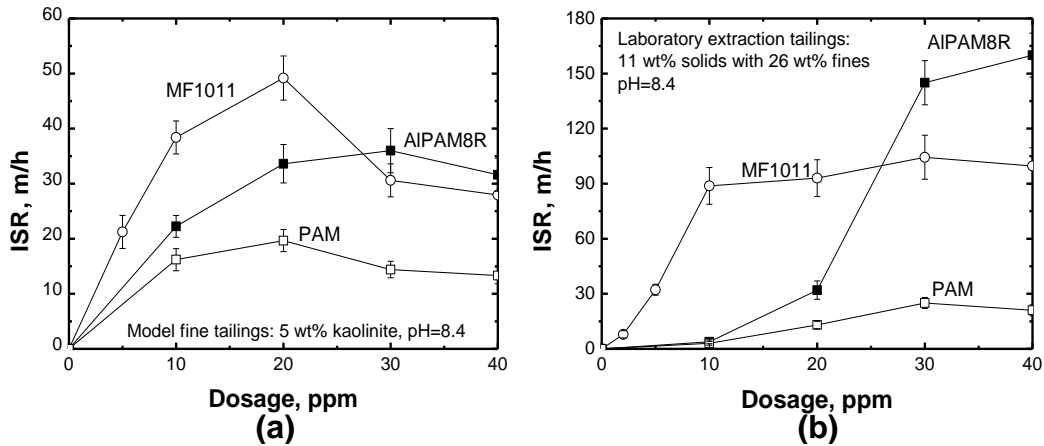


Figure A-6 Comparisons of initial settling rate of flocculated (a) model fine tailings; and (b) laboratory exaction tailings with PAM, MF1011 and AI-PAM.

Laboratory extraction tailings were also used to study the mechanism of AI-PAM in settling and filtration. Likewise, the settling behaviour of MF1011 and PAM had similar settling trend due to their similar structures, i.e., a single acrylamide chain. Figure A-6 (b) shows that for both MF1011 and PAM, the optimum dosage was 30 ppm. Besides the different polymer chain length, corresponding to different viscosity and molecular weight (see Table A-2), led to faster settling rates of MF1011 than those of PAM at given dosage. Figure A-6 (b) also shows that the settling rate of AIPAM8R were significantly higher than those of PAM, although they have similar intrinsic viscosity. The settling rate of AIPAM8R was significantly higher than that of PAM and MF1011 at the dosage of 30 ppm.

After settling for 5 minutes, the volume of sediments were recorded and compared for each polymer at different dosages as shown in Table A-3.

Table A-3 Sediment volume of flocculated laboratory extraction tailings by different polymers at different dosages

MF1011						
Dosage, ppm	2	5	10	20	30	40
Volume, mL	17.7	18.4	15.4	15.4	15.4	14.9
AIPAM4R						
Dosage, ppm	N/A		10	20	30	40
Volume, mL	N/A		34	23	18.5	20
AIPAM6R						
Dosage, ppm	N/A		10	20	30	40
Volume, mL	N/A		34	18	19	20
AIPAM8R						
Dosage, ppm	N/A		10	20	30	40
Volume, mL	N/A		26.4	19.2	19.4	19.5
AIPAM6H						
Dosage, ppm	N/A		10	20	30	40
Volume, mL	N/A		17.8	19	17.9	18

Figure A-7 shows the solids content by weight in sediment of flocculated laboratory tailings with polymers addition at different dosages.

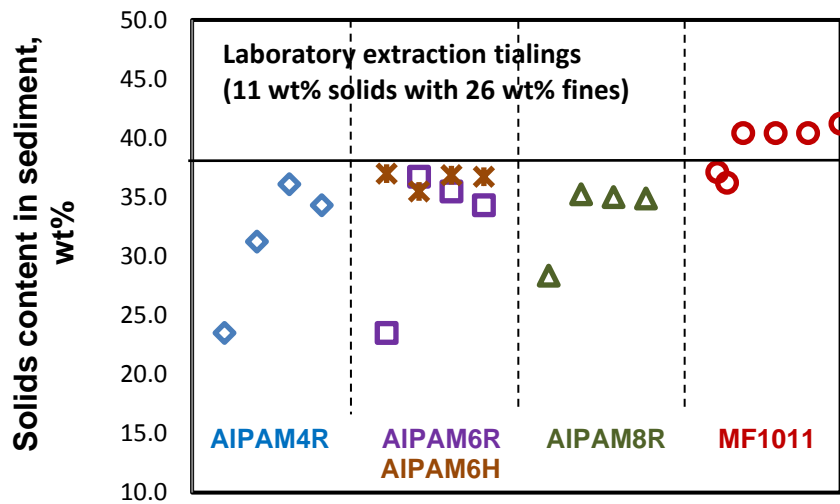


Figure A-7 Solids content in sediment of flocculated laboratory extraction tailings with polymers addition at different dosages.

The most solids contents of sediment for AI-PAMs were 30-33%, and most solids contents of the sediment for MF1011 were 38-42%. The sediment of MF1011 was more compact than AI-PAMs.

Figure A-8 shows the schematic of why sediment of MF1011 is more compact than AI-PAM.

The hydrocarbon chains of anionic PAM (e.g. MF1011) become more stretched at high pH (e.g. pH 8.4) due to the electrostatic repulsion among negatively charged particles surface [1]. These repulsive forces cause the polymer molecule chains to extend and produce loops and tails, which lead to the formation of large open-structure flocs shown in Figure A-8 (a),

resulting in compact sediments subsequently [2].

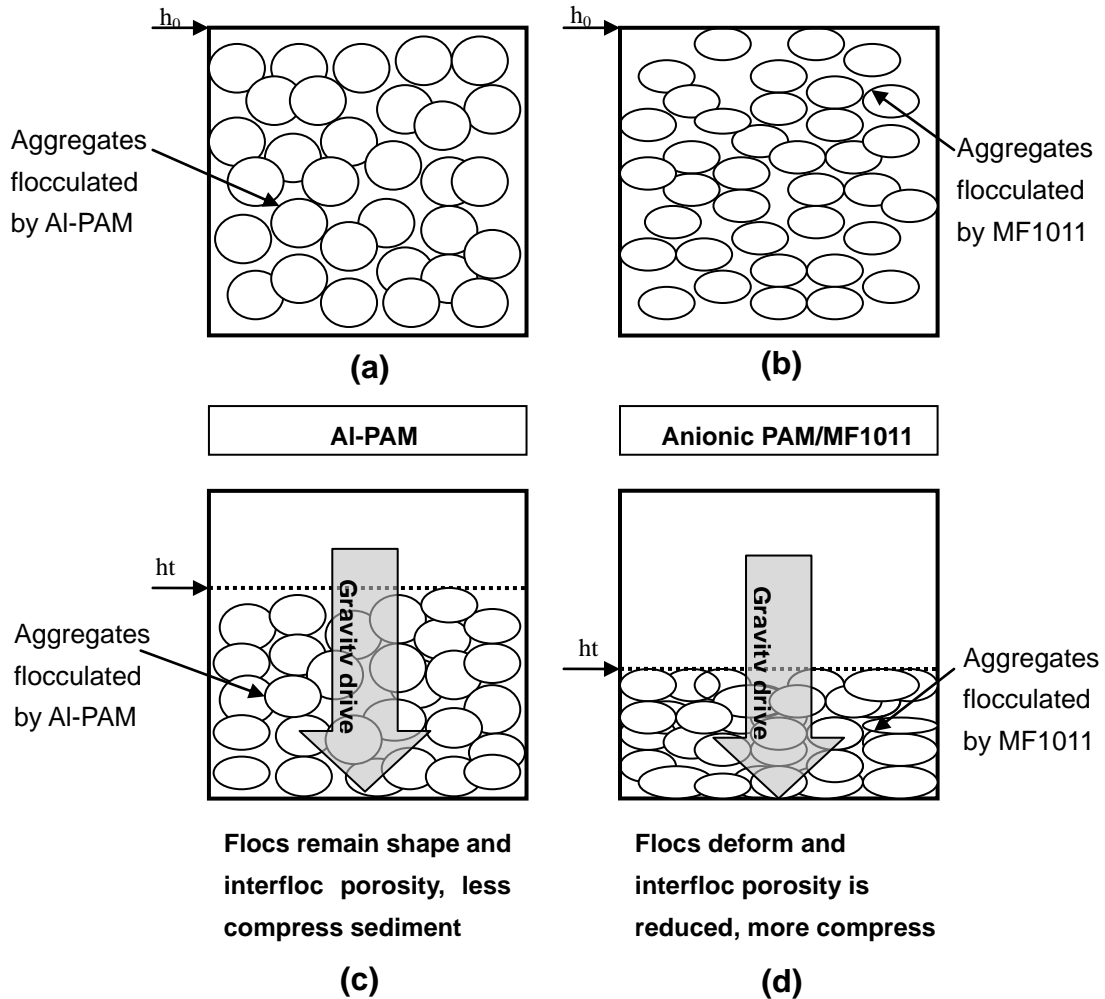


Figure A-8 Schematic of why sediment of MF1011 is more compact than Al-PAM.

Based on the above results, the following conclusions can be drawn:

1. For the polymers with same structure, higher molecular weight gives better flocculation performance.
2. At a given molecular weight, the existing of $\text{Al}(\text{OH})_3$ colloid core

makes the whole polymer positively charged, and hence enhances the ability of flocculation.

In previous work, TGA (Thermo-gravimetric Analysis) and adhesion force tests were conducted to further investigate the structure characteristics of Al-PAM [3].

In Figure A-9, there are three peaks representing the temperature at where PAM, (PAM+ Colloid) mixture and Al-PAM (e.g.H-1 in Figure A-9), respectively, are broken. The temperature for Al-PAM is the highest as more energy to break the bond is needed. This would indicate that the connection between aluminum and polymer is stronger. Therefore, Young et al. assumed that Al-PAM is a star-like hybrid polymer, in which core is the Al(OH)_3 colloid and polyacrylamide chains are the arms [3]. In other words, Al-PAM is not a simple physical mixture of PAM and Al(OH)_3 . It was observed that a simple blend of PAM and Al(OH)_3 colloid cannot bring out an efficient and stable flocculation.

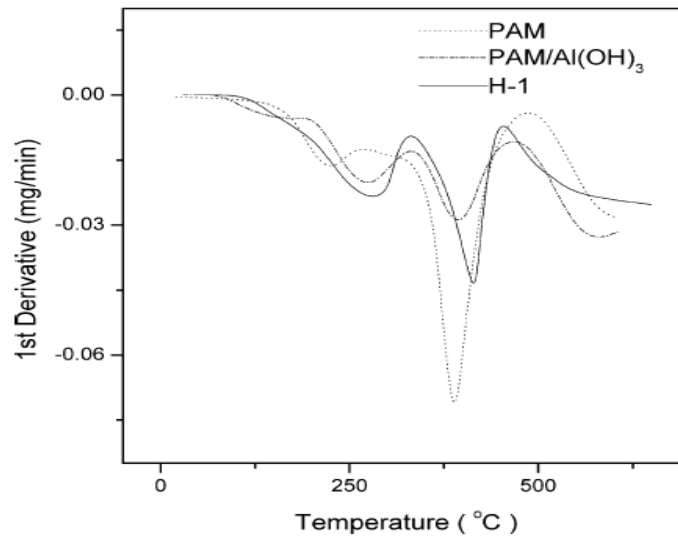


Figure A-9 TGA curves of H-1(Al-PAM), PAM, and Al(OH)₃/PAM blend [3].

Figure A-10 shows that the adhesion force of a single PAM chain to clay was not strong (e.g.250 pN), but the adhesion force between Al-PAM and clay particles was much stronger (1250 pN) than that between PAM and clay [3].

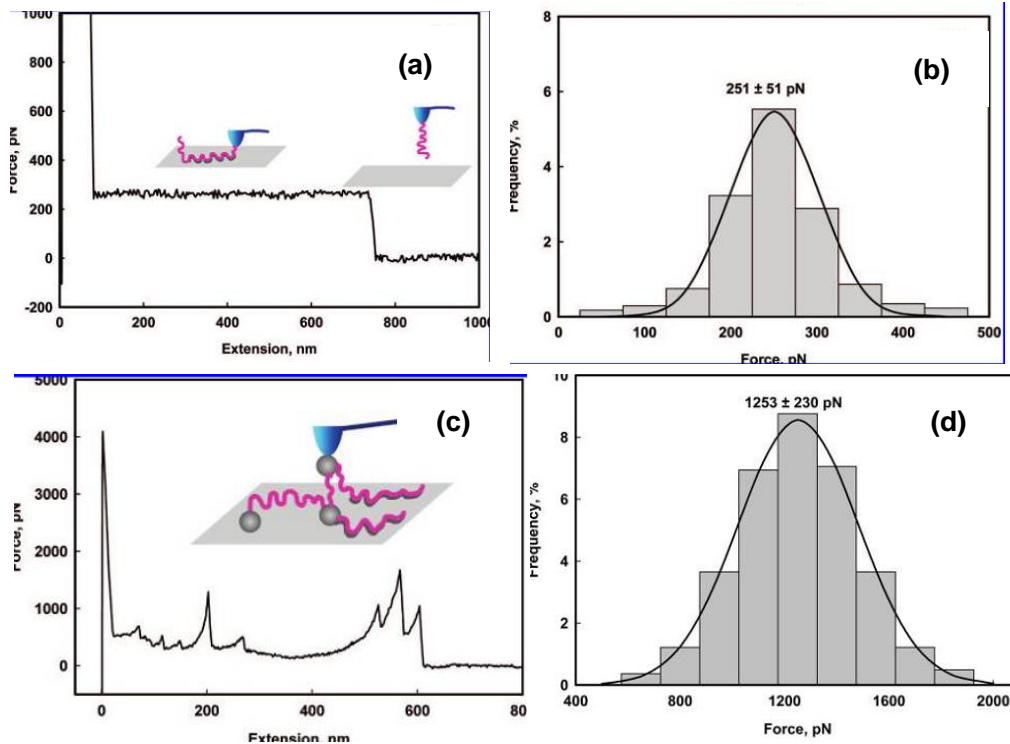


Figure A-10 (a)&(b) Adhesion force of a single PAM chain to clay; (c)&(d) adhesion force of Al-PAM to clay [5].

This is not only because of electrostatic interactions between $\text{Al}(\text{OH})_3$ colloids and the particle surface, but also due to a strong affinity between aluminum and oxygen in the form of $-\text{O}-\text{Al}-\text{O}-$, by which $\text{Al}(\text{OH})_3$ colloidal particles could adsorb onto the silica surface [4].

The dramatic Al-PAM-induced flocculation at least comes from two mechanisms [4]. One is coagulation-flocculation mechanism, which is both electrical neutralization and bridging roles synergism at the same time. It has been known that there are two components in Al-PAM: centered $\text{Al}(\text{OH})_3$ colloidal (group of $\text{Al}(\text{OH})^{2+}$, $\text{Al}(\text{OH})_2^+$ and $\text{Al}(\text{OH})_3$) particles and

PAM arm chains. The electrostatic repulsion is reduced among the particles in solution because of the attachment of positive charged Al-colloidal particles and negatively charged particles, and at the same time PAM chains can bridge clay particles through hydrogen bonding.

Another mechanism is accredited to the star-like molecular structure of Al-PAM [4], which is more beneficial to the bridging process compared to linear chain molecules because of the easy accessibility of PAM chains of Al-PAM to clay particles. The multi-chains stretching to the space have more chances to catch the particles and thus the formed primary flocs are associated to nearby flocs (see Figure A-11), leading to the formation of larger flocs of a raspberry structure [4].

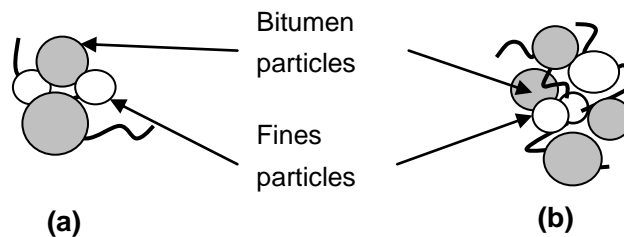


Figure A-11 Schematic of flocs by (a) single chain polymer; and (b) star-like polymer with the similar chain length.

Appendix B - Effect of bitumen content on settling and filtration of diluted mature fine tailings

In this section, diluted mature fine tailings (DMFT) was used to investigate the effect of bitumen content on settling and filtration performance. The original industrial mature fine tailings (MFT, from Syncrude) has about 40 wt% solids, in which more than 90 wt% content is fines. The selected MFT was diluted with de-ionized water to a suspension containing 5% solids by weight. It was found in the previous tests (Alamgir et al., 2009) that effect of polymer was not visible when dilution ratio was not low enough (e.g. weight ratio of MFT to water=1:4). Here, DMFT-HC stands for diluted mature fine tailings after removal of bitumen content. The bitumen content of DMFT was less than 3 wt%, and the bitumen content of DMFT-HC was less than 1 wt%.

Figure B-1 shows the settling and filtration results of flocculated diluted mature fine tailings with different bitumen content.

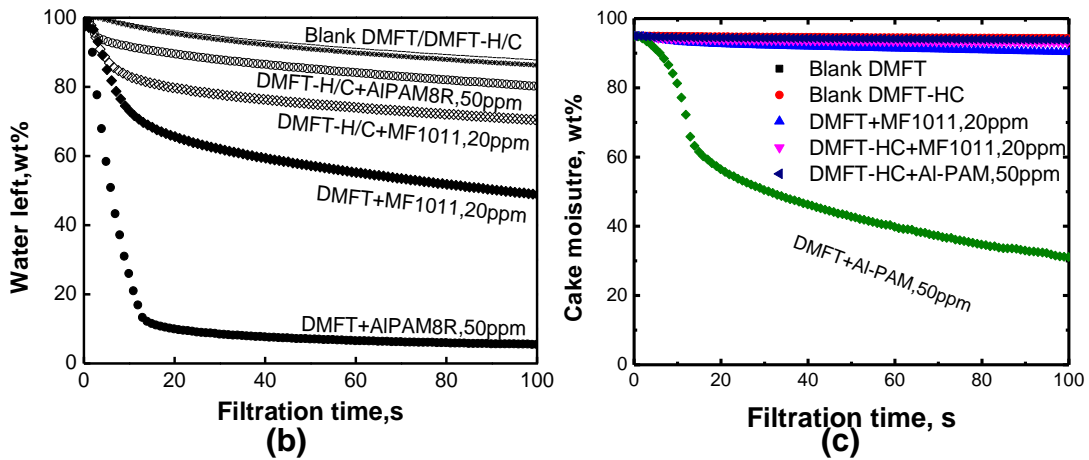
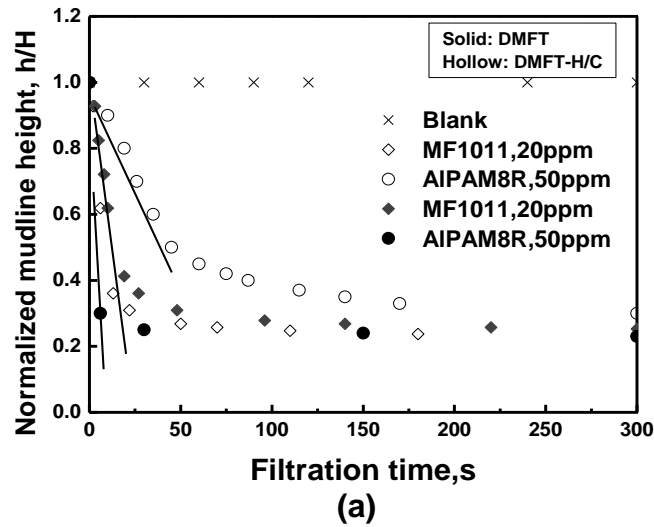


Figure B-1 Comparisons of (a) settling; (b) water left percent in the total water of tailings; and (c) moisture content in the filter cake of the diluted MFT with different bitumen content at selected dosages of each polymer.

Figure B-1 shows the results are consistent with the comparisons of the laboratory extraction tailings. Further removal bitumen did not improve either settling or filtration of the diluted MFT.

References

1. Sabah, E.; Erkan, Z. E., *Interaction mechanism of flocculants with coal waste slurry*. Fuel, 2006. **85**(3): p. 350-359.
2. Nasser, M. S.; James, A. E., *The effect of polyacrylamide charge density and molecular weight on the flocculation and sedimentation behaviour of kaolinite suspensions*. Separation and Purification Technology, 2006. **52**(2): p. 241-252.
3. Yang, W. Y.; Qian, J. W.; Shen, Z. Q., *A novel flocculant of Al(OH)(3)-polyacrylamide ionic hybrid*. Journal of Colloid and Interface Science, 2004. **273**(2): p. 400-405.
4. Sun, W.; Long, J.; Xu, Z. H.; Masliyah, J. H., *Study of Al(OH)(3)-polyacrylamide-induced pelleting flocculation by single molecule force spectroscopy*. Langmuir, 2008. **24**(24): p. 14015-14021.